Université de Montréal

# Genetically engineering the mouse genome to study the role of the Phosphotyrosyl Phosphatase Activator (PTPA) gene in the response to oxidative stress

Par Cyril Sabbah

Programme de Biologie Moléculaire

Faculté des études supérieures

Mémoire présenté à la faculté des études supérieures
en vue de l'obtention du grade de Maître ès science (M.Sc.)
en biologie moléculaire

Août 2005

Université de Montréal

Faculté des études supérieures

Ce mémoire intitulé :

Genetically engineering the mouse genome to study the role of the Phosphotyrosyl Phosphatase Activator (PTPA) gene in the response to oxidative stress

Présenté par:

Cyril Sabbah

a été évalué par un jury composé des personnes suivantes

| | |
|---|---|
| Eric Milot | Président Rapporteur |
| Dindial Ramotar et Elliot Drobetsky | Directeurs de Recherche |
| Edward Bradley | Membre du Jury |

**Résumé**

L'oxygène est indispensable à la vie aérobique. Cependant, certains métabolites de cette molécule peuvent devenir des espèces oxygénées activées (EOA), des radicaux libres extrêmement réactifs pouvant causer des dommages à plusieurs composants cellulaires tels que les lipides, les protéines et l'ADN. Les EOA sont une source de stresse inévitable et permanent puisqu'elles sont générées par des processus endogènes; ces molécules sont des sous-produits de la respiration cellulaire et sont générées par des cellules immunitaires pour combattre l'infection de corps étrangers. De plus, ils sont produits à la suite de l'exposition à plusieurs agents exogènes tels que certaines longueurs d'onde émises par le soleil ainsi que de nombreux métaux et drogues. Par conséquent, les cellules ont développés plusieurs mécanismes qui permettent d'empêcher ou de réparer les dommages dus aux EOA. Notamment, la réparation par excision des bases est la voie principale de réparation de l'ADN endommagé par ces radicaux libres, permettant d'éviter à ce que les lésions oxydatives deviennent des mutations permanentes. Cependant, si ces mécanismes sont altérés, les cellules peuvent devenir particulièrement vulnerables face aux dommages causés par les EOA. En effet, de nombreuses pathologies sont associées au stress oxydatif, tels que certaines maladies cardiovasculaires, neurodégénératives, le diabète et le cancer. Une meilleure connaissance des gènes impliqués dans la réponse cellulaire face aux stresses oxydatifs pourrait nous permettre de mieux comprendre ces maladies sur le plan biologique.

Lors d'un criblage de souches de levures mutantes, l'homologue du gène Phosphotyrosyl Phosphatase Activator (PTPA) humain, RRD1, à été identifié comme jouant un rôle important dans le maintient de l'intégrité de l'ADN exposé aux EAO. Quoique le mécanisme d'action et la fonction précise de PTPA ne soient pas bien caractérisés, plusieurs évidences suggèrent que ce gène joue un rôle dans plusieurs processus biologiques, dont certains étant liés à la carcinogenèse. Etant donné l'importance du stresse oxydatif dans l'initiation de certains types de cancer et du rôle de PTPA dans le maintien de l'intégrité l'ADN face à ce stresse, nous avons chercher à étudier ce gène chez les mammifères en produisant de souris ayant soit une délétion, soit une surexpression de la protéine Ptpa. Nous avons préparé la construction d'ADN en vue de créer des souries knockout «conditionnelle » pour ce gène, et avons générer des

colonie de souris ayant intégré une copie supplémentaire du gène PTPA fusionné avec une protéine dérivée de la protéine fluorescente verte sans, pour autant, exprimer le transgene. Une fois que ces souris manipulées génétiquement seront établies, elles pourront être exposées a divers sources de stresse oxydatif. Ceci permettrait l'étude du fonctionnement de PTPA dans la réponse aux EOA.

Mots clés : PTPA, RRD1, stress oxydatif, UVA, dommages à l'ADN, souris transgénique, souris knockout, cre-loxP, protéine verte fluorescente

**Abstract**

Oxygen molecules are essential for aerobic life. However, certain free radical metabolites of oxygen molecules, Reactive Oxygen Species (ROS), can cause significant damage to cellular lipids, proteins and DNA. ROS are a constant threat to cellular integrity as they are produced by endogenous processes; they are normal byproducts of cellular respiration and are produced by cells of the immune system to combat foreign organisms. In addition, exogenous agents such as a subset of solar wavelengths and a number of drugs and metals also generate ROS. Consequently, cells have developed a number of methods of containing the damaged caused by ROS, including the Base Excision Repair pathway, the primary line of defense against oxidative DNA damage, which prevents the accumulation of irreversible mutations. Therefore, cells in which these mechanisms are altered have increased susceptibility to ROS-induced damage. Indeed, a variety of conditions and diseases, such as cardiovascular and neurodegenerative diseases, diabetes, and cancer have been associated to oxidative stress. Therefore, the study of genes involved in the cellular response to ROS may achieve a greater understanding of the biology of these diseases.

In searching for genes that are involved in the response to oxidative stress, our laboratories have previously identified the yeast homologue of the human Phosphotyrosyl Phosphatase Activator (PTPA) gene as playing an important role in maintaining the integrity of DNA in response to oxidative stress. Although studies have not yet revealed its specific function or mechanism of action, data suggest that PTPA may have a number of important cellular functions, many of which are consistent with a function of PTPA in pathways related to carcinogenesis. Given the clinical importance of oxidative stress in certain types of cancer as well as PTPA's involvement in maintaining DNA integrity, our laboratories sought to elucidate this gene's function in mammals by generating PTPA knockout and transgenic mice. Recent advances that allow for a high degree of "tailoring" of the mouse genome have prompted us to design a targeting vector that will enable the generation of "conditional" knockout mice. In addition, we have produced animals having integrated a DNA construct which was anticipated to express the Ptpa protein fused with a variant of the Green Fluorescent Protein within their genome, although these did not express the transgene *per se*. When mouse lines with the Ptpa

deletion and overexpression will be established, these animals can be exposed to oxidative stress-causing agents. It is expected that these experiments will further our understanding of this gene's role in the response to oxidative stress.

Keywords: PTPA, RRD1, oxidative stress, UVA, DNA damage, transgenic mice, knockout mice, cre-loxP, green fluorescent protein

## Table of Contents

**List of figures**

## List of tables

**List of abbreviations**

ES: embryonic stem

HR: homologous recombination

DNA: deoxyribose nucleic acid

PTPA: Phosphotyrosyl Phosphatase Activator

BER: Base Excision Repair

NER: Nucleotide Excision Repair

dNTP: deoxyribonucleoside triphosphate

dCTP: Deoxycytidine 5'-triphosphate

PCR: polymerase chain reaction

Neo: neomycin gene conferring resistance to G418

Puro: puromycin gene conferring resistance to puromycin

Amp: gene conferring resistance to ampicillin

Kan: gene conferring resistance to kanamycin

UV: ultraviolet

Ex: Excitation maximum

Em: Emission maximum

pSK: Bluescript cloning vector

EYFP: Enhanced Yellow Fluorescent Protein

## Acknowledgments

First and foremost, I would like express my gratitude my research directors, Dr. Dindial Ramotar and Dr. Elliot Drobetsky for having granted me the chance to embark on this ambitious and challenging project, as well as for their patience throughout my studies. This has been a truly worthwhile learning experience.

In addition, I owe a debt of gratitude to the members of the labs. The moral and technical support that they have provided throughout my studies was greatly appreciated. In particular, I thank Julie Douville for her constant support, advice and laborious efforts. Many friendships have been fostered through this project.

Last but certainly not least, I would like to thank my family for their encouragement and guidance. Finally, a special thanks to my wife and daughter who patiently tolerated my absence "outside of standard working hours," and have endured the occasional work-related mood swings, seemingly inherent to scientific research.

# 1. Introduction

## 1.1. Oxidative stress and disease

### 1.1.1. The Oxygen Paradox

Oxygen is a mixed blessing for aerobic life. On the one hand, it is essential for cellular respiration and energy metabolism. Yet this molecule can become a potent agent capable of causing significant damage to various macromolecules. Denham Harman (1956) first developed the notion that oxygen can be detrimental to the cell, hypothesizing that oxygen free radicals are involved in general cellular damage, mutagenesis, cancer and aging. Since then, this hypothesis has been extensively researched (Droge, 2000; Behrend *et al.*, 2003), and many other conditions are currently associated with oxygen cytotoxicity, including neurodegenerative and heart diseases (Lebovitz *et al.*, 1996; Norata *et al.*, 2003) and diabetes (Nath *et al.*, 1984).

Oxygen molecules become toxic when their metabolites are activated, via a series of intercellular chemical reactions, into free radical reactive oxygen species (ROS), or molecules with an unpaired electron in their outer valence shell. ROS can be very unstable and highly reactive, "attacking" neighbouring, generally non-radical, molecules in seeking to fill their valence shell. In the process, reactive oxygen species damage the "donor" molecules, effectively transforming these into free radicals, which in turn, will also seek to fill their outer valence shell. Thus, a single free radical can cause a chain reaction, potentially damaging multiple cellular components (Turrens *et al.,* 2003).

### 1.1.2. Cellular Toxicity of ROS

Reactive oxygen species cause damage to cellular lipids, proteins and DNA. ROS-mediated lipid peroxidation could disrupt the fluidity and permeability of the cytoplasmic and mitochondrial membranes, interfering with the proper functioning of membrane-bound proteins (Van der Vliet and Bast, 1992). Reactive oxygen species can also disrupt protein function by causing site-specific amino acid modifications, altering proteic electrical charge or triggering peptide fragmentation (Grune *et al.*, 1997). Finally, ROS can produce a variety of DNA lesions, including modified bases (Téoule and Cadet,

1978), oxidized apurinic/apyrimidinic sites (Mitra *et al.*, 2002) and strand breaks resulting from damage to the sugar moiety of DNA (Dizdaroglu *et al.*, 1975). These damages can eventually give rise to permanent mutations (Loeb and Preston, 1986). One frequent oxidative DNA lesion is the 7,8-dihydro-8-oxoguanine (8-oxoG) (Grollman and Moriya, 1993). Left unrepaired, this premutagenic lesion can become an irreversible G·C→T·A transversion (Shibutani *et al.*, 1991; Cheng *et al.*, 1992). Interestingly, such transversions are often present in cancerous cells, particularly in oncogenes and tumour suppressor genes (Aguilar *et al.*, 1993; Jones *et al.*, 2004; Yokota and Kohno, 2004). Another example of the mutagenic effects of ROS, is the deamination of normal cytosine nucleic acids into the premutagenic 5-hydroxyuracil and uracil glycol lesions, which can lead to a C·G→T·A transition if left unrepaired (Kreutzer *et al.*, 1992).

Oxygen free radicals are often so reactive that they do not diffuse more than a few molecular diameters before reacting with another molecule (Pryor *et al.*, 1996). Thus, the damage localized within the nucleus is probably the result of free radicals produced later in the free radical chain reaction. In fact, quantitatively speaking, it has been estimated that DNA may be the least significant target of ROS (Marnett, 2000). Nonetheless, it is estimated that one human cell produces up to 10,000-20,000 oxidative DNA lesions in a 24-hour period (Ames *et al.*, 1993; Jackson and Loeb, 2001). In addition, damage incurred by DNA is qualitatively of great significance because; whereas other cellular components can be newly synthesized when damaged, unrepaired DNA can lead to permanent and irreversible mutations.

### 1.1.3. Sources of ROS

It would be expected that organisms would seek to minimize their exposure to reactive oxygen species. However, the formation of ROS is neither abnormal nor rare. As mentioned, ROS produced by mitochondria are natural by-products of cellular respiration, continuously and inevitably endangering cells (Cadenas and Davie, 2000). Further, higher eukaryotes actively produce oxygen free radicals. Neutrophils and macrophages exploit free radical toxicity by generating ROS as a means of destroying foreign bodies during inflammation (Chong *et al.*, 1989; Roos *et al.*, 2003).

In addition, humans are exposed to a variety of exogenous sources of oxidative stress, including ionizing radiation (Ward, 1989), cigarette smoke (Churg, 2003), trace metals found in industrial waste, such as lead, mercury and cadmium (Ercal *et al.*, 2001), and various therapeutic and experimental drugs such bleomycin and adriamycin (Kappus, 1987) and the model carcinogen, 4-NQO (Ramotar *et al.*, 1998). Oxidative stress is also generated upon exposure to the ultraviolet (UV) subset of solar radiation. The sun emits UV light of all wavelengths, commonly categorized as UVA (400 nm - 320 nm), UVB (320 nm - 290 nm), UVC (290 nm - 100 nm) Although UVC is extremely genotoxic, it is not a major public health concern because wavelengths of less than 300 nm are largely absorbed by ozone in the stratosphere before it reaches the Earth (Latarjet, 1935). Consversely, UVA and UVB wavelengths reach the Earth. These generate chemically distinct types of DNA damage these wavebands. However, both UVA and, to a lesser extent, UVB, can generate ROS (Cadet *et al.*, 2005). Thus, these exogenous sources of ROS are compounded to the endogenous "load" constantly challenging the integrity of the cell.

### 1.1.4. Cellular Defence Against ROS Insult

Organisms have adapted to the continuous and unavoidable exposure to oxygen free radicals by developing several strategies to attenuate ROS cytotoxicity. Various superoxide dismutase (SOD), catalase and glutathione peroxidase enzymes constitute an important line of defence. Briefly, SOD can convert two superoxide radicals ($O_2^{\cdot -}$) into less reactive hydrogen peroxide ($H_2O_2$) (Noor *et al.*, 2002), which is subsequently, converted into water and oxygen in a process mediated by catalase and glutathione peroxidase (de Haan, 1995). In addition, higher eukaryotes produce antioxidants, molecules that provide free radicals with an electron to fill their outer valence shell (Jacob and Burri, 1996). Together, these mechanisms allow the cell to contain the effects of oxygen free radicals.

However, preventative measures are insufficient to protect the integrity of DNA, which cannot be newly re-synthesised once mutations have incurred. Consequently, cells have developed mechanisms to repair oxidative lesions before these become permanent mutations. Most important is the Base Excision Repair (BER) pathway, in which a

variety of proteins acts sequentially to remove the base and sugar moieties of the damaged nucleic acid, incorporating the appropriate undamaged nucleic acid in its place. Briefly, a DNA glycosylase is recruited to the site of the lesion, disassociating the base from the sugar moiety of the nucleic acid and creating an apurinic/apyrimidic (AP) site (Figure 1). Subsequently, an AP endonuclease disrupts the sugar backbone, leaving behind a gap in the double stranded structure of the DNA. This gap is filled by a DNA polymerase, and the newly incorporated nucleic acid is ligated to the DNA by a ligase (Fortini *et al.*, 2003).

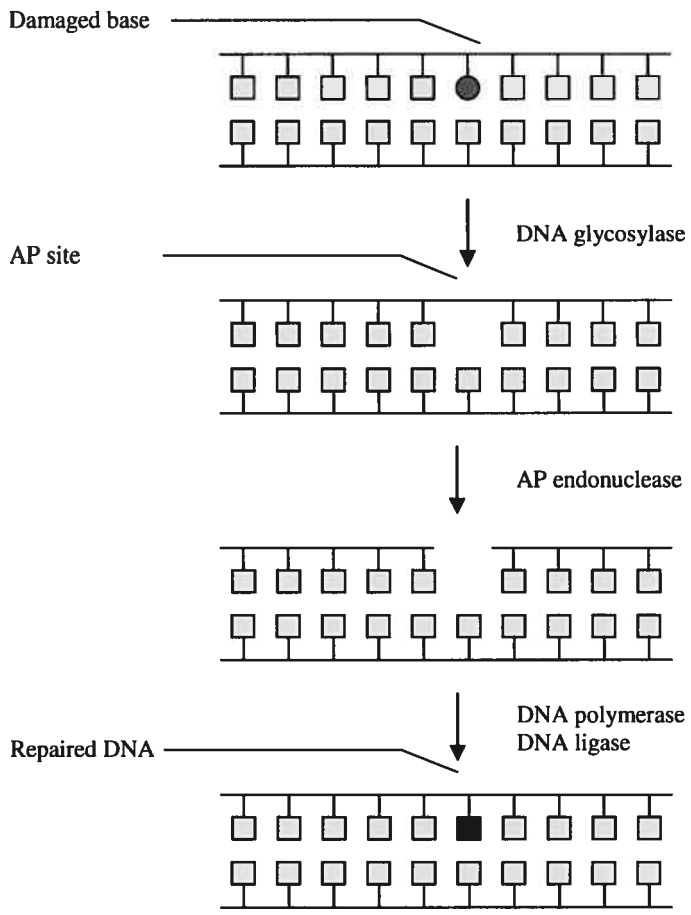


**Figure 1:** Base Excision Repair pathway. This is the most important for the repair mechanism of oxidative DNA lesions

The repair proteins, such as DNA glycosylases and AP endonucleases, are relatively well conserved in organisms (Barzilay and Hickson, 1995; McCullough *et al.*, 1999). Studies in yeast and mammalian cells have demonstrated that cells with a deficiency in one or several of these genes show an increase in premutagenic lesions and, sometimes, a hypersensitivity to oxidative stress-inducing agents (Walker *et al.*, 1994, Doetsch *et al.*, 2001, Kim *et al.*, 2002).

Although BER is the primary response to oxidative stress-induced DNA lesions, other mechanisms also contribute to the repair of these lesions. For example, UVC generates dipyrimidine photoproducts lesions (chemically distinct from oxidative lesions) which are primarily repaired by the Nucleotide Excision Repair (NER) pathway. Nonetheless, there is some overlap of these repair pathways; the NER and other repair mechanisms contribute to the repair of oxidative DNA lesions, albeit to a lesser extent relative to the BER (Scott *el al.*, 1999, Rybanska and Pirsel, 2003).

### 1.1.5. Mutagenic effect of ROS and Melanoma

Oxidative damage to DNA may be a significant factor in the dramatic increase of melanoma incidences rates in North America, Europe and Australia in the 1970s and 1908s (Armstrong and Kricker, 1994, Hall *et al.*,1999). The highly mutagenic UVB component of solar radiation has long been established as the major cause of this disease (de Gruijl, 2000). However, there is a growing consensus that solar UVA plays a more significant role in the development of melanoma than was first thought. This is supported by several experiments conducted in murine and human cell lines, whole animals, as well as a number of epidemiological studies (Jones *et al.*, 1987, Lundgren *et al.*, 1988, Sterenborg and van der Leun, 1990, Setlow *et al.* 1993, and Ley, 1994). In addition, various lines of evidence indicate that oxidative stress plays a significant role in cutaneous carcinogenesis. For example, it has been demonstrated that normal melanocytes from melanoma patients have increased sensitivity to peroxidizing agents (Grammatico *et al.*, 1998), that the skin antioxidant defense system is impaired in melanoma cells and normal melanocytes of these patients (Picardo *et al.*, 1996). Further, antioxidant supplementation was found to have a photoprotective effect on cells (Lopez-Torres *et al.*, 1998). Another study demonstrated that compounds that generate oxygen

free radicals increase the effect of malignant conversion of cancerous skin cells (Athar *et al.*, 1989). The authors of this report present the hypothesis that the accumulation of genetic lesions and strand breaks and chromosomal aberrations induced by ROS hasten the process by which cells become malignant.

Thus, although UVB is incontestably more genotoxic than UVA and remains the major factor in the incidence of melanoma, there is growing evidence that UVA-induced reactive oxygen species may play a role in this carcinogenesis that is more significant than was initially thought.

## 1.2. The Involvement of the Phosphotyrosyl Phosphatase Activator Gene in the Response to Oxidative Stress

### 1.2.1. Identification of Genes with a Role in the Response to Oxidative Stress

Given the significant impact of oxidative stress upon human health, our laboratories were interested in identifying novel genes that perform key functions in the cellular response to this type of stress, particularly those that play a role in the repair of ROS-induced DNA damage. Initially, the budding yeast *Saccharomyces cerevisiae* was chosen as the organism in which to conduct this search because its genome is well characterized and relatively easy to manipulate. In addition, fundamental processes, including DNA repair pathways, are well conserved from yeast to humans. Isolating oxidative stress response genes in yeast could lead to the identification of novel functions of new or previously characterized genes in humans.

As described by Ramotar *et al.* (1998), a wide panel of yeast mutants were subjected to a three-step screen. Initially, mutants showing hypersensitivity to 4-nitroquinoline 1-oxide (4-NQO) were isolated. This drug generates two different types of DNA damage: genotoxic "bulky" lesions, primarily repaired by NER, and oxidative DNA lesions, primarily repaired by the BER pathway. Mutants obtained from this initial screen were expected to demonstrate hypersensitivity to 4-NQO due to defects in a number of mechanisms, including the NER and BER pathways. To differentiate the ROS-response mutants from the ones with other defects, the 4-NQO hypersensitive strains were exposed to UVC (254 nm UV light). The mutants showing full cross-sensitivity to the genotoxic

effects of UVC were precluded from further study because these were likely to carry defects in the NER. Conversely, the mutants exhibiting normal sensitivity to UVC were retained. The latter carried mutations in candidate genes having a ROS-specific function. The final step consisted of characterizing these yeast strains, identifying the mutated genes and confirming their role in the cell's response to oxidative stress.

### 1.2.2. PTPA Involvement in Maintaining DNA Integrity upon Exposure to Oxidative Stress

When the mutants were characterized, it was found that several ROS-hypersensitive strains carried a mutation on RRD1, one of the two yeast homologues of the human Phosphotyrosyl Phosphatase Activator (PTPA). This gene was subsequently deleted in various wild-type yeast backgrounds and exposed to different oxidative stress-inducing agents. In addition to the previously observed hypersensitivity to 4-NQO, RRD1-defecient cells were hypersensitive to other ROS-inducing agents including UVA, UVB, and diamide. Conversely, these strains were not hypersensitive to genotoxic agents that do not cause oxidative stress, such as 254 nm-UV. Further, genetic complementation tests were performed by transforming RRD1-deficient yeast cells with vectors driving the constitutive expression of RRD1. This successfully restored normal UVA and 4-NQO resistance. It was also shown that strains lacking RRD1 exhibited a hypermutable phenotype in normal conditions, as well as an increased frequency of chromosomal breakage in comparison to wild-type strains. This phenotype was exacerbated when cells were treated with 4-NQO. Together, the data strongly suggested that Rrd1 plays a role in maintaining the integrity of DNA in cells challenged with oxidative stress.

### 1.2.3. Complexity of PTPA Functions

Although PTPA, the mammalian homologue of yeast RRD1, has been the subject of numerous studies since it was identified in 1990, very little is known about its function. The Ptpa protein was found to be an activator of protein phosphatases of type 2A (PP2A), a family of phosphatases that is both structurally complex and multifunctional. Much like PP2A, PTPA seems to be involved in a multitude of pathways. Its complexity has rendered focused and precise studies difficult to perform.

In addition, two recent reports have showed that this gene activates a broad spectrum of PP2A's activities (Fellner *et al.*, 2003; Longin *et al.*, 2004), contrary to what had been assumed for over a decade. Accordingly, hypotheses and speculation of possible roles of PTPA have, until recently, been based on data that was later shown to be false. It is in the context of the complex functions of PP2A and PTPA and erroneous assumptions concerning Ptpa's biochemical function as a PP2A activator that the fragmented literature on this gene should be surveyed. Although no clear model of Ptpa action mechanism emerges from the literature, it does not negate the finding that this gene plays an important role in maintaining DNA integrity in response to ROS insult. Rather, the sum of Ptpa-related data indicates that this protein is involved in a number of cellular processes, a subset of which is associated with mutagenesis and carcinogenesis.

**1.2.3.1. PP2A Proteins are Multifunctional Phosphatases Involved in Carcinogenesis**

Protein phosphatases of the family 2A are multifaceted at the biochemical and structural levels. Their primary biochemical function is to dephosphorylate phosphorylated serine and threonine residues (Waelkens *et al.*, 1987). However, PP2A also exhibits a low basal level of phosphotyrosine phosphatase activity (Chernoff *et al.*, 1983; Foulkes *et al.*, 1983). Conserved in organisms, PP2A is structurally complex. Minimally, the phosphatase exists as a dimer consisting of a C-catalytic subunit and an A-structural subunit. Both of these subunits can exist in two isoforms in mammals (Mayer *et al.*, 1991; Groves *et al.*, 1999). This core dimer can associate with a regulatory component, subunit B, to form a trimeric holoenzyme. This subunit, made up of four distinct families (B, B', B'', B''') and their isoforms (Gentry and Hallberg, 2002), is involved in targeting the PP2A holoenzyme to the appropriate cellular compartment and in providing substrate specificity (Zolnierowicz *et al.,* 1996). In addition to these, a number of subunits that are structurally and functionally similar to PP2A exist. These PP2A-like proteins include PPP6C, the mammalian homologue of *S. cerevisiae* SIT4 (Bastians and Ponstingl, 1996, Bastians *et al.* 1997). Only a few holoenzymes of PP2A have been isolated in humans, but it has been estimated that more than 40 different combinations of trimeric complexes could be formed (Janssens and Goris, 2001).

The phosphatases of type 2A in lower organisms share many, but not all, of these features. For example, in contrast to mammalian PP2A, *S. cerevisiae* has numerous C subunits, but these do not have known functional isoforms. In addition, there are fewer B subunits, and consequently there are far fewer possible holoenzyme combinations (Gentry and Hallberg, 2002).

It appears that the various components of the holoenzymes and their isoforms have some partially non-redundant functions. An example of this in yeast arises from a genetic study involving the deletions of the *S. cerevisiae* B-subunits CDC55 and RTS1, which demonstrated that CDC55-deficient strains exhibit defective cytokinesis and abnormal cell morphology while RTS1-deficient strains are temperature sensitive. It was also shown that the over-expression of one gene did not compensate for the deletion of the other (Zhao *et al.*, 1997), further indicating that these B-subunits are involved in distinct pathways.

Even isoforms of a given subunit may have non-redundant functions. A striking example of this was provided by Götz *et al.* (1998), who demonstrated that the β isoform of subunit C could not compensate for the embryonic lethality phenotype observed in the targeted deletion of the α isoform in mice, despite their strong homology (97% amino acid identity).

Given the number of potential holoenzymes and the possibility that these have at least partially non-redundant functions, it is not surprising that PP2A is associated with a variety of biological processes including the cell cycle (Karaiskou *et al.*, 1999), DNA replication (Lin *et al.*, 1998), transcription (van Zyl *et al.*, 1992), RNA splicing (Mermoud *et al.*,1998), translation (Di Como *et al.*, 1996) and morphogenesis (Healy *et al.*,1991; Heller *et al.*,1998). In addition, PP2A is an important cellular target of invading toxins and viruses (Garcia *et al.*, 2000).

There are various lines of evidence associating PP2A with cancer. For example, okadaic acid, a strong inhibitor of PP2A activity has been found to promote tumour formation in the skin of mice (Suganuma *et al.*, 1988), and a number of studies have demonstrated loss-of-function mutations in A-subunit isoforms of patients with lung and breast carcinomas and colorectal and colon cancers. (Wang *et al.*; 1998; Takagi *et al.*; 2000; Calin *et al.*, 2000; Ruediger *et al.*, 2001). Further, PP2A has been found to

facilitate the cellular response to oxidative stress by dephosphorylating members of the retinoblastoma (Rb) family of tumour suppressor proteins. These proteins have a variety of functions including regulating the E2F transcription factor. This regulation plays an important role in mediating the events leading to the progression/arrest of the cell cycle (Muller *et al.*, 2000). Cicchillitti *et al.* (2003) demonstrated that upon exposure to hydrogen peroxide, a drug that generates significant levels of oxidative stress, PP2A acts to dephosphorylate Rb proteins, causing E2F to arrest cell growth. This phosphatase is also involved in melanoma; a mutation of the B subunit 56γ-1 gene was shown to exacerbate the progression of this cancer (Ito *et al.*, 2003). Thus, PP2A is involved in a number of pathways, a subset of which is consistent with a role in carcinogenesis, melanoma progress and the response to oxidative stress.

#### 1.2.3.2. PTPA: A Survey of the Literature

Initially, most research relating to Ptpa sought to elucidate its biochemical function as an activator of PP2A. Later reports focused primarily on genetic and proteomic features of PTPA in different organisms, and more recent studies have principally elaborated on its function at the cellular level. Whereas the biochemical literature has not led to any real understanding of Ptpa's role in the cell, a number of important features and phenotypes have been identified.

#### 1.2.3.3. Biochemical Functions of Ptpa

As mentioned, PP2A can exist as a dimer or trimer, and has two phosphatase activities. It is primarily a Ser/Thr phosphatase, but also exhibits a basal level of tyrosyl phosphatase activity (Chernoff *et al.*, 1983, Foulkes *et al.*, 1983). Initial in vitro assays identified Ptpa as an activator of the tyrosyl phosphatase activity of the dimeric form of PP2A. These assays excluded the possibility of PTPA activating the trimeric holoenzyme (Cayla *et al.*, 1990) or being involved in the Ser/Thr phosphatase activity of PP2A. Consequently, early studies involved determining the effect of Ptpa on subunits A and C of PP2A only. However, two recent studies indicate that these assumptions were incorrect; PTPA's main function was found to be the activation of the Ser/Thr phosphatase activity of the PP2A *trimeric* holoenzyme in vivo (Fellner *et al.*, 2003; Longin *et al.*, 2004). Both reports propose different biochemical models in which Ptpa

regulates the C-subunit's activity by mediating conformational changes of PP2A. However, these findings are not definitive and it is unclear if they will be instrumental in defining a cogent biological function for PTPA.

**1.2.3.4. Ptpa Protein is Conserved in Organisms**

Homologous Ptpa proteins have been identified in *S. cerevisiae* (Rrd1 and Rrd2), *S. pombe* (Accession Z98980), *Drosophila melanogaster*, *Xenopus laevis* (Van Hoof *et al.*, 1998), as well as many mammals ranging from the rabbit, mouse and dog to humans (Cayla *et al.*, 1990; Cayla *et al.*, 1994; Van Hoof *et al.*, 1994). Mammalian Ptpa appears to be ubiquitous; the protein is present in the brain, liver, kidney, muscle, spleen, pancreas and fat cells of the rabbit and dog (Cayla *et al.*, 1994) as well as various independent cell lines derived from mice and humans (Cayla *et al.*, 1994; Fellner *et al.*, 2003).

There are some significant differences between the Ptpa proteins of the different organisms. For instance, although mammalian Ptpa proteins are highly homologous to each other (for example, 97% amino acid identity is observed between human and rabbit Ptpa), less similarity is observed between mammalian proteins and those of lower eukaryotes (for example, 50% homology is observed between drosophila and human Ptpa). In addition, *S. cerevisiae* and drosophila proteins are considerably larger than their orthologues in vertebrates; whereas the latter are 37 kDa, the former contain an extended 10 kDa C-terminal tail (Van Hoof *et al.*, 1998). Nonetheless, certain regions are highly conserved in all organisms (Figure 2). Van Hoof *et al.* (1998) demonstrated that these regions have functional significance by showing that targeted deletions of the conserved areas altered PTPA activity in vitro. Further, genetic complementation studies, in which RRD1-deficient yeast strains were transformed with a vector driving the expression of the mammalian Ptpa protein successfully reversed some phenotypes of the mutant strain (Douville *et al.*, 2004).

The presence of Ptpa is crucial to cell survival; yeast strains deficient in both PTPA genes are not viable (Rempola *et al.*, 2001) and the inhibition of Ptpa translation by RNA interference causes mammalian cell lines to undergo apoptosis (Fellner *et al.*, 2003).

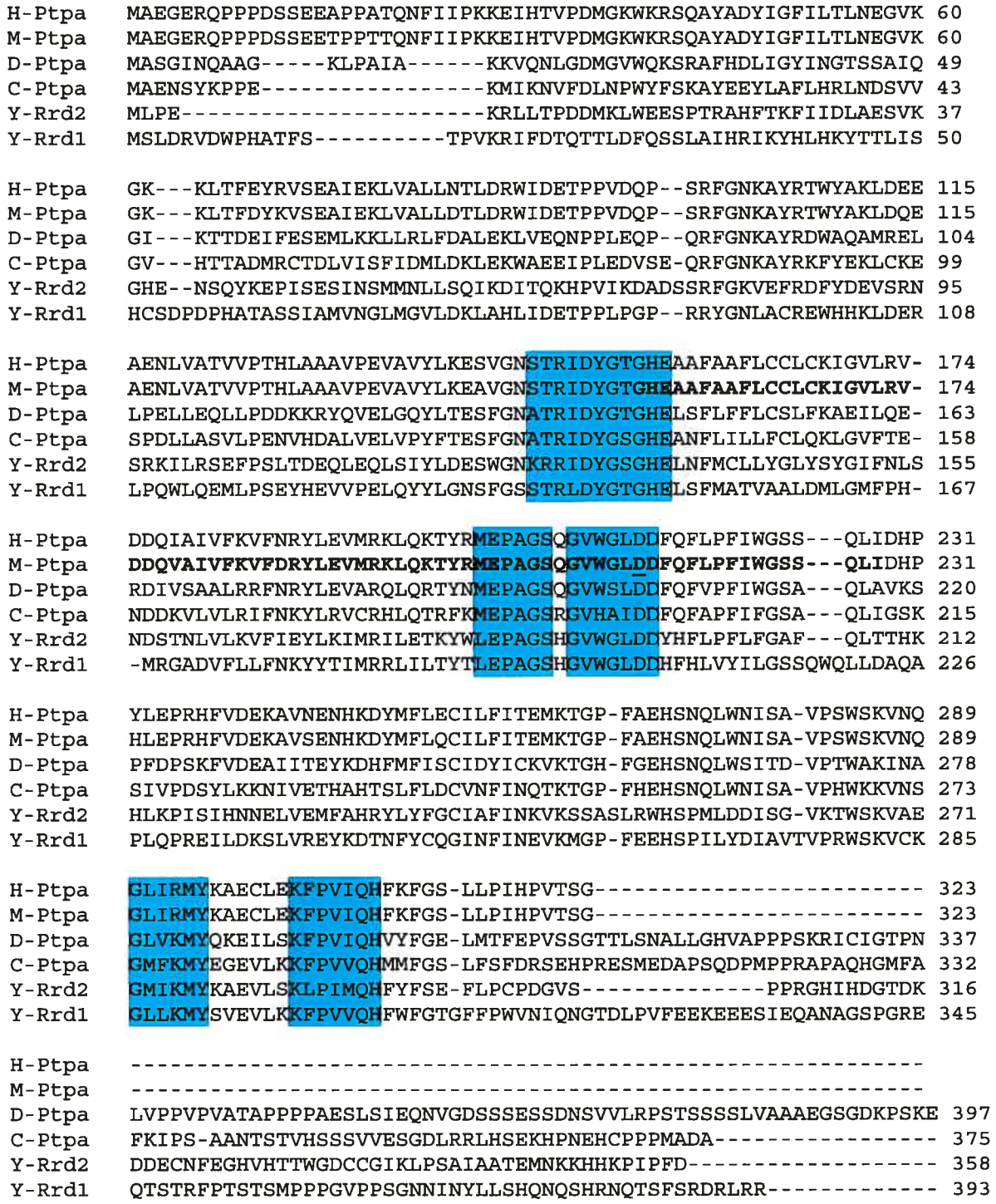


**Figure 2:** Ptpa is conserved in organisms. Human (H), mouse (M) *D. melanogaster* (D), *C. elegans* (C), both *S. cerevisiae* (Y) proteins. Highlighted sequences correspond to highly conserved regions. Amino acids in bold correspond to the targeted sequence (see section 4.1.5).

The ubiquity of Ptpa expression in mammalian tissues, the presence of the highly conserved regions and the apparent necessity of this protein for cell survival in yeast and mammalian cell lines indicate that Ptpa performs vital cellular functions.

### 1.2.3.5. Genetic Features of PTPA

The coding sequence for the human PTPA gene was found to be localized at chromosome 9q34, spanning 60 kb. The genomic sequence consists of 10 exons and 9 introns. The promoter region lacks the traditional TATA sequence for transcription initiation. However, it was observed that several features of housekeeping genes are present in the PTPA promoter sequence (Van Hoof *et al.*, 1995). For example, many housekeeping genes have a 200-1000 bp unmethylated, typically GC-rich, CpG island spanning the promoter region, frequently extending into the first exon (Bird, 1986). Accordingly, the PTPA promoter sequence has an average GC content of more than 70% and an unmethylated CpG island well into its first exon (from position -159 to +91) (Janssens *et al.*, 1999). Although the promoter sequence was found to have many putative binding sites for a variety of transcription factors (including Myc, NF-κB and Myb), only the Yin Yang 1 (YY1) transcription factor was found to bind PTPA's promoter sequence to initiate transcription (Janssens *et al.*, 1999). Interestingly, this transcription factor has been associated with cervical and breast cancer (Dong *et al.*, 1994; Nayak and Das 1999) as well as hepatocarcinogenesis (Parija and Das, 2003).

Finally, several alternative splicing products of Ptpa (transcripts β-η) were identified, of which only the β transcript was detected by western blotting (Janssens *et al.*, 2000). However, in vitro assays revealed that this product did not activate the tyrosyl phosphatase activity of PP2A. It was thus concluded that these products have limited biological function and are the result of splicing errors. The more recent data indicating that Ptpa activates the Ser/Thr phosphatase activities now casts doubt on this result; Ptpa β may well have a functional role in vivo.

### 1.2.3.6. PTPA's Role in Response to Oxidative Stress and in Pathways Related to Carcinogenesis

Douville *et al.* (2004) have recently confirmed that Rrd1 plays a role in the response to oxidative stress and have demonstrated that this function is dependent upon

Rrd1 interaction with Sit4, a yeast PP2A-like catalytic subunit. Indeed, yeast strains deficient for Rrd1, Sit4, or both exhibit equal sensitivity to 4-NQO, indicating that these proteins function in a common pathway. Further, these two proteins were found to physically interact with each other. Despite this progress, no clear mechanism of action can be assigned to Ptpa. Still, several lines of evidence support the notion that PTPA is involved in carcinogenesis.

The p53 tumour suppressor gene was found to be a target of Ptpa. This gene represses PTPA transcription by binding to its TATA-less minimal promoter, preventing the YY1 transcription factor from binding to the region (Janssens *et al.*, 2000). Indeed, p53 is known to repress the transcription of a number of genes by binding their TATA-less promoters (Kley *et al.*, 1992, Sandri *et al.*, 1996).

In addition, numerous studies have also associated Rrd1 to the cell cycle in yeast, although its precise role is still a subject of controversy. Dr. Goris' group have published data suggesting that Rrd1 functions in negative regulation through Start (Van Hoof *et al.*, 2000), excluding involvement in the G2/M transition (Van hoof *et al.*, 2000). Conversely, Mitchell and Sprague (2001) found that Rrd1 *does* function in the G2/M transition and that it may play a role in the *positive* regulation of G1. Thus, although it is unclear how and at what stage, PTPA appears to be involved in the progression of the cell cycle.

Another line of evidence linking PTPA to cancer is a proteomic analysis of a human hepatocellular carcinoma cell line HCC-M. The study revealed a number of proteins that were expressed at abnormal levels in these cells, including Ptpa (Ou *et al.*, 2001). Interestingly, this proteomic analysis also detected thioredoxin peroxidase (Seow *et al.*, 2000), an important enzyme in regulating the intracellular redox environment (Gasdaska *et al.*, 1995). Although preliminary, given the relationship of oxidative stress, DNA damage and chronic inflammation with the increased risk of liver cancer (Wang *et al*, 2002; Ichiba *et al*, 2003), the data is fully consistent with PTPA's putative function in the cellular response to oxidative stress.

In addition, the chromosomal location of the human PTPA gene on chromosome 9q34 may be a corroborating factor. This region contains genes associated with a number of diseases such as bladder cancer (Kimura *et al.* 2001), several types of leukemia

(Kaneko *et al.*, 1988; von Lindern *et al.* 1990; Huntly *et al.*, 2003), as well as amyotrophic lateral sclerosis (Chance *et al.*, 1998).

Together with the data on PP2A, the literature supports a role for PTPA in the cellular response to oxidative stress as well as the cellular processes associated with carcinogenesis.

**1.2.3.7. Phenotypes Associated with PTPA**

Given the broad spectrum of cellular processes in which PP2A is involved, it is not surprising that Ptpa, too, has many functions. Indeed, Ptpa is implicated in a number of pathways that appear unrelated to its role in maintaining DNA integrity in the response to oxidative stress. For example, yeast cells deficient in RRD1 or RRD2 display phenotypes similar to those observed in yeast strains deficient in PP2A subunits. Most notably, deletion of RRD1 causes defects in bud morphology formation that are similar to the ones obtained in strains with a deletion of two yeast PP2A catalytic subunits, PPH1 and PPH2. Yeast strains carrying a deletion of the RRD2 gene exhibit altered microtubule dynamics, resembling the phenotype obtained upon deletion of a PP2A regulatory B, CDC55 (Van Hoof *et* al, 2001). In addition, Rrd1 and Rrd2 also function in the HOG1 kinase pathway (Rempola *et al.*, 2000), which is essential for mediating cellular response to increased external osmolarity (Brewster *et al.*, 1993), again unrelated to the response to ROS.

Finally, Ptpa also functions in the TOR (Target of Rapamycin) pathway in *S. cerevisiae*. In yeast, this complex pathway is important for sensing nutrient availability before initiating cellular division. Thus, the proteins in this pathway regulate translation initiation, ribosome biosynthesis (Powers and Walter, 1999), transcription of numerous enzymes involved metabolic pathways (Schmelzle and Hall, 2000), and amino acid import (Beck *et al.*, 1999). Rapamycin mimics nutrient deficiency, causing yeast cells to arrest growth and to behave physiologically as if they were starved, via the TOR pathway. However, cells lacking RRD1 are resistant to the starvation mimetic affect of rapamycin (Rempola *et al.*, 2000). This suggests that the Ptpa protein may be central to the complex TOR pathway.

These cellular pathways are, apparently, unrelated to each other. However, the accumulation of unrelated findings concerning Ptpa's functions may eventually help shape an understanding of its broader function. For example, Ptpa's involvement in the TOR pathway may shed light on its function within the response to oxidative stress. Di Como and Arndt (1996) have demonstrated that Sit4, the PP2A catalytic subunit found to interact with Rrd1 to respond to oxidative stress, is also a target of a protein known to be implicated in the TOR pathway, Tap42. In addition, a number of studies have indicated that dysregulation of the Target of Rapamycin pathway generates "a favorable oncogenic environment" (Huang and Houghton, 2003). Therefore, although it is not clear how this network of complex interactions functions, later studies may demonstrate a convergence of the different PTPA-related pathways.

## 1.3. Manipulating the Mouse Genome to Study Gene Function and Disease

### 1.3.1 Genetically Modified Mice

Genetic manipulation of mammalian cells has proven to be a useful means of studying gene function. However, the refinement of molecular biology techniques has led to a growing trend of studying biological processes in laboratory animals. Most widespread is the manipulation of the mouse genome, which enables studies on genes and their impact on animal health relatively rapidly and at a low cost in comparison to research on other mammals. Two of the most common methods used are the targeted deletion and integration of specific genes into the mouse genome.

Creation of these mice consists of four essential steps: (i) the engineering of a DNA construct; (ii) the integration of the construct within the genome of embryonic stem (ES) cells or fertilized oocytes; (iii) the transfer of these cells to a pseudo-pregnant female who will then give birth to the genetically manipulated mice, and finally; (iv) the strategic pairing of offspring to produce a colony of genetically modified mice.

There are major differences between the production of knockout and transgenic mice. Typically, the former involves electroporating the DNA construct into mouse ES cells. The aim of this step is to replace endogenous DNA sequences with the construct

via homologous recombination (HR). Since this is a relatively rare event, ES cells must be carefully selected before being transferred into a pseudo-pregnant female. Conversely, creating transgenic mice requires the DNA construct to be microinjected directly into a fertilized oocyte. There is no need to grow cells in vitro for selection since the integration of the construct DNA does not need to occur at a specific locus (Cheah and Behringer, 2001; Richa, 2001).

Despite these progresses, there is an ever-growing need to develop techniques that will enable a higher degree of "tailoring" of the mouse genome. A number of technologies have recently been developed, refining classical manipulation methods by combining them with strategies that allow for greater versatility, such as conditional targeted deletions and the use of the Green Fluorescent Protein (GFP).

### 1.3.2 Conditional Knockout Mice

At the molecular level, the strategy used for gene targeting essentially consists of modifying a specific portion of this gene, thought to be important for the proper functioning of the resulting protein, via homologous recombination (HR). A crucial step is the design of the targeting vector. The DNA construct must be designed to contain two regions of high homology to the targeted gene for HR. These flank a sequence that would disrupt the function of the translated protein. For example, one common approach is to replace an important exon of the targeted gene with a marker for antibiotic resistance. Upon electroporation of embryonic stem cells and homologous recombination, the ES cells will carry an antibiotic resistance gene *in lieu* of this exon (Figure 3), and will translate truncated, non-functional protein of the targeted gene.

The traditional strategy for targeted deletions has one major disadvantage: the entire organism is defective for the specific gene throughout its development and in all tissues. It may be difficult to design and perform precise experiments on animals in which the gene disruption is ubiquitous. Worse, the targeted deletion could lead to embryonic lethality, making it impossible to study gene function during the postnatal period.

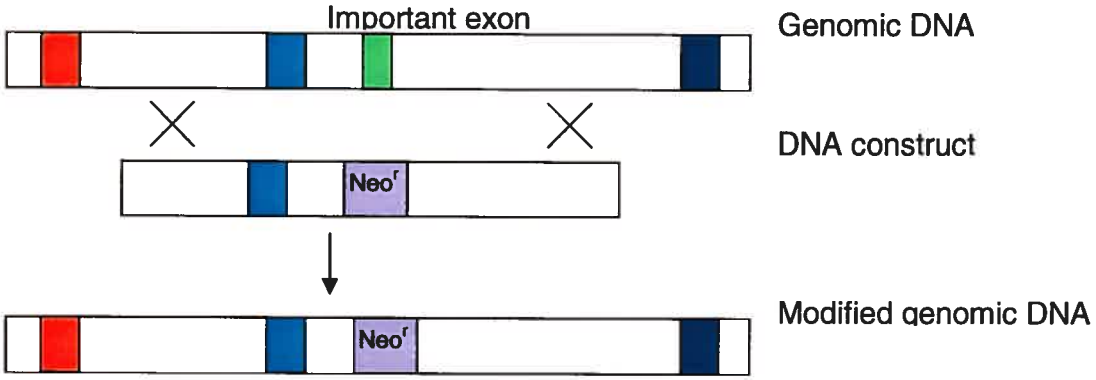


**Figure 3:** Homologous recombination between the targeting vector and the endogenous gene. A portion of the gene is disturbed by the integration of the modified DNA construct.

A method of circumventing these challenges is the creation of conditional knockout mice, designed to carry the gene deletion in a subset of tissues and/or at a moment in their lifespan chosen by the experimenter. Thus, temporal and spatial conditional knockouts allow the knockout event to occur post-partum, preventing the problem of embryonic lethality, and/or in specific tissues, enabling a more focused experimental design. Commonly used tools for developing such conditional knockouts are the Cre/loxP and Flp/frt systems. The Cre/loxP system is based on a recombination that occurs in bacteriophage P1 (Austin *et al.*, 1981). The Cre recombinase of this bacteriophage recognizes and mediates recombination between two specific, 34 base-long loxP sequences (Figure 4). In knockout studies, the targeting vector is engineered with loxP sites flanking the sequences of the mouse genome that are to be deleted. In contrast to traditional targeted deletions, the purpose of the homologous recombination between the DNA construct and the genomic DNA in ES cells is not to delete or disrupt sequences in all tissues, but rather, to incorporate the loxP, which will then facilitate the removal of genomic sequences at a later time and/or in specific cell types. The loxP sequences are engineered within the intron sequence so that these genomic modifications have little chance of altering the expression or activity of the resulting protein. These loxP-mice are subsequently crossed with mice expressing the Cre recombinase, under either an induci-

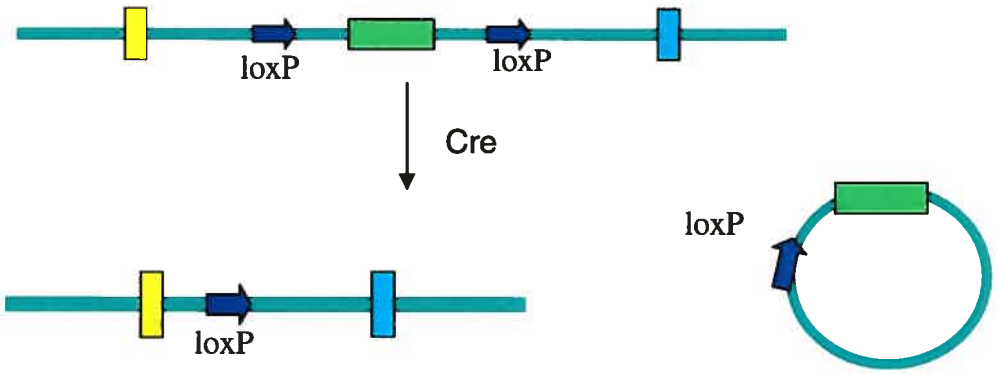


**Figure 4:** The Cre recombinase mediates recombination between loxP sites. This effectively deletes the loxP-flanked sequences.

ble or a tissue-specific promoter (or both), resulting in mice carrying the loxP sites as well as the Cre recombinase. The offspring of this cross are wild-type with regards to the targeted gene; only when and where the recombinase is expressed does the recombination between the loxP sites finally occur, deleting the sequence flanked by loxP sites (Orban *et al.*, 1992). Thus, if the Cre recombinase is under the control of an inducible promoter, the knockout event occurs only upon recombinase induction; if the promoter is tissue-specific but not temporally controlled, only this tissue type will become deficient for the targeted gene throughout development. Tissues that are not induced to express the recombinase will express wild-type, full-length protein.

The Flp/frt system is based on *S. cerevisiae* (Broach and Hicks, 1980) and functions in a manner that is analogous to the Cre/loxP system, the Flp recombinase mediating the recombination between two 48 bp-long frt sites. The Flp/Frt approach is rather efficient and used relatively frequently in cells lines. Although it is less commonly used for generating conditional knockout mice because of certain technical restrictions, these constraints are being gradually overcome (Rodriguez *et al.* 2000), making this a more appealing system.

### 1.3.3 The Use of Green Fluorescent Protein Variants in Mice

The use of the Green Fluorescent Protein (GFP), derived from the jellyfish *Aequorea victoria*, has helped create transgenic mice that are more versatile. The main chemical and physical properties of the GFP were detailed in the late 1970s (Prendergast *et al.*, 1978) but it was not for several years that it was used a tool for biological study in other organisms, such as *C. elegans* (Chalfie *et al.*, 1994), *D. melanogaster* (Wang *et al.*, 1994) and the zebrafish (Amsterdam *et al.*, 1995). Ikawa *et al.* (1995) produced the first transgenic mouse lines, having integrated the GFP gene in their genome and expressing fluorescence in a variety of tissues.

The original GFPs' relatively low emission and excitation spectra allow for fluorescence observation upon exposure to a standard handheld UV lamp. In the last decade, many variants of this protein have been developed, each with slightly different characteristics. These GFPs can have several applications in mammals. They can be expressed as tags on either the C or N terminals of proteins, and used as non-invasive reporters of gene expression. In addition, the intensity of fluorescence can be used for typing of transgenics (homozygote vs. hemizygote), and as a means for screening for transgenic offspring at birth (Hadjantonakis and Nagy, 2001).

The applications are not limited to fluorescence visualization at the macroscopic level. Indeed, GFPs can be visualized at every stage of animal development. Embryonic and primary cells obtained from tissues expressing fluorescence could be cultured and the fluorescence viewed microscopically to determine intracellular protein localization, or used in FACS analyses.

Thus, the transgenic approach, when coupled with GFP technologies, can be an extremely practical and powerful tool for genetic studies.

### 1.3.4. Genetically Engineering the Mouse Genome to Study Genes Involved in the Response to Oxidative Stress

Mouse studies have been useful in shaping our understanding of the biological functions of specific genes involved in the response to oxidative stress. For instance, a mouse model for familial amyotrophic lateral sclerosis (ALS) in which mice bear mutations on the SOD1 gene was developed. These animals were found to exhibit

enhanced oxyradical production and lipid peroxidation, as well as several other typical features of oxidative stress (Kruman *et al.*, 1999). Another report shows that SOD2-deficient mice have increased levels of DNA damage and incidences of cancer (Van Remmen *et al.*, 2003). Kim *et al.* (2004) demonstrated that transgenic mice that overexpress the Sod1 protein have increased resistance to oxidative stress induced by kainic acid. These examples highlight how manipulating specific genes provides insight into the genetics and biology of disease at the level of the entire organism.

Unfortunately, this direct link between gene and health is much less evident in studies examining genes involved in the Base Excision Repair pathway. For instance, Ogg1 is a DNA glycosylase, which removes the oxidative lesion 8-oxoG in the early steps of this repair pathway. It was hypothesized that mice lacking this important glycosylase would accumulate damaged bases and mutations, and therefore, be at a significantly higher risk for free-radical-induced pathology. Surprisingly, $OGG1^{-/-}$ mice exhibited an increase in lesion frequency, but showed no noticeable health problems (Klungland *et al.*, 1999, Minowa *et al.*, 2000). Indeed, the phenotype of hypermutability, with no accompanying increase in disease, was observed in other mouse studies involving targeted knockouts of other DNA glycosylases such as alkyladenine glyocosylase (Bevin *et al.*, 1997) and Nth1 (Cunningham *et al.*, 2002). Similarly, mice deficient for the DNA polymerase β, the polymerase responsible for filling the gap left by the endonuclease upon excision of the damaged base, exhibit an accumulation of DNA damage while lacking any noticeable increase in pathological conditions (Cabelof *et al.*, 2002). Thus, it appears that BER proteins have considerably redundant functions.

Further, other repair mechanisms are also involved in attenuating the effects of a deficiency in BER genes. For example, the Cockayne syndrome B (CSB) protein is typically associated with both transcription-coupled (TCNER) (Le Page *et al.*, 2000) and global (GNER) Nucleotide Excision Repair pathways (Sunesen *et al.*, 2002). However, $OGG1^{-/-}/CSB^{-/-}$ mice accumulate more premutagenic 8-oxoG lesions than either $OGG1^{-/-}$ or $CSB^{-/-}$ mice (Osterod *et al.*, 2002), indicating that CSB protein functions in repairing oxidative lesions, albeit to a lesser extent in comparison to OGG1.

Interestingly, although genetic studies in mice have not been successful in establishing a direct correlation between gene and pathology, epidemiological studies in

humans suggest that disruption of the BER pathway may increase susceptibility to disease. For example, one noteworthy study indicates that individuals who have low levels of Ogg1 are at increased risk to lung cancer (Paz-Elizur *et al.* 20003).

In sum, the relationship between the repair of oxidative DNA damage and health is complex. As more animal studies are performed, the relative role played by individual genes, and how these genes act in concert to prevent, cause or increase susceptibility to diseases, can be better assessed.

## 1.4. Rationale

Although vital, oxygen molecules pose a permanent threat to aerobic cells. When metabolized into free radicals, these can cause significant damage to essential cellular components, including DNA. Generated as by-products of natural biological processes and as the result of exposure to various exogenous agents, including the UVA component of solar irradiation, exposure to reactive oxygen species is continuous and unavoidable. Cells have consequently developed complex prevention mechanisms and DNA repair networks to cope with this paradoxical situation. However, if these mechanisms fail, organisms are at increased risk to oxidative damage and mutagenesis. Indeed, a number of conditions and diseases are associated with oxidative stress.

The RRD1/PTPA gene was found to play an important role in the cellular response to oxidative stress in yeast. Although it appears to have several distinct functions, several lines of evidence corroborate Ptpa's putative role in mediating the response to oxidative DNA damage. Further, several features of the PTPA gene suggest it is involved in pathways related to carcinogenesis. Our laboratories aspired to elucidate this gene's precise function in the cellular response to oxidative stress and to determine how altering it may affect mammalian health. Genetically manipulated mice are powerful tools to illuminate the function of specific genes and their contribution to overall health. Therefore, we sought to generate two types of genetically manipulated mice to study PTPA: conditional knockout mice, in which this gene could be temporally or spatially disrupted, and transgenic mice that would, express Ptpa fused to a GFP in addition to the endogenous levels of Ptpa protein.

# 2. Materials and methods

## 2.1. Cloning Techniques

### 2.1.1. Preparation of Competent Cells for Cloning

To prepare competent *E. coli* DH5-α cells, a small amount of bacteria was scraped from the frozen stock and allowed to grow in 5mL LB medium with 6mM $MgSO_4$ at 37°C for approximately 18 hours. The 5mL of culture was subsequently added to 200 mL of LB containing 6mM $MgSO_4$. This larger culture was again incubated at 37°C until the optical density was established to be between 480 nm and 550 nm. When this density was reached, the bacteria was allowed to cool on ice for 5 minutes, after which they were placed in 50mL falcon tubes and centrifuged at low speed (4000 rpm) at 4°C for 20 minutes. Resulting bacterial pellets were obtained and re-suspended in 20mL of TFB I, incubated on ice for 10 minutes, and centrifuged again at low speed (4000 rpm) at 4°C for 10 minutes. The bacterial pellet was re-suspended in 2mL cold TFB II, aliquoted in sterile eppendorf tubes (200 μL/tube) and stored at -80°C. One tube of prepared competent *E. coli* was used for one transformation.

### 2.1.2 Transformation of Competent Cells with Plasmid DNA

An aliquot of competent bacteria was placed on ice for five minutes. Ligated DNA fragments or a circularized plasmid were added to the bacteria and left on ice for an additional 30 minutes. The bacteria were then incubated at 42°C for 90 seconds, after which 1mL of LB was added. The cells were allowed to recover from the heat shock and to begin expressing the antibiotic resistance gene for one hour at 37°C , after which they were plated on LB agar plates containing 0.1 mg/ml of ampicillin and or 0.5 mg/ml kanamycin (depending on the plasmid) and incubated for 16 - 24 hours at 37°C.

### 2.1.3. Mini-and Maxi-Preparation Methods for Plasmid Purification

Bacterial colonies were picked and inoculated in 3mL of LB medium for 16 - 24 hours at 37°C. Small scale plasmid purification (1.5mL bacterial culture) was performed as described by Birnboim and Doly (1979). Larger scale purifications (50 - 500mL of

bacterial culture) were performed using the same ratio of solutions. Protein contaminants were eliminated by standard phenol/chloroform extractions.

### 2.1.4. Restriction Digestions and DNA Modification for Cloning

After the plasmid purification, the DNA was digested with restriction enzymes that would enable us to determine if the desired construct was indeed obtained. Usually, for plasmid verification, approximately 250 - 500ng were digested with the appropriate restriction enzymes for 1 - 4 hours with 5 units of the appropriate enzyme and buffer dilution in a total volume ranging from 15 to 20μL, and then placed at the appropriate temperature (usually 37°C). Larger scale restriction digestions were performed when the DNA was to be used for cloning purposes; up to 10μg of DNA was used, with 20 units of enzyme and the appropriate buffer dilution in a total reaction volume ranging from 20 to 40μL.

When a vector plasmid was linearized with compatible ends, digested DNA was treated with 5 units of Calf Intestinal Alkaline Phosphatase (CIAP) (Promega) for 45 minutes. The CIAP supplied by Promega is sufficiently versatile to work in virtually all restriction digestion buffers, and was therefore added directly to the restriction digestion reaction.

Although restriction digestion was routinely used as a method of confirming that the appropriate clone was obtained, the integrity of loxP sites, s as well as certain clones were confirmed by automated sequencing using the Research Center's ABI PRISM 3100 Genetic Analyzer (Applied Biosystems), following the manufacturer's protocols and procedures.

### 2.1.5. Polymerase Chain Reaction to Generated Clonable Fragments

The Polymerase Chain Reaction (PCR) was used to amplify fragments, thereby enabling the engineering of convenient restriction sites for cloning. Typically, the program consisted of 30 cycles, each consisting of a denaturing step (95°C for 1 minute), an annealing step (52°C for 1 minute), an elongation step (72°C for 2 minutes/kb to be amplified), and a final long elongation step (72°C for 10 minutes). PCR reactions were performed in appropriate reaction buffer dilution (buffer supplied with the enzyme) with

3mM $MgSO_4$, 1μg of each oligonucleotide, 0.5mM of each dNTP, 25 - 100ng of template DNA with 1 - 3 units of Pfu polymerase in a total volume of 100μL. The Pfu was used because it possesses a proofreading activity, decreasing the chance of errors taking place during the amplification process.

### 2.1.6. Fragment Purification for Cloning

Fragments obtained by restriction digestion were resolved and observed on ethidium bromide-stained 1% agarose gels. The specific fragments to be used for cloning were physically removed from the gel using a blade, and purified using Amersham GFX-Gel Purification Kit.

### 2.1.7. Ligation Reactions for Cloning of DNA Fragments

Relative concentrations of purified DNA fragment were estimated visually on an agarose gel. To maximize cloning efficiency, three ligations were usually performed, each with varying vector:insert ratios ranging from molar ratios of 1:2 to 1:10. Ligations were performed in volumes ranging from 10μL to 15μL, using 10 units of Promega or New England Biolabs ligase and the appropriate buffer dilution. The duration and temperature of incubation varied from 1 hour ligation reactions at room temperature, to 16 - 24 hour ligation reactions at 16°C.

### 2.1.8. General Cloning Strategies

Three strategies were used for the creation of the various constructs. The first was the standard plasmid digestion and fragment purification followed by ligation and transformation in competent bacteria. The second strategy involved amplifying fragments of DNA using specially designed primers to engineer restriction sites for cloning and/or other short sequence within the amplified product. After the PCR reaction, the amplified DNA could simply be restriction-digested, purified and ligated as in the first strategy. The third strategy differs from the others in various respects: no phosphatase treatment was performed on linearized plasmids, and fragments were not purified from agarose gels. Instead, this type of cloning was performed on large fragments that could not easily be resolved from undigested, supercoiled plasmid on

agarose gel or when only one restriction site was available for cloning in the DNA sequences to be ligated. Thus, plasmids were restriction-digested with a single enzyme, ethanol-precipitated and ligated directly. This method could only be performed when the plasmids carried different resistance genes (ampicillin and kanamycin). Therefore, only constructs containing both plasmids could grow in media containing both antibiotics. The enrichment of positive clones by double selection compensated for the increased chance of obtaining undigested or religated plasmids due to the fact the DNA was not gel purified or treated by CIAP.

## 2.2. Generating Transgenic Mice

### 2.2.1. Micorinjection of the Oocyte and Breeding Procedures

The DNA construct microinjected into mouse oocytes was prepared by other members of the laboratory and subsequently implanted in pseudo-pregnant females. The microinjection of the linearized DNA construct into fertilized mouse oocytes and the transfer to pseudo-pregnant females was performed by the Animal Facility of the Recherche Guy-Bernier Research Centre according to the protocols approved by the Centre's Committee for Animal Protection. The pseudo-pregnant females carried these fertilized oocytes to term. Pups were born three weeks after the microinjection and thereafter weaned and crossed with fertile mice CD-1 males or females. The pups resulting from this second cross were weaned and screened for transgene integration at the age of 3 weeks or older. When a mouse was established as transgenic, it was crossed with a transgenic sibling, when possible, or with a CD-1 mouse. Thus, independent families of transgenic mouse lines were generated. Mice were routinely weaned at the age of three weeks. All matings and screening procedures were performed when mice were at least three weeks of age.

### 2.2.2 Screening for Transgenic Mice

#### 2.2.2.1. Extraction of Mouse Tail Genomic DNA

Southern blotting is the method of choice for reliable detection of transgene integration. Screenings were performed on DNA purified from mouse tail clippings.

Approximately 1 cm of tail was cut from the mice, digested in Tail Mix for 4 - 16 hours and purified by gentle mixing, first with phenol and then with chloroform, for a period of five minutes. This mixture was centrifuged at 12,000 X g for 5 minutes, after which the supernatant containing the DNA was transferred to an eppendorf tube containing 1mL of 100% ethanol, incubated at -80°C for 10 minutes and centrifuged at 12,000 X g for 10 minutes. Following the ethanol-precipitation, DNA was washed with 70% ethanol and resuspended in water containing approximately 20 ng/mL of RNAse A. The concentration of the DNA was obtained using the spectrometer.

**2.2.2.2. Restriction-Digestion and Treatment of Genomic DNA for Southern Blotting**

Approximately 15μg of genomic DNA were restriction-digested with 50 units of BamHI for 6 - 16 hours. The digested DNA was run on a 1% agarose gel until the DNA was sufficiently resolved as visualized by ethidium bromide staining and exposition to UV light. The agarose gel was placed in a depurination buffer for ten minutes, after which the agarose gel was soaked twice for 30 minutes, first with denaturing and then with neutralizing solutions.

**2.2.2.3. Transfer of DNA to the Nitrocellulose Membrane**

A reservoir containing 20 X SSC was prepared, in which two agarose gel-sized Whatman filters and one gel-sized Hybond $N^+$ nitrocellulose membrane (Amersham) were soaked. An elevated surface was placed within the reservoir, upon which lied a large strip of Whatman paper, extending on two parallel ends into the SSC buffer. The treated agarose gel was place upside down on this elevated Whatman paper. The pre-wetted nitocellulose membrane and the two Whatman filters were place on the membrane and air bubbles were removed. The sides of the agarose gel were sealed and the reservoir covered with saran wrap. Approximately three inches of paper towel were placed on top of the filters, upon which was placed a weight of approximately 500g.

The DNA transfer onto the nitrocellulose membrane was allowed to take place overnight. The DNA was fixed to the membrane by exposing the membrane to UV for one minute.

### 2.2.2.4. Preparation of the Radioactive Probe

The vector used for microinjection in the mouse blastocyst, cPTPA-EYFP, was restriction-digested with NotI and BamHI. This digestion yields two fragments; including the 1.5kb fragment corresponding to the PTPA and EYFP sequences. This fragment was purified from the gel as described in section 2.1.6. Approximately 50ng of the purified fragment were denatured at 95°C for 3 minutes, placed on ice for 2 minutes and labelled with radioactive dCTP using Ready-To-Go DNA Labelling Beads (-dCTP) (Amersham). Briefly, the kit supplies a pre-dispensed reaction mix in bead form. The bead containing a Klenow fragment is activated upon the addition of the radioactive dCTP and the denatured DNA. After the 15 minute labelling reaction, the Klenow fragment was inactivated by adding 2μL of 0.5 M EDTA, as recommended by the manufacture. The unincorporated radioactive dCTP was removed using ProbeQuant G-50 micro columns (Amersham) following the supplier's protocol.

#### 2.2.2.5. Hybridization of Radioactive Probe to DNA on Nitrocellulose Membrane

The membrane was transferred to a hybridization bottle. Approximately 10mL of ULTRAhyb Ultrasensitive Hybridization Buffer (Ambion) were added to the bottle for a two hofur pre-hybridization treatment. The radioactive probe was denatured at 95°C for 3 minutes, placed on ice for 2 minutes and added to the bottle containing the membrane and ULTRAhyb buffer. The probe was allowed to hybridize with the genomic DNA overnight at 42°C, as recommended by the UltraHyb manufacturer.

#### 2.2.2.6. Membrane Washes and Exposition

After the completion of the hybridization step, the membrane was quickly washed with wash solution I. To remove non-specific hybridization, additional 20-minute washes were performed; three with wash solution II, and three with wash solution III. All washes were carried out at 65°C. Membranes were exposed with a film at -80°C using two intensifying screens for a minimum of 36 hours. More stringent washes or longer expositions were performed depending on the intensity of the signal and on the level of background.

## 2.2.3. Dissections and Preservation of Individual Organs for Protein Extractions

In order to verify if the transgene was expressed, animals were sacrificed and different tissues stored for protein analysis. Mice were sacrificed by the Animal Facility staff. Dissections were performed and individual organs were immediately frozen in liquid nitrogen. After this initial freeze, they were placed in screw cap tubes, which were kept immersed in the liquid nitrogen. The kidneys, liver, heart, lungs, spleen, pancreas, intestine and skin tissue were obtained and stored at -80°C. For protein extractions, approximately 100ng of tissue and 100µL of Protein Extraction Buffer were placed in a Potter–Elvehjem glass homogenizer on ice. The tissue was crushed on ice until there were no discernable pieces of the organ left. The resulting mixture was then transferred to a sterile eppendorf tube and was centrifuged at 10,000 X g for 10 minutes at 16°C. The supernatant was removed and the concentration was estimated using the Bradford assay (Bradford, 1976). Protein extracts were always maintained on ice.

## 2.2.4. Western blotting

### 2.2.4.1. Protein SDS-PAGE Electrophoresis

Tissue proteins were resolved on 10% SDS-Page gel. The resolving portion of the gel was poured into the mould and the upper layer levelled by quickly covering it with ethanol. The gel was allowed to polymerize for at least 20 minutes. During this time, the stacking gel was prepared. Once the resolving portion of the gel was polymerized, the ethanol was replaced with stacking gel and the comb adjusted to the apparatus. Upon polymerization, the entire gel was placed in the electrophoresis cast and 1L of 1X migration buffer was added. Approximately 50µg of protein were loaded per well of the SDS-PAGE for a period of 90 minutes at 120V.

### 2.2.4.2. Transfer of Proteins to the Nitrocellulose Membrane

Before proceeding with the transfer, the gel, a Hybond ECL membrane and four 3MM Whatman filters cut to match the size of the gel were soaked in transfer buffer for 15 minutes. The transfer was set up by placing the membrane facing immediately the gel. Two Whatman papers were placed facing the other side of the membrane and gel. The

stack of gel and membrane sandwiched by Whatman filters was placed in the transfer apparatus, to which 1L of transfer buffer was added. The apparatus was transferred to a cold room and was placed in an ice reservoir to prevent overheating. The transfer was typically performed for 1 hour at 100V. Protein transfer was confirmed by colouring the membrane with Ponceau S.

#### 2.2.4.3. Membrane Blocking, Blotting and Exposure

The membrane was saturated for 30 minutes at 37°C (or overnight at 4°C) in TBST with 5% skim milk. The membrane was then washed twice with TBST for a period of 5 minutes. The primary antibody was prepared by adding antibody to 2% milk in TBST (1/1000 dilution for PTPA-specific antibody, a gift from Dr. Egon Ogris, or 1/5000 for Clontech's GFP-specific antibody). The membrane was incubated with the PTPA antibody at 4°C overnight or with the GFP antibody at room temperature for 1 hour. This incubation period was followed by two additional 5 minute TBST washes. Subsequently, the membrane was incubated with the secondary antibody (mouse anti-IgG with peroxydase for the GFP antibody, and rabbit anti-IgG with peroxydase for the PTPA antibody), diluted 1/1000 in 2% milk dissolved in TBST for 1 hour. This was followed by four additional 5 minute TBST washes.

During the last wash, equal volumes of the detection solutions 1 and 2 of the Amersham ECL kit were mixed together. The total volume of ECL mix was of 0,125 $mL/cm^2$ of membrane. After the final wash, the membrane was sponged dry, covered with the ECL mix and incubated at room temperature for 1 minute. Excess liquid was removed from the membrane with a Whatman filter. The membrane was then enveloped in Saran wrap, placed in a cassette and exposed to a film for various times ranging from one second to 2 minutes before exposure.

### 2.2.5. Macroscopic EYFP Detection

Many systems allow for the macroscopic visualization of EYFP in mice. Indeed, certain companies can provide equipment that is sufficiently sensitive to detect fluorescence through the mouse skin. Therefore, dissections need not be performed to visualize fluorescence of mouse inner organs.

These GFP visualization devices essentially consist of a bright light equipped with two filters: one that limits the wavelengths that will reach the fluorescent animal (the excitation filter), and one that limits the wavelengths that are viewed by the experimenter (the emission filter). However, most of these systems are rather costly and require many accessories. Our laboratories employed a more cost effective system that allows for macroscopic assessment for fluorescence in live and recently sacrificed mice, namely the Clare Chemical Dark Reader Spot Lamp. This lamp is equipped with an excitation filter that allows wavelengths between 400nm and 520nm. In addition, viewing goggles consisting of emission filters that allow only wavelengths over 540nm to pass through were also used. This combination of excitation and emission wavelengths is appropriate for viewing of EYFP (EYFP Ex Max = 513nm; Em Max = 517nm). However, the major setback of this system is that it does not come equipped with cameras or with filters that can be adjusted to standard photographic equipment. In addition, the light source is not sufficiently strong to detect fluorescence through mouse skin. As such, GFP detection of inner organs can only be performed if dissections are carried out and individual organs are exposed to the filtered light and observed with the viewing goggles. This is especially disadvantageous when fluorescence is being used as a method to screen animals, because to identify transgenic mice, the mice must be sacrificed and are therefore *de facto* excluded from further study. Still, although the Spot cannot detect fluorescence on inner organs, EYFP should be observable on hairless tissue such as ears and feet or on hairless pups less than ten days of age.

## 2.6. Media, Buffers, Antibiotics and Solutions

### 2.6.1. Media

LB (Luria Bertani) medium

Bacto tryptone, 10g; bacto yeast extract, 5g; NaCl, 10g; dissolved in 1L distilled water.

LB agar solid medium

Bacto tryptone, 10g; bacto yeast extract, 5g; NaCl, 10g; agar, 6g; dissolved in 1L distilled water.

## 2.6.2. Antibiotics

Ampicillin, 1 g; dissolved in 10 mL distilled water, sterilized by filtration.

Kanamycin, 0.5 g; dissolved in 10 mL distilled water, sterilized by filtration.

## 2.6.3. Oligonucleotides Used as Primers for PCR Reactions

The primers were sometimes designed to engineer new restriction sites (underlined), or other sequences, such as loxP (in italics). When possible, the primer was almost entirely complementary to the template sequence, modifying as few bases as possible to maximize amplification efficiency. Otherwise, the entire restriction sequence was added to the extremity of the primer.

| Oligonucleotide | Sequence | Composition | Application |
|---|---|---|---|
| F1-mPTPA-UP | GCTTGATATCGAATTCGG ATCCTTTTCTTT | Template sequence | Cloning loxP site in pCS1 |
| R1-mPTPA-BglII-LoxP | CCATGCTagatct*ATAACTTC GTATAATGTATGCTTACGA AGTTAT*AGTAACAAATGAG TCCTTGCC | BglII, loxp, template sequences | Cloning loxP site in pCS1 |
| F4-PGKNeo-EcorI-NheI | GCTAGCGAATTCGCTAGC GGTGGCGGCCGAAGTTC CTATTCT | EcoRI, NheI, template sequences | Cloning PGKNeo in pCS2 plasmid |
| R4-PGKNeo-XhoI-RI-NheI | GCTAGCCTCGAGGCTAGC ATAACTTCGTATAATGTAT GCTAT | NheI, XhoI, template sequence | Cloning PGKNeo in pCS2 plasmid |
| T3 Primer | TTAATTGGGAGTGATTTCC C | pSK sequence | Sequencing pCS1 |
| T7 primer | GTAATACGACTCACTATA GGGC | pSK sequence | Sequencing |

**Table 1.** Oligonucleotide primers used for PCR amplification of fragments for cloning or for verifying orientation of ligated fragments. F – sense primer; R – antisens primer.

## 2.6.4. Buffers

50 X TAE

Tris base, 242g; Glacial Acetic Acid, 57.1mL; EDTA, 18.6g; distilled $H_2O$ water, completed to 1L.

Resolving gel buffer

Tris Base: 18.17 g ; SDS 0.4 g ; completed with distilled water to 100 mL; pH adjusted to 8.8 with HCl

Stacking gel buffer

Tris Base, 6.06g; SDS, 0.4g ; completed with distilled water to 100mL; pH adjusted to 6.8 with HCl.

5X Migration Buffer for SDS-PAGE

Tris-base, 15.1g; Glycine, 94g; SDS 20% 25mL; distilled water, completed to 1L.

Transfer buffer for Western Blot

Tris-base, 9.1g ; glycine, 43.2g; methanol 100% 600mL; SDS 20% 7.5 mL; distilled water, completed to 3L.

Tail Mix

10mM Tris, pH= 8.0; 5mM EDTA; 1% SDS; 0.3M NaOAc ;200 µg/ml Proteinase K.

Protein Extraction Buffer

25mM Hepes (pH=7.4); 150 mM NaCl; 1mMATP; 3mMMg$Cl_2$; 0.2mM phenylmethylsulfonyl fluoride; 1 g/ml aprotinin; 10 g/ml leupeptine; 10 g/ml pepstatine.

## 2.6.5. Solutions

Agarose

5g dissolved in 500mL TAE 50X.

TFB I

30mM KOAc; 10mM Cacl2·2H2O; 50mM MnCl2·4H2O; 100mM KCl, 15% (v/v) glycerol-water.

TFB II

10mM MOPS; 75mM CaCl2·2H2O; 10mM KCl, 15 % v/v glycerol-water.

Mini-prepare solutions

Solution I : 50mM glucose; 25mM-Tris-HCl; 10mM EDTA; pH adjusted to 8.0 with HCl.

Solution II : 0.2M NaOH, 1% SDS.

Solution III : 3M KoAC ; 2 M $CH_3COOH$ glacial.

Depurination solution

HCl, 21.4mL;completed with distilled water to 1L.

Denaturing solution

NaCl, 175.32g; NaOH: 40g; completed with distilled water to 2L.

Neutralizing solution

Tris-HCl, 121.14g ; NaCl, 175.32g ; completed with distilled water to 2L; pH adjusted to 7.0.

20X SSC Solution

NaCl, 175.3g; Sodium citrate, 882g, completed with distilled water to 1L; pH adjusted to 7.0.

Wash solutions I, II, III

2X SSC, 0.1% SDS; 1X SSC, 0.1% SDS; 0.1X SSC, 0.1% SDS, respectively.

10 % Resolving Gel for SDS-PAGE

Acrylamide (29:1), 3.35mL; resolving gel buffer, 2.5mL; ammonium persulfate 10% 100μL; distilled water, completed to 10mL; TEMED, 10 μL.

Stacking Buffer 5 %

Acrylamide (29:1), 1.4mL; stacking gel buffer, 1.3mL; ammonium persulfate 10% 100μL; distilled water, completed to 10mL; TEMED, 10μL.

TBST

Tris-HCl, 1M, pH 8.0: 20mL; NaCl 5M, 30 mL; Tween 20%, 5mL; completed with distilled water to 1L.

# 3. Results

## 3.1. Cloning of PTPA-Neo-loxP

### 3.1.1. General Cloning Considerations

The design and cloning of the targeting vector is complex and involves several plasmids. Generally, our strategy involved creating three independent vectors: pCS7, pCS8 and pCS9. Fragments from these plasmids could be cloned to obtain the final vector, pCS10, in the future.

Briefly, the mouse PTPA gene is composed of 10 exons. Our laboratories have previously isolated exons 5 - 10, which span approximately 10 kb. DNA of this length can be difficult to manipulate in cloning applications. Therefore, the first constructs were designed to isolate a smaller, more workable PTPA fragment. We constructed plasmids pCS and pCS1 to isolate 4.7 kb of the 5' end of the 5 - 10 exon portion of the gene. We then integrated the first loxP site in pCS1, 5' of exon 6 (pCS2), and subsequently, an frt-PGKNeo-frt-loxP cassette (for positive selection), 3' of exon 7 (pCS4).

Two other plasmids were prepared parallel with these cloning steps. The aim of constructing pCS7 was to modify a PGKPuro cassette (for negative selection) for future cloning into pCS4. pCS9 was designed to allow us to subclone a portion of the PTPA gene that could later be inserted into this pCS7 plasmid. Thus, this step would lengthen the sequence of the 3' end of the PTPA gene, forming the final clone, pCS10. Upon linearization with XhoI, this construct could be used for gene targeting in ES cells. This final clone has not yet been completed.

The cloning strategy involves ten different vectors. A schematic representation of each procedure is included to help conceptualize the cloning design. In these illustrations only selected restriction sites are shown, and can be used as landmarks. The position of the restriction sites is included as an additional reference point and for restriction digestion analysis. The portion of a given plasmid that was sub-cloned is outlined with a black line within its parent plasmid. When cloning was performed using an amplified

DNA fragment, the template plasmid as well as the amplified product are illustrated. Every individual plasmid is drawn to scale with respect to its various regions and components. However, due to the variable sizes of plasmids, ranging from 3 - 18 kb, these were not illustrated to scale with respect to each other.

Most clones were identified by performing restriction digestions of candidate plasmids isolated from bacterial colonies. Extensive restriction analysis was generally carried out to confirm the authenticity of a clone. For simplicity, only a subset of this analysis appears in the figures presented here. The restriction digestions presented in the figures were selected because they clearly demonstrate that a correct clone, in which the insert has been incorporated in the appropriate orientation, has been obtained. In some instances, restriction digestion of plasmids was not sufficient to confirm that the correct clone was obtained. In these cases, plasmid DNA was sequenced.

### 3.1.2. Cloning of pCS

The first cloning step consisted of removing approximately 3 kb from the 3' end of the genomic PTPA sequence. Digestion of pPTPA with SmaI yields bands of approximately 10 and 3 kb. The 10.8 kb band, consisting of the 5' end 8 kb of the PTPA fragment and the pSK vector, was isolated and ligated to form pCS (Figure 5).

A number of restriction digestions demonstrate that the correct clone was obtained (Figure 5B). As expected, pCS is linearized to approximately 10 kb when digested with SmaI (lane 3). When pCS is digested with SacI (lane 4), bands of 2.1, 2.6, 2.9 and 3.2kb are observed. The deleted sequence contained several SacI site. Had the 3' end *not* been deleted, additional bands of 0.58, 1.5, 2.3, 3.3kb would have been observed. Finally, digestion with NheI (lane 5) is also consistent only with the expected pCS clone. A 1.8 kb fragment occurs upon NheI digestion of both pPTPA and pCS, but the second fragment of 9kb is consistent with loss of the PTPA 3 kb 3' fragment to form pCS.

The faint band observed above the 9kb fragment upon digestion with NheI represents undigested DNA. Partial digestion of plasmid can occur for several reasons: loss of restriction enzyme activity, suboptimal buffer conditions, or the presence of impurities in plasmid DNA. The buffer used for this digestion was provided by the enzyme manufacturer and was routinely used in the laboratory without difficulty, and

SmaI and SacI enzymes have fully digested the plasmid DNA, indicating that it was free of digestion-inhibiting impurities. Therefore, it seems more likely that this unexpected band resulted from enzyme activity loss rather than suboptimal buffer conditions or the impurity of plasmid DNA.

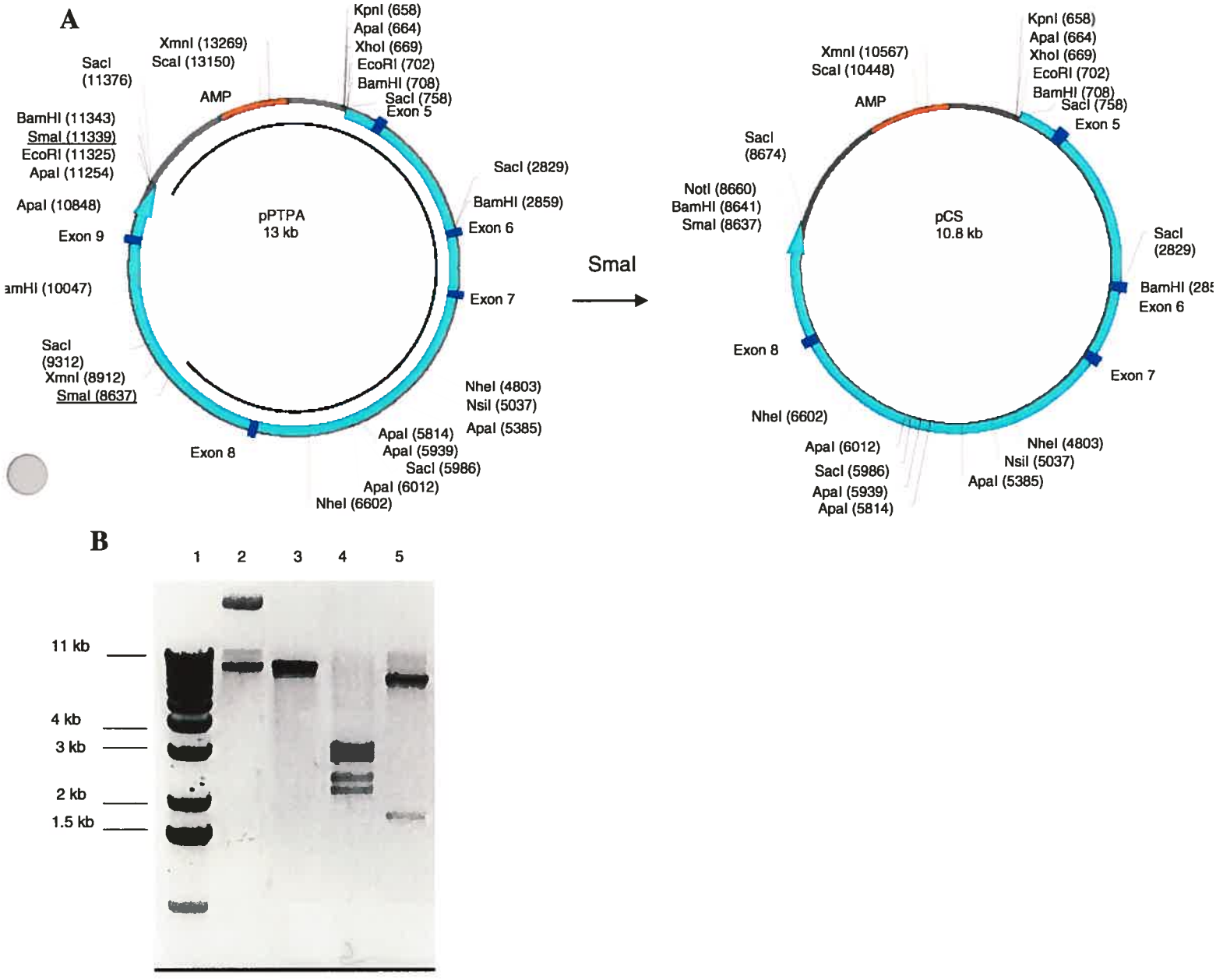


**Figure 5:** Cloning of pCS. *A*. Schematic representation of the clone. *B*. Agarose gel indicating that the pCS clone was obtained (Lane 1, 1 kb ladder; Lane 2, pCS undigested; Lane 3, pCS digested with SmaI; Lane 4, pCS digested with Sac I; Lane 5, pCS5 digested with NheI).

### 3.1.3. Cloning of pCS1

The goal of the next cloning step was to further shorten the PTPA fragment. A 4.7 kb fragment consisting of exons 5 - 7 was generated by digesting pCS with ApaI. This fragment was cloned into the ApaI-linearized pSK (Strategene's Bluescript vector). Two orientations were obtained, of which one (pCS1) was retained for subsequent cloning steps. Thus, the pCS1 vector consists of 4.7 kb of the 5' end of the PTPA gene within a pSK (Figure 6).

Generation of uncontaminated insert posed a significant difficulty in producing this clone. Indeed, digesting pCS with ApaI generates several fragments of different sizes, including one fragment of 5.4 kb, corresponding to the sequence between the ApaI sites at positions 6,012 and 667 of pCS. Despite running the digested pCS vector on the agarose gel for an extended period of time, the 5.4 kb and the desired 4.7 kb fragments migrated in close proximity to one another. This made it difficult to physically isolate the correct band without contamination from the larger fragment.

Digestion with ApaI (Figure 6B) and Kpn (Figure 6C) indicates that the desired fragment was inserted in the pSK vector. As expected, the ApaI digestion generates 2.9 kb and 4.7 kb bands. Had the 5.4 kb contaminant been inserted in the linearized vector, the digestion would have generated 2.9 and 5.4 kb bands. This is consistent with the KpnI digestion, which yields a single fragment below the 8 kb marker band. Had the incorrect insert been incorporated, the linearized fragment would have migrated to above this band, to approximately 8.4 kb.

These digestions did not provide information about the orientation of the plasmid, nor do they prove conclusively that the correct fragment was ligated to the vector. This uncertainty led us to seek a way to confirm the authenticity of this clone rapidly and irrefutably. Therefore, the candidate pCS1 plasmid was sequenced using the T3 primer,

**Figure 6:** Cloning of pCS1. *A.,* Schematic representation of the clone. *B.* Agarose gel indicating the pCS1 clone was obtained (Lane 1, 1 kb ladder; Lane 2, undigested pCS1; Lane 3, pCS1 digested with ApaI) *C.* Agarose gel indicating the pCS1 clone was obtained (Lane 1, pCS1 digested with KpnI; Lane 2, undigested pCS1; Lane 3, 1 kb DNA ladder).

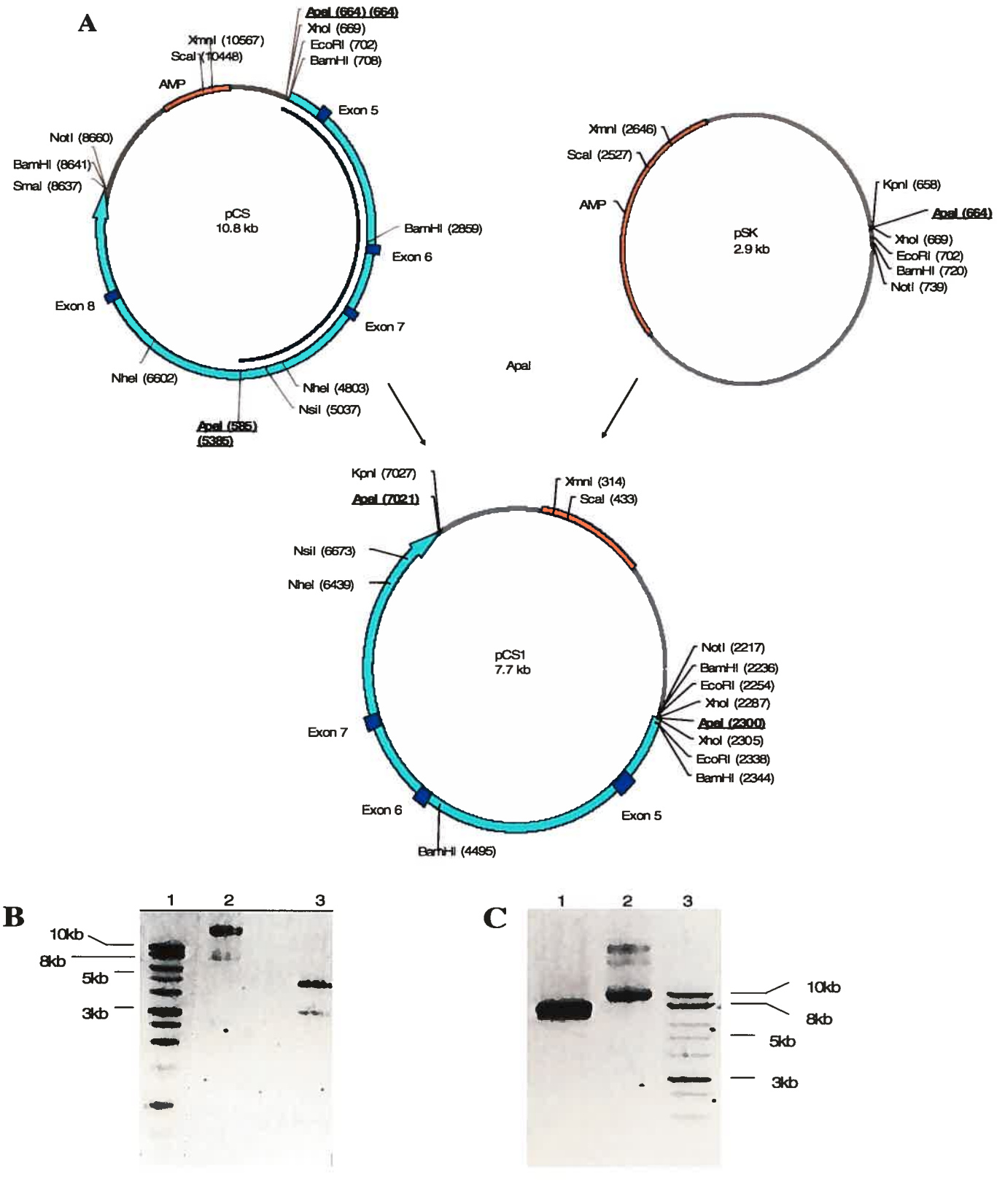
A
ApaI (664) (664)
XhoI (669)
EcoRI (702)
BamHI (708)
XmnI (10567)
ScaI (10448)
AMP
Exon 5
NotI (8660)
BamHI (8641)
SmaI (8637)
pCS
10.8 kb
BamHI (2859)
Exon 6
Exon 8
Exon 7
NheI (6602)
NheI (4803)
NsiI (5037)
ApaI (585)
(5385)
XmnI (2646)
ScaI (2527)
AMP
KpnI (658)
ApaI (664)
pSK
2.9 kb
XhoI (669)
EcoRI (702)
BamHI (720)
NotI (739)
ApaI
KpnI (7027)
ApaI (7021)
XmnI (314)
ScaI (433)
NsiI (6673)
NheI (6439)
pCS1
7.7 kb
NotI (2217)
BamHI (2236)
EcoRI (2254)
XhoI (2287)
ApaI (2300)
XhoI (2305)
EcoRI (2338)
BamHI (2344)
Exon 7
Exon 6
Exon 5
BamHI (4495)
B
1
2
3
10kb
8kb
5kb
3kb
C
1
2
3
10kb
8kb
5kb
3kb

which provides the sequence 5' of the NotI site (2,217), into the PTPA gene. The sequence obtained was consistent with the expected plasmid as presented in Figure 6.

### 3.1.4. Cloning of pCS2

We sought to incorporate a loxP site 5' of exon 6, at the position of BamHI (4,495) of pCS1. To do this, a 2.2kb portion on the 5' end the PTPA gene pCS1 was amplified using pCS1 as a template. Oligonucleotide primers were designed to include the loxP sequence and restriction sites to facilitate cloning. The sense primer, F1-mPTPA-UP, consisted of sequence complementary to the PTPA gene, and the anti-sense primer, mPTPA-BglII-loxP, contained the 34 bp-long loxP sequence, a BglII site for cloning, and the PTPA-complementary sequence. To obtain pCS2, the amplified PCR product was digested with BamHI and BglII, and ligated with the 5.5 kb fragment from BamHI-digested pCS1. BamHI and BglII generate compatible ends. However, ligation of these ends disrupts both of these sites (Figure 7).

Initially, pCS2 was confirmed by restriction digestion analysis. Figures 7B and 7C indicate that the insert was integrated in the vector in the expected orientation. Digestion of pCS2 with BamHI linearizes the plasmid to approximately 7.7 kb (Figure 7B). This would only be possible if one of the BamHI sites on the pCS1 plasmid had been disrupted by ligation with a BglII end. The correct orientation is demonstrated by the digestion of pCS2 with SacI, which generates 2.1 and 4.6 kb bands (Figure 7C). Had the insert been incorporated in the opposite orientation, the SacI sites would have been within 50 bp from each other, yielding bands of 7.6 kb and 50 bp. In addition to the 2.1 and 4.6 kb bands obtained upon SacI digestion, a faint band of approximately 9 kb can be observed (Figure 7C). This corresponds to the same molecular weight as the undigested DNA (Lane 2), indicating that the 9kb band represents plasmid which was not successfully digested by the SacI enzyme (see section 3.1.2.).

Two aspects of this construct prompted us to sequence parts of the plasmid. First, differences between pCS2 and pCS1 are minimal, making it difficult to distinguish them exclusively on the basis of restriction digestion. Sequencing the vector would best confirm the integration and orientation of the fragment. The T3 primer, which allows

sequencing 5' of the NotI site (2,217), confirmed that the PCR product had been incorporated in pCS1 in the correct orientation.

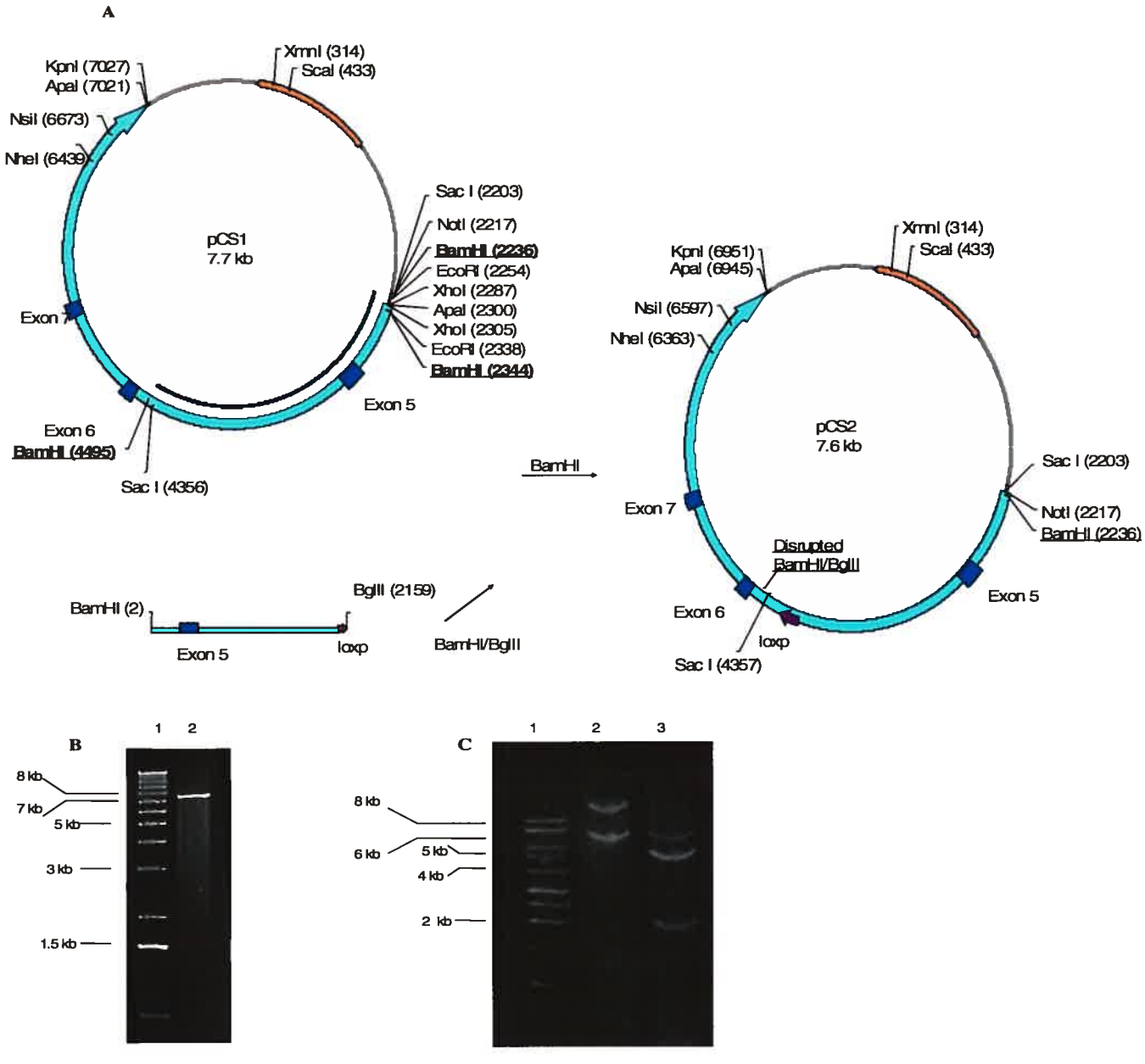


**Figure 7:** Cloning of pCS2. *A.*, Schematic representation of the clone. *B.* Agarose gel indicating the pCS2 clone was obtained (Lane 1, 1kb ladder; Lane 2, pCS2 digested with BamHI). *C.* Agarose gel indicating the pCS2 clone was obtained (Lane 1, 1 kb ladder; Lane 2, pCS2 undigested; Lane 3, pCS2 digested with SacI).

In addition, it has been demonstrated the Cre recombinase can only mediate the recombination between two identical loxP sequences (Chatterjee *et al.*, 2004). Therefore, we sought to confirm the integrity of the loxP site before proceeding further. We used the R1-mPTPA-BglII-loxP oligonucleotide to sequence the plasmid and demonstrated that the loxP had not been modified during the amplification process. The primer sequenced several bases past this site, providing further evidence that the correct clone had been obtained.

### 3.1.5. Cloning of pCS4

Following the insertion of the first loxP site, the PGKNeo-loxP sequence was inserted into pCS2 to form pCS4. To do this, the pK-11 plasmid, containing the PGKNeo flanked by frt sites and a loxP site identical to the one designed in pCS2, was amplified by PCR. The primers, (F4-PGKNeo-EcorI-NheI and R4-PGKNeo-XhoI-RI-NheI), were engineered such that the amplified product would have NheI sites in both extremities. NheI-linearized pCS2 was ligated to the NheI-digested PCR product. Thus, the resulting pCS4 plasmid contains the PGKNeo cassette flanked by frt sites, one loxP site located 3' of the cassette (8,255), and one located 5' of exon 6 (4,419) (Figure 8).

Several digestions allowed us to confirm that the PGKNeo-loxP was inserted in the vector with the appropriate orientation (Figure 8B). Digesting pCS4 with NheI (lane 4) reconstituted the vector and insert used to construct the clone (2.2kb PGKNeo-loxP vector, and 7.6kb pCS2 insert). The other digestions provide evidence that the correct orientation was obtained. BamHI digestion (Lane 2) indicates bands of 3.8 and of 5.8 kb. This is consistent only with fragment insertion with the correct orientation; incorrect orientation would have generated fragments of 4.4 and 5.5 kb. Digestion with KpnI generates the expected bands of 0.59 and 8.9 kb (Lane 3); the opposite orientation would have produced 2.6 and 7.1 kb fragments.

**Figure 8:** Cloning of pCS4. *A.*, Schematic representation of the clone. *B.* Agarose gel indicating the pCS4 clone was obtained (Lane 1, undigested pCS4; Lane 2, pCS4 digested with BamHI; Lane 3, pCS4 digested with KpnI; Lane 4, pCS4 digested with NheI; Lane 5, 1 kb DNA ladder).

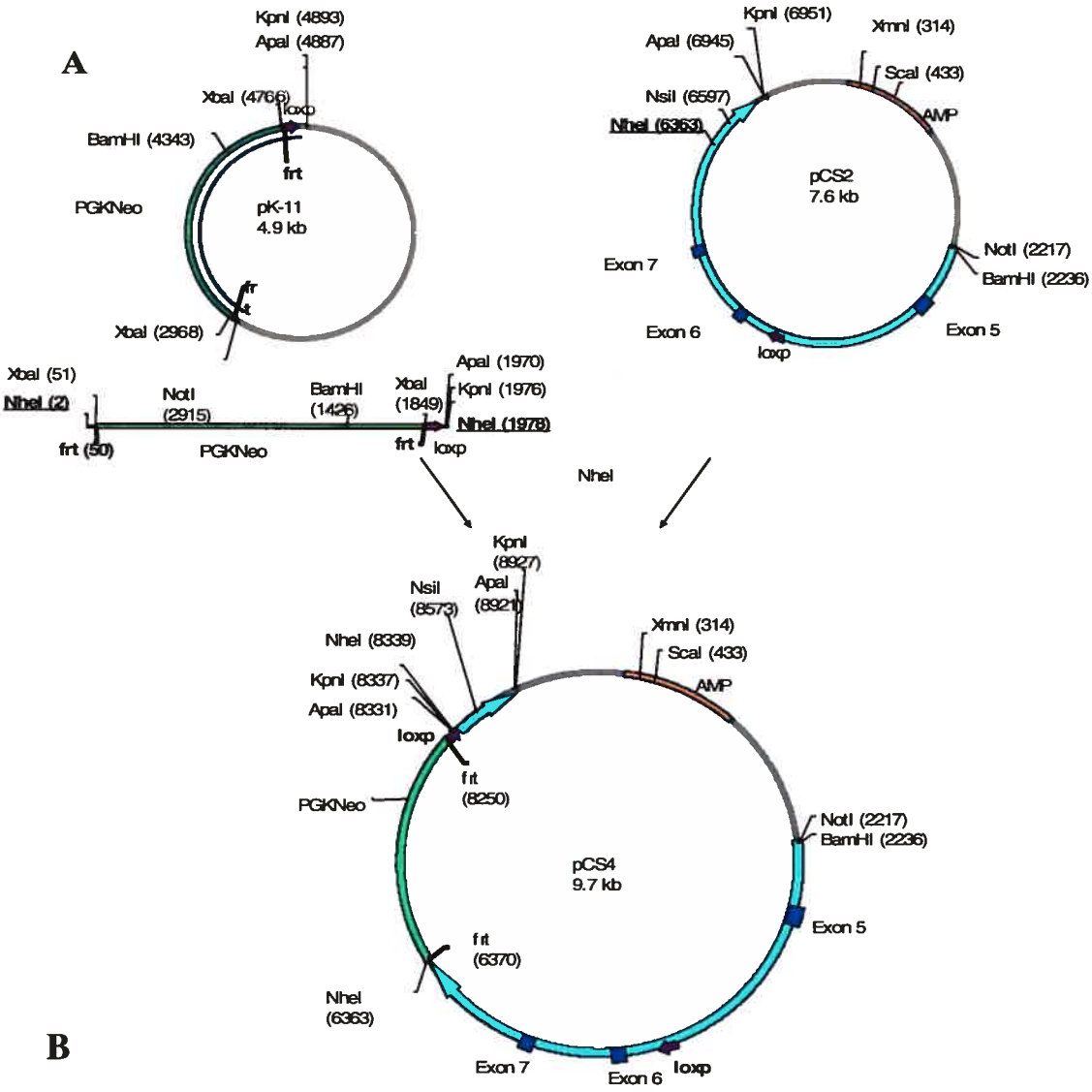
A
KpnI (4893)
ApaI (4887)
XbaI (4766)
loxp
BamHI (4343)
frt
PGKNeo
pK-11
4.9 kb
XbaI (2968)
KpnI (6951)
ApaI (6945)
XmnI (314)
ScaI (433)
NsiI (6597)
NheI (6363)
AMP
pCS2
7.6 kb
NotI (2217)
BamHI (2236)
Exon 7
Exon 6
Exon 5
loxp
XbaI (51)
NheI (2)
NotI
(2915)
BamHI
(1426)
XbaI
(1849)
ApaI (1970)
KpnI (1976)
NheI (1978)
frt (50)
PGKNeo
frt
loxp
NheI
KpnI
(8927)
NsiI
(8573)
ApaI
(8921)
XmnI (314)
ScaI (433)
NheI (8339)
KpnI (8337)
AMP
ApaI (8331)
loxp
frt
(8250)
PGKNeo
NotI (2217)
BamHI (2236)
pCS4
9.7 kb
Exon 5
frt
(6370)
NheI
(6363)
Exon 7
Exon 6
loxp
B
1
2
3
4
5
9kb
7kb
6kb
4kb
2kb
0.5k

We also sought to confirm the integrity of the loxP through sequencing the DNA of the site. The T7 primer allows us to obtain the sequence immediately 5' of the KpnI site at position 8,927. The orientation of the insertion and the integrity of the loxP site were also confirmed by this sequencing.

A smear appears in all lanes, including Lane 5, which contains the 1 kb DNA ladder. The ladder was used routinely and did not usually produce smearing. This suggests that this smear was not the result of nuclease contamination from the DNA samples or enzyme reaction mixtures. Rather, this smear is probably the result of migrating the agars gel at a high speed. Because the effects of this rapid migration are uniform, the position of the bands relative to those in the 1kb ladder lane reflects the true molecular weight of the fragments.

### 3.1.6. Cloning of pCS5

It has been hypothesized that recombination frequency of the targeting vector may increase with the length of the homologous arms (see section 4.1.4.). The construction of plasmids pCS, pCS1, pCS2 and pCS4 allowed us to incorporate the loxP, frt, and neomycin sequences within the PTPA gene, leaving the 5' and 3' end arms of PTPA homology of 4.1 kb and 610 bp, respectively. The aim of designing plasmids pCS5 and pCS9 was to lengthen the 3' arm. Two clones were required for this step because the PTPA sequence that was intended to lengthen this arm of homology did not contain restriction sites that would allow us to clone this fragment directly in pCS4. Therefore, the specific goal in the construction of pCS5 was to engineer sites in the sequence of homology to facilitate future cloning steps.

We produced pCS5 by ligating the 1.8 kb fragment obtained by digesting pCS with NheI, with XbaI-linearized pBluescript (Figure 9). The NheI and XbaI digestions generate compatible ends, which are disrupted when ligated.

A restriction digestion analysis indicates that the pCS5 has been obtained (Figure 9B). The digestion of the construct with XhoI linearized the 4.7kb plasmid (lane 3). Had the vector re-circularized, this digestion would have generated a linearized 2.9 kb band. XhoI and NcoI double digestion produced 3.6 and 1.1 kb bands, as expected (lane 4); the incorrect orientation would have given 0.7 and 4.0 kb bands. This digestion also

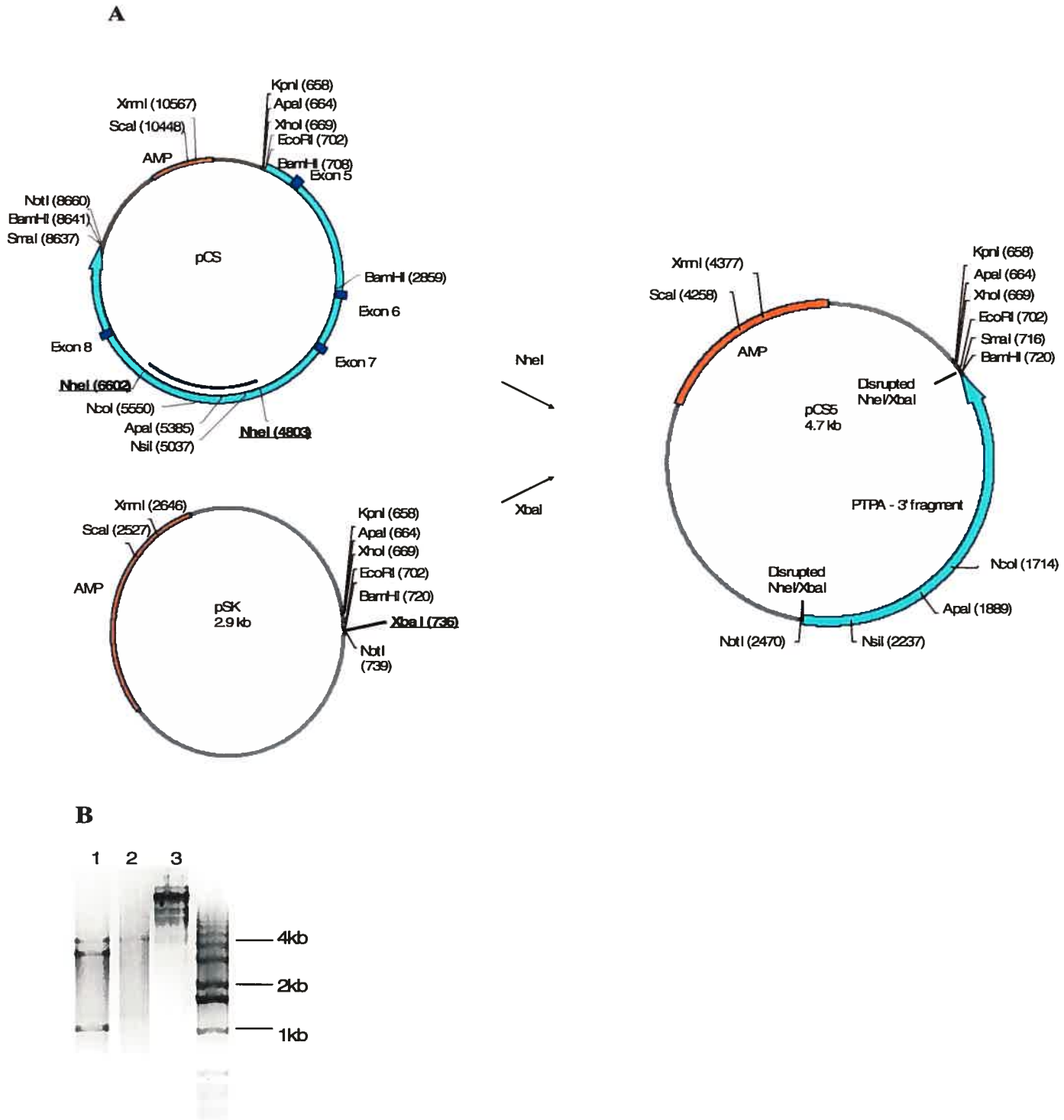


**Figure 9:** Cloning of pCS5. *A.* Schematic representation of the clone. *B.* Agarose gel indicating the pCS5 clone was obtained (Lane 1, pCS5 digested with NcoI and XhoI; Lane 2, pCS5 digested with XhoI; Lane 3, pCS5 undigested; Lane 4, 1 kb DNA ladder).

generated a 4.7 kb fragment, representing linearized plasmid that was only digested at one site. Given that digestion with XhoI alone was very effective (lane 3), and since this double XhoI/NcoI digestion was performed in a common buffer as recommended by the manufacturer's protocol, it would appear that this 4.7 kb band was generated because of incomplete NcoI activity.

A smear appears in all bands, including the 1kb DNA ladder, which was used routinely in the laboratory without difficulty. As indicated earlier, this suggests that the smear was caused by too rapid migration of the agarose gel rather than DNAse contamination. This rapid migration has little effect on the migration patterns of the fragments. Therefore, the position of the bands in relation to the DNA ladder reflects the true length of these fragments.

### 3.1.7. Cloning of pCS9

The PTPA sequence in pCS5 is to be used in the final cloning step, aimed at increasing the length the 3' end of the gene in the targeting vector. This plasmid contains an XhoI site, 3' of the genomic sequence (position 669). However, it was anticipated that the final construct, pCS10, would linearize with this enzyme. Therefore, we sought to disrupt this site in pCS5, making the linearization of pCS10 with XhoI possible. This was achieved by digesting pCS5 with SalI and XhoI, enzymes generating compatible ends, and re-circularizing the plasmid to form pCS9 (Figure 10). The ligation of these ends disrupts both SalI and XhoI sites. With the XhoI destroyed, pCS9 could be used to construct pCS10.

As expected, XhoI and SalI digestion of pCS9 produced bands at the same position as the undigested plasmid (Figure 10B, lane 2). Conversely, the digestion with NcoI and XhoI linearized the plasmid the 4.7 kb plasmid. Had the plasmid not been properly altered, the XhoI/SalI and NcoI/XhoI digestions would have produced a 4.7 kb, and 1.1 and 3.6 kb fragments, respectively.

A

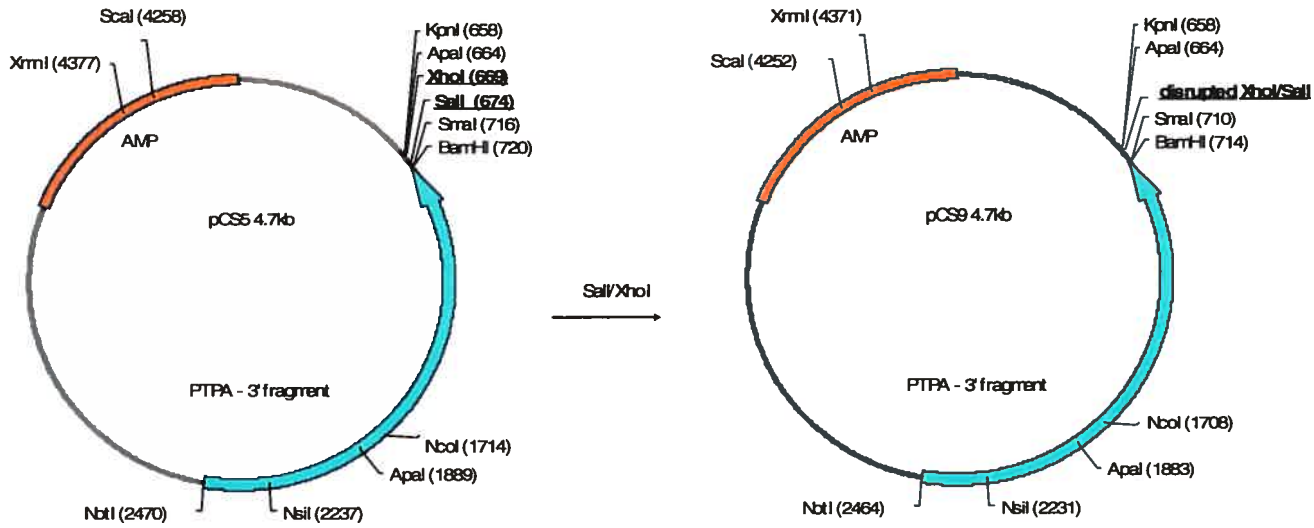


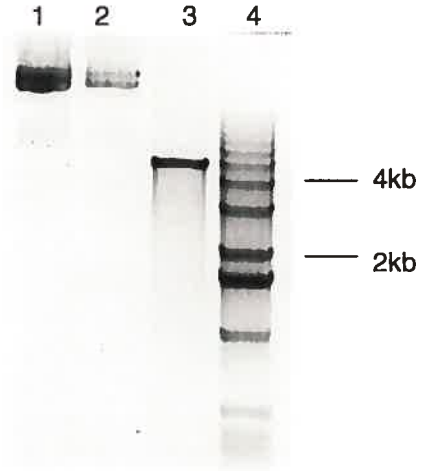


**Figure 10:** Cloning of pCS9. *A.*, Schematic representation of the clone. *B.* Agarose gel indicating the pCS9 clone was obtained (Lane 1, pCS9 undigested; Lane 2, pCS9 digested with XhoI and SalI; Lane 3, pCS9 digested with NcoI and XhoI; Lane 4; 1 kb DNA Ladder).

### 3.1.8. Cloning of pCS6

Two plasmids, pCS6 and pCS7, were designed in preparation for cloning the PGKPuro cassette required for negative selection in ES cells, in either extremity of the PTPA gene. These steps were required because of the absence of restriction sites that would allow the direct integration of PGKPuro in the pCS4 plasmid.

pCS6 was constructed by isolating the PGKPuro-Ampicillin fragment from the BamHI-digested pEV-Puro plasmid, ligating it within the BglII-linearized EYFP plasmid containing the kanamycin resistance gene (Figure 11). This allowed us to select bacteria with resistance to both ampicillin and kanamycin, enriching for candidate plasmids that contain both sequences to be ligated (see section 2.1.8). A number of clones containing different copy numbers of PGKPuro-Ampicillin fragment in different orientations were obtained. pCS6 was retained because it contained two copies of the PGKPuro cassette in the same orientation. This feature facilitated the following cloning step (see section 2.1.8.), in which the ampicillin resistance gene was disrupted.

Restriction analysis indicates that the plasmid retained for future constructions contains the vector and two adjacent copies of the insert sequences in the same orientation (Figure 10). BamHI digestion of pCS6 generated bands of 3.6 and 7.8 kb (Figure 10B). Had the plasmid contained less than two inserts, the resulting plasmid would have generated a single band because of the disruption of one BamHI site by ligation with the BglII-digested ends. Therefore, this band pattern eliminates the possibility that only one copy of PGKPuro-Amp was ligated into the pEYFP vector.

The EcoRI further demonstrates that two inserts in the same orientation were integrated to form pCS6. Bands of 3.4 and 4.7 kb were obtained (lane 3), consistent with the plasmid as presented in Figure 10. It is important to note that the 3.4 kb band is actually composed of the combined fragments of two identical PGKPuro sequences found within an individual plasmid. Had the opposite orientation been obtained, fragments of 6.8 and 4.7 kb would have been observed.

Digestion with XhoI further confirms that pCS6 has two copies of the insert in the same orientation. As expected, bands of 6.1, 3.4 and 1.9 kb were obtained (lane 4). Only the construct as presented in Figure 10A can account for this pattern.

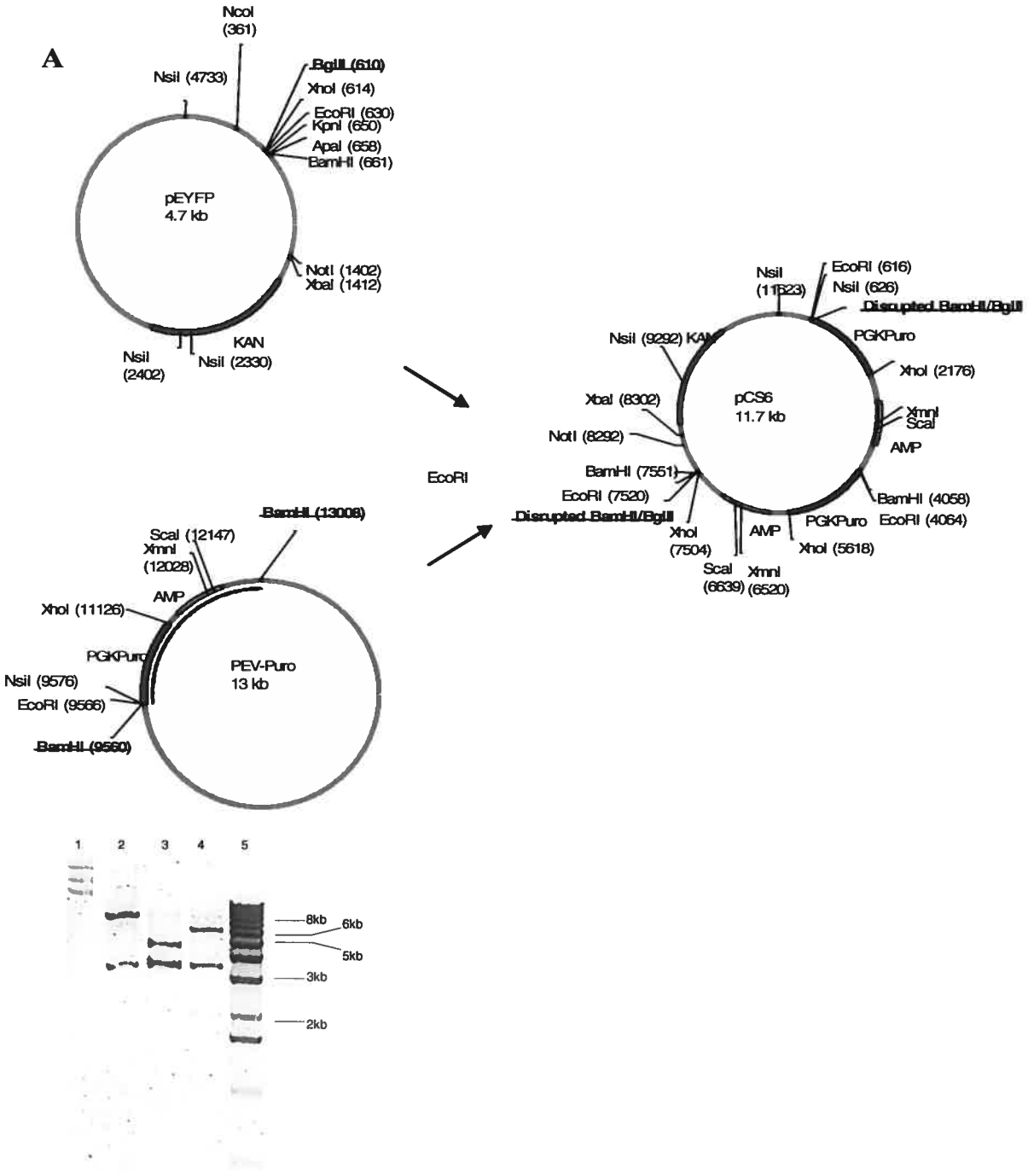


**Figure 11:** Cloning of pCS6. *A.*, Schematic representation of the clone. *B.* Agarose gel indicating the pCS6 clone was obtained (Lane 1, pCS6 undigested; Lane 2, pCS6 digested with BamHI; Lane 3, pCS6 digested with EcoRI; Lane 4, pCS6 digested with XhoI).

### 3.1.8. Cloning of pCS7

It was anticipated that future cloning steps would be difficult because they involved ligating large fragments. Since our strategy consisted of enriching for clones containing vector and insert via double kanamycin/ampicillin selection, we sought to disrupt the ampicillin gene in pCS6. The resulting construct, pCS7, would be resistant to kanamycin only, enabling us to employ this double selection strategy in future cloning steps.

To restore pCS6 sensitivity to ampicillin, the plasmid was digested with blunt end-generating XmnI and ScaI enzymes. In this plasmid, these sites are only located within the ampicillin resistance gene. The 8.1 kb fragment isolated from this digestion, which included the intact kanamycin resistance gene as well as the PGKPuro cassette, was re-ligated. The resulting pCS7 plasmid therefore consisted of one copy of the PGKPuro gene within the pEYFP vector and one copy of the truncated, non-functional, ampicillin-resistance gene (Figure 12). Positive and negative selection with standard doses of kanamycin and ampicillin allowed us to enrich for clones that had lost the gene conferring resistance to the latter.

Restriction digestion analysis confirmed that the correct clone was obtained. Digestion with XhoI generated bands of 1.8 and 6.5 kb (Figure 12B). Digestion with EcoRI, and BamHI (Figure 12C) linearized the plasmid near the 8 kb band of the 1 kb DNA ladder. These patterns are only consistent with the pCS7 plasmid as presented in Figure 12A.

### 3.1.9. Cloning of pCS8

The three subsequent cloning steps consisted of piecing together the fragments of interest from pCS4, pCS9 and pCS7. The pCS4 vector contains a portion of the PTPA gene, the PGKNeo cassette, and the loxP and frt sites. The final element required for the construct was the addition of the PGKPuro cassette for negative selection. Since no restriction sites were available for the standard integration of PGKPuro within pCS4, pCS8 was constructed by digesting pCS4 and pCS7 with NotI and then ligating the linearized plasmids (Figure 13). Since pCS7 confers resistance to kanamycin only and

pCS9 confers resistance to ampicillin, the pCS8 ligation product was enriched for by selection of bacteria resistant to both antibiotics.

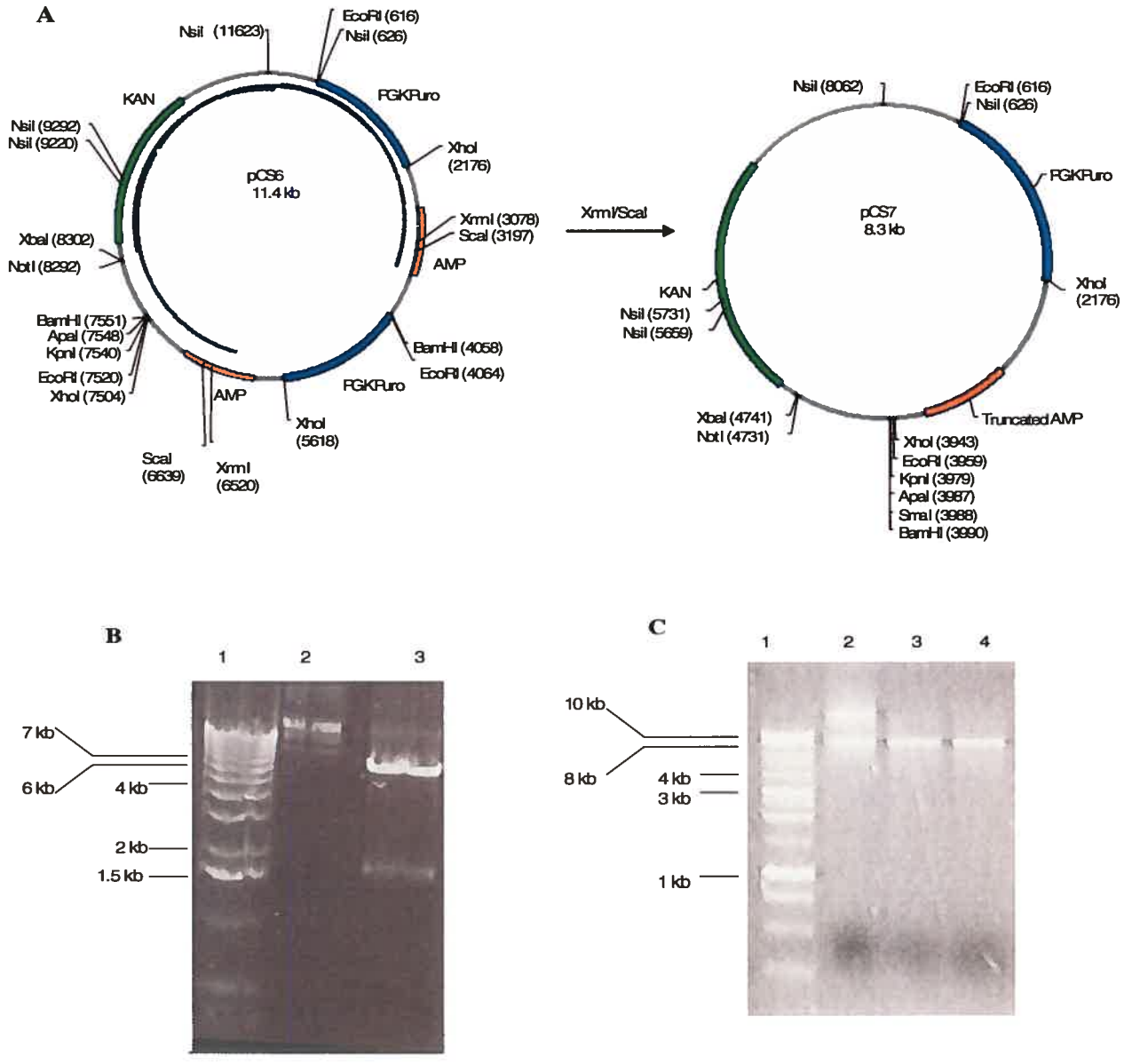


**Figure 12:** Cloning of pCS7. *A.* Schematic representation of the clone pCS7 clone was obtained (Lane 1, 1kb ladder; Lane 2, pCS7 undigested; pCS7 digested with XhoI). *C.* Agarose gel indicating the pCS7 clone was obtained (Lane 1, 1 kb ladder; Lane 2, pCS7 undigested; Lane 3, pCS7 digested with EcoRI; Lane 4, pCS7 digested with BamHI).

Restriction digestion analysis allowed us to determine with greater certainty that the expected clone was obtained (Figure 13B). It is important to mention that in this construct, the orientation of ligated fragments was of little relevance. The presence of the PGKPuro sequence is required for the purpose negative selection in ES cells. Therefore, cells that have undergone homologous recombination would be expected to have eliminated this sequence. We developed strategies to allow us to utilize ligated plasmids in either of the possible orientations.

Digestion with NotI generates two bands of lengths equal to those of fragments used to create pCS8, approximately 8 and 10 kb (lane 4). As expected, digestion with EcoRI generates fragments of 3.6 kb and approximately 14kb (lane 3), consistent with clone as presented in Figure 13A. ApaI digestion (lane 2) generates bands of 7.5 and 10 kb, as expected for this orientation. Had the opposite orientation been obtained, this digestion would have generated 3.6 and 13.8 kb bands.

### 3.1.10. Future Cloning of pCS10

pCS8 contains all the elements necessary for gene targeting: 5' portion of the pPTPA plasmid, as well as both selection cassettes, and loxP and frt sites. However, the 3' end of the PTPA sequence proper is 0.6 kb in length. This length may be insufficient to guarantee efficient homologous recombination (see section 4.1.4.). Therefore, although not absolutely necessary, one additional cloning step could be performed to lengthen this sequence in the hopes of increasing recombination frequency. The pCS9 plasmid consists of the portion of PTPA that is immediately 3' of the PTPA sequence of pCS8. Indeed, the NsiI located at position 11,087 of pCS8 corresponds to the NsiI site of pCS9, at position 2,237. These plasmids could be fused by ligating NsiI-linearized pCS9 with the 13.2 kb fragment generated by digestion of pCS8 with this same enzyme. Ligation in the correct orientation will allow for the addition of 1.6 kb of the PTPA sequence on the 3' end of the PTPA-Neo-loxP sequence (Figure 14A).

**Figure 13:** Cloning of pCS8. *A*. Schematic representation of the clone. *B*. Agarose gel indicating the pCS8 clone was obtained (Lane 1, pCS8 undigested; Lane 2, pCS8 digested with ApaI; Lane 3, pCS8 digested with EcoRI; Lane 4, pCS8 digested with NotI).

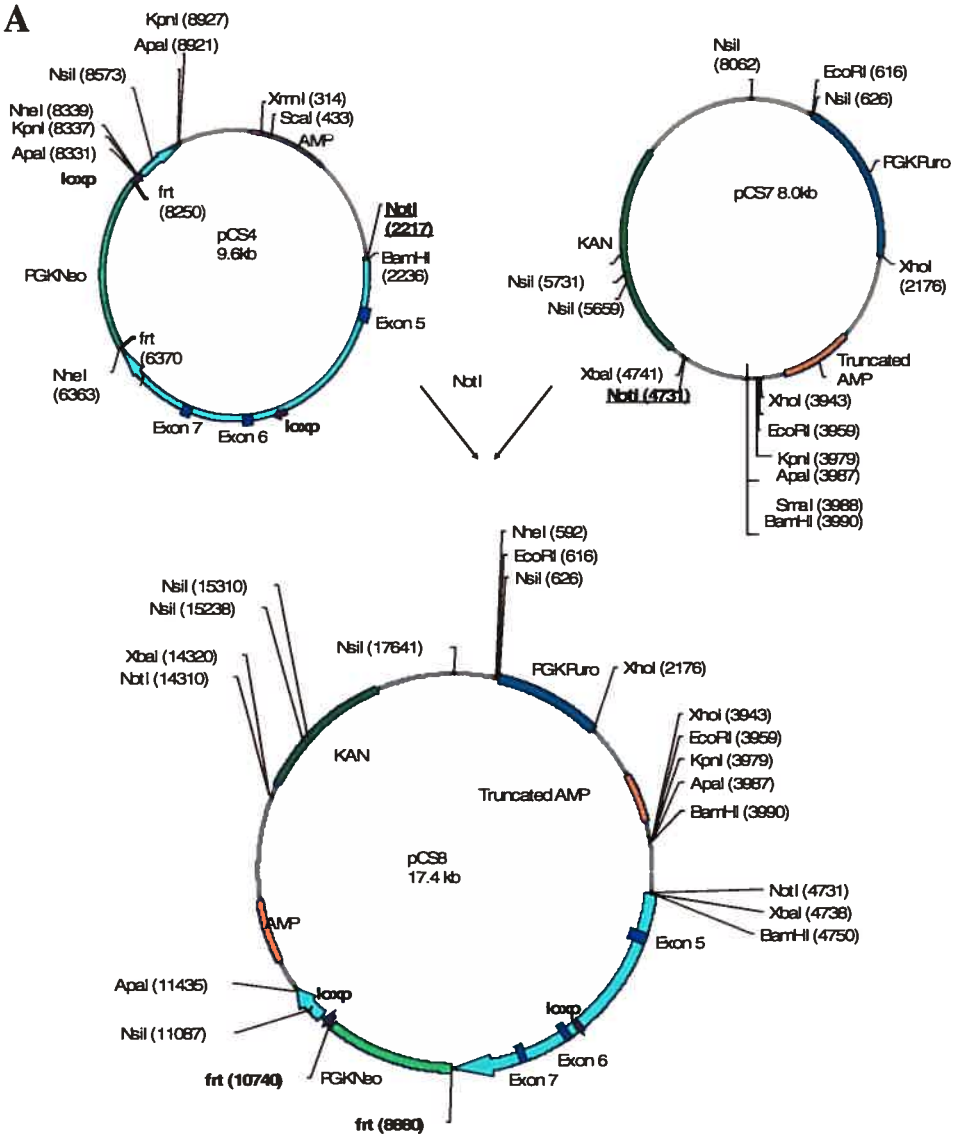
A
KpnI (8927)
ApaI (8921)
NsiI (8573)
NheI (8339)
KpnI (8337)
ApaI (8331)
loxp
frt (8250)
XmnI (314)
ScaI (433)
AMP
NotI (2217)
BamHI (2236)
Exon 5
pCS4 9.6kb
PGKNeo
frt (6370
NheI (6363)
Exon 7
Exon 6
loxp
NotI
NsiI (8062)
EcoRI (616)
NsiI (626)
PGKPuro
pCS7 8.0kb
KAN
NsiI (5731)
NsiI (5659)
XhoI (2176)
XbaI (4741)
NotI (4731)
Truncated AMP
XhoI (3943)
EcoRI (3959)
KpnI (3979)
ApaI (3987)
SmaI (3988)
BamHI (3990)
NheI (592)
EcoRI (616)
NsiI (626)
NsiI (15310)
NsiI (15238)
XbaI (14320)
NotI (14310)
NsiI (17641)
PGKPuro
XhoI (2176)
XhoI (3943)
EcoRI (3959)
KpnI (3979)
ApaI (3987)
BamHI (3990)
KAN
Truncated AMP
pCS8 17.4 kb
NotI (4731)
XbaI (4738)
BamHI (4750)
Exon 5
AMP
ApaI (11435)
loxp
NsiI (11087)
loxp
Exon 6
frt (10740)
PGKNeo
Exon 7
frt (8880)
B
1 2 3 4 5
10kb
8kb
6kb
3kb
0.5kb

The kanamycin resistance gene of pCS8 will be lost, but all other sequences will be intact. If many colonies are obtained, this restoring of kanamycin sensitivity will allow for negative selection to facilitate the screening process before performing restriction digestion analysis on candidate clones.

Unfortunately, attempts to achieve this clone have failed so far. In fact, a number of trials have produced ligated fragment and insert, yet only the incorrect orientation of insertion was obtained.

When pCS10 is obtained, this plasmid will be linearized with XhoI (14B). The resulting 13.3 kb fragment will contain the PTPA, loxP, frt, PGKNeo and PGKPuro sequences, and will have lost the truncated ampicillin gene. This construct will be purified and electroporated into ES cells for the eventual creation of PTPA-loxP mice.

## 3.2 Transgenic mice

### 3.2.1. Screening for Transgenic Mice by Southern Blot

A DNA construct designed to drive Ptpa-EYFP expression in mice was prepared by other members of our laboratories. The construct was microinjected in fertilized oocytes and transferred to pseudo-pregnant females by the Centre de Recherche Guy-Bernier Animal Facility staff and 22 founder mice were carried to term (mice 1 - 22). Of these animals, a fraction were expected to have integrated the construct into their genome. However, since the chromosomal integration of the construct occurred at a postzygotic stage, these mice were expected to be mosaic, with transgene incorporation in only a subset of cells. Therefore, transgene inheribitability would only be possible in founder mice that carried this exogenous DNA in their germline cells. In accordance with Mendelian patterns of inheritance, a quarter of the progeny of these "ancestral" mice would be expected to carry the transgene in all cell types. Therefore, the founder animals were crossed with fertile CD-1 mice of the opposite sex, and the resulting litter was screened for transgene integration by southern blot.

Since animals were expected to carry the transgene in either all or none of their cell types, any tissue could have enabled us to perform the screen. We purified DNA

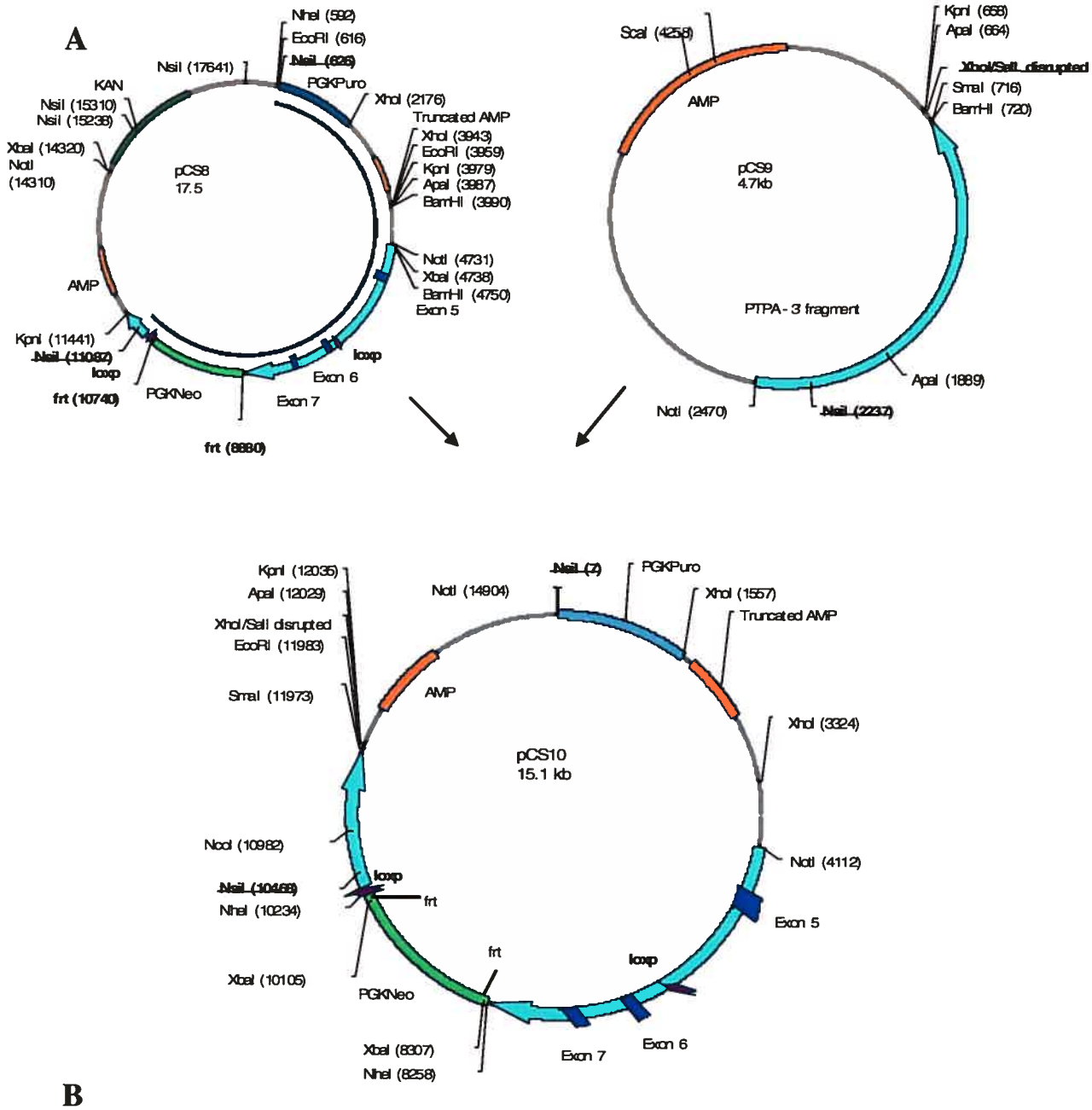


**Figure 14:** Future cloning of pCS10, (A) before and (B) after linearizing with XhoI (B) for electroporation into ES cells.

from mouse tails because this procedure provides the greatest yield possible without requiring the animal to be sacrificed. Extracted DNA was screened by southern blotting, using a radioactive-labelled copy of the full-length PTPA-EYFP construct as a probe.

Two major constraints throughout the screening process were the variable quality and the relatively low quantity of DNA extracted from mouse tails. Consequently, southern blots often revealed smearing of lanes, indicative of DNA degradation, and bands of variable intensities. Yet, data amassed from several of these southern blots suggested that three potential founder transgenic animals, mice 6, 7 and 16, had been obtained (Figure 15).

A number of mice were derived and screened from these three animals. The quantity of genomic DNA extracted from mouse tail clippings was usually not sufficient to perform more than one southern blot for any given animal. Therefore, it was not possible to replicate the procedure or to screen candidate transgenic mice more rigorously. Had greater DNA yields been obtained, we would have repeated the southern blot using probes consisting of variable portions of this construct. This would have allowed us to confirm that the transgene had been fully and stably integrated in the genome in candidate mice.

The southern blot data of transgenic animals from mouse line 6 (Figure 15A) highlights how more rigorous southern blotting could have further substantiated our results. Transgenic offspring of a founder mouse are identical with respect to the locus of transgene integration in the genome. Therefore, DNA extracted from animals derived from mouse 6, digested and hybridized with the same enzyme and radioactive probe, should have generated bands of the equal molecular weight on the southern blot. However, as illustrated in Figure 15A, two siblings from this mouse line appear to have produced bands of different sizes. Several possibilities can account for this discrepancy. For example, it is possible that a meiotic recombination event occurred at a locus immediately flanking the site of the transgene insertion in one of the animals, such that the transgene was in greater proximity to a BamHI site (used to digest the genomic DNA) in one mouse than in the other. In such an eventuality, the transgene would be localized within BamHI fragments of different lengths, as detected in the southern blot. Alternatively, the different bands appearing on the southern blot may also be the result of

rearrangement, such as a deletion of a portion of the transgene. It also possible that this discrepancy is related to DNA degradation. Indeed, a "blotchy" smear appears below the band on lane 4 (Figure 15A), suggesting that the probe hybrdizied DNA at lower molecular weights. This is consistent with hybridization of degraded DNA, which typically generates a broad signal spanning wide range of molecular weights. Thus, had mouse tail DNA extraction generated sufficient quantities of DNA, we would have replicated this southern blot. Additional blots, in which genomic DNA would have been digested with different enzymes and probed with different portions of the PTPA-EYFP construct, would have been performed, which would have allowed us to explore the reason for the discrepancy in banding patterns in siblings.

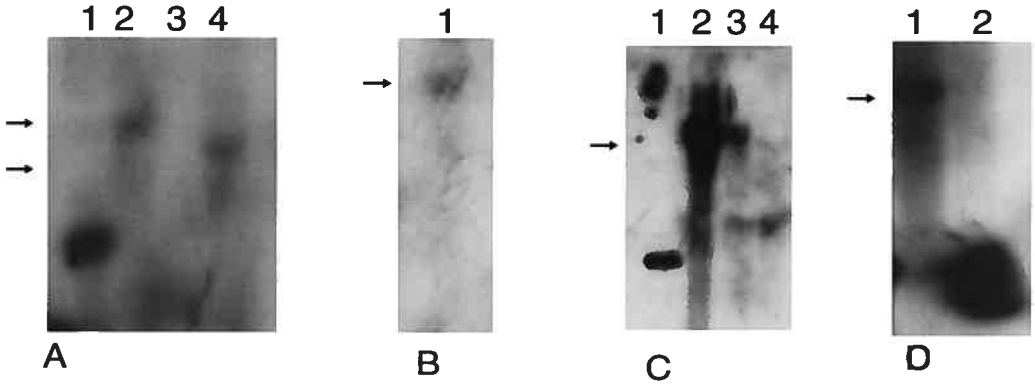


**Figure 15:** Southern blots for offspring of transgenic mice 6 (*A*, *B*), 7 (*C*) and 16 (*D*). *A.*, Lane 1, the DNA used to design the probe, as a positive control; Lane 2 and 4; transgenic mice; Lane 3, wild-type mouse. *B,* Lane 1, transgenic mouse. *C,* Lane 1, the DNA used to design the probe, as a positive control; Lanes 2 and 3 transgenic mice. *D.* Lane 1, transgenic mouse; Lane 2, the DNA used to design the probe, as a positive control.

There is also some ambiguity in the southern blot for animals from mouse line 7 (Figure 15C). In addition to the relatively intense signal (lane 3), a faint band of lower molecular weight appears on the southern blot film. This band is approximately the same molecular weight as the unique band observed in an adjacent lane (lane 4), in which was loaded the DNA of non-transgenic offspring of mouse 7. This band may represent weak, non-specific hybridization of the radioactive probe to the genomic DNA. Alternatively, the "blotchy" appearance of the band may be indicative that the perceived signal is an

artefact of the blotting protocol rather than the result of probe hybridizing to mouse DNA. Replicating the southern blot would have allowed us to determine the true nature of this unexpected signal.

Thus, the results obtained from our southern blot screening were not always clear and did not demonstrate unequivocally that transgenic animals were obtained. Three offspring of mouse 6 appeared to have integrated the transgene in their genome, but all three generated faint signals in the southern blot. However, since three potentially positive mice were identified, of which two corresponded to the same molecular weight (Figure 15A, lane 2 and Figure 15B), we considered that it was worthwhile to further investigate whether or not these mice were truly transgenic and actually expressed Ptpa-EYFP. Only two offspring from mouse 7 appeared to carry the transgene. Yet, the strong intensity of the signal for both these animals prompted to us to explore the possibility that animals from this mouse line expressed Ptpa-EYFP. Mouse line 16 provided less compelling evidence as only one offspring revealed a positive signal in the southern blot. Still, given that our laboratories had decided to pursue the investigation of two candidate mouse families, it was decided that this third line, although uncertain, would be also explored. Indeed, we hypothesized that given the wide range of pathways in which Ptpa is involved, it was possible for the transgene expression to have a deleterious or lethal effect on the animals. In such a case, fewer transgenic mice would develop to adulthood than would normal mice, accounting for the lack of transgene detection in line 16. Thus, our overall strategy consisted of exploring two mouse lines that had produced positive results by southern blot in two or more offspring of founder animals, and one line that was perhaps more tenuous, but that was potentially of interest given the function of Ptpa.

These candidate transgenic animals were crossed with fertile CD-1 mice in order to expand these into large mouse lines. Birth and development patterns appeared normal for all three lines. This is particularly noteworthy for mouse line 16; had the transgene expression caused a serious and deleterious effect, either it would have been expected that fewer pups be born, or that animals have a greater propensity to disease. These normal patterns strongly suggested that the hypothesized adverse effects of Ptpa-EYPFP expression could not account for the lack of transgene detection in mouse-line 16.

### 3.2.2. Assessing Transgene Expression by Western Blotting

The southern blotting for transgene integration into genomic DNA did not permit us to fully characterize candidate transgenic mice because of initial difficulties in optimizing DNA extraction techniques and insufficient DNA yields. Conversely, large quantities of protein can be extracted from virtually any tissue. In addition, our laboratories possessed effective and specific antibodies for Ptpa and EYPF. Therefore, our laboratories sought to examine the possibility of transgene expression in candidate animals by western blot.

Protein was extracted from various tissues, including the liver, kidneys, lungs, heart, intestine, spleen and skin from the animals in which a signal was detected by southern blotting as well as offspring derived from matings with CD-1 mice. Western blots were performed with these tissues with both anti-GFP and anti-Ptpa antibodies. GFP variants are 27kDa proteins. Therefore, fused to Ptpa (37kDa), the expression of the transgene was expected to have a molecular weight of 64 kDa.

The anti-Ptpa antibody detected several non-specific bands. Several peptides were detected by this antibody, as is generally the case for polyclonal antibodies. Yet, this anti-Ptpa effectively detected the 37 kDa endogenous Ptpa protein. However, in comparing adjacent lanes for wild-type control and candidate transgenic protein extracts, the western blot did not reveal transgenic-specific bands of 64 kDa (Figure 16A) or any other weight.

The monoclonal anti-GFP antibody revealed one strong signal of approximately 40 kDa as well as a few faint bands. This strong signal probably does not represent Ptpa protein. The secondary antibody for the GFP blot is a *mouse* anti-IgG. This band likely represents a component of a mouse protein recognized by this anti-IgG.

Figure 16 illustrates western blots performed for an animal from mouse line 6 for which appeared positive by southern blot. Similar patterns were observed for animals of all other mouse lines. Thus, molecular methods indicated that the candidate transgenic mice did not express the transgene in the specific tissues screened.

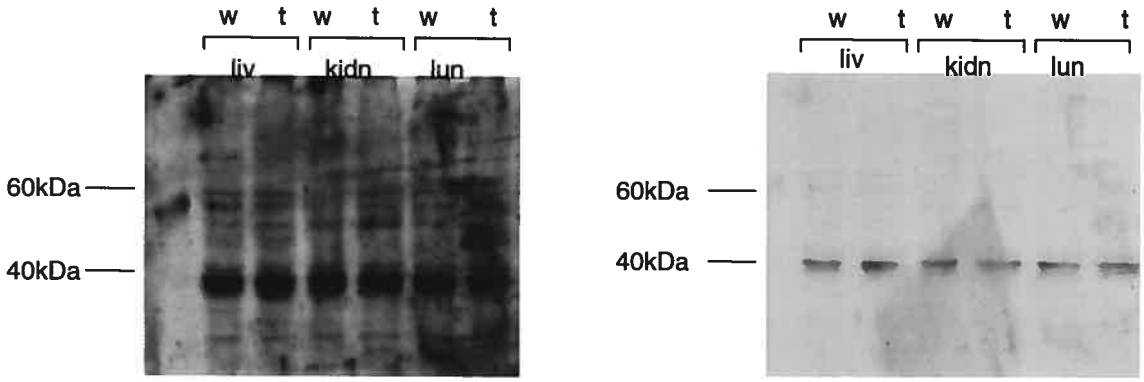


**Figure 16:** Western blotting for detection of transgene expression using (A) anti-PTPA and (B) anti-GFP antibodies (*wt*, wild-type; *t*, transgenic).

### 3.2.3. Macroscopic Observation of EYFP to Assess Transgene Expression

Having failed to identify animals expressing Ptpa-EYFP by western blot, we hypothesized that perhaps only very specific tissues expressed the transgene. In addition, we also hypothesized that In order to rapidly test for gene expression in many animals and a greater number of organs, we sought to screen for EYFP fluorescence macroscopically. Therefore, a large number of wild-type and potentially transgenic animals from families 6, 7 and 17 were sacrificed, dissected and observed under the Clare Chemical Dark Reader Spot Lamp using viewing goggles. Unfortunately, one of the short-comings of the Spot Lamp is that it does not allow for photographs of animals to be taken.

Consistent with the western blot results, no fluorescence was detected on the hairless surfaces of mice (such as feet or ears), or in hairless pups. In anticipation of a mosaic pattern of expression of the transgene, animals were sacrificed and dissected. Viewing approximately 15 individuals from the three mouse lines, including the candidate mice identified by southern blotting did not reveal any fluorescent tissue type in any animal. The only exception was an individual from the transgenic family 16, whose seminal vesicle seemed to fluoresce. However, this was not observed in any other

animals, including siblings of the mouse in question. In addition, since this individual had been sacrificed, we were not able to exploit this possibility further. Consequently, it seems that the transgenic mice generated did not express the transgene to any significant extent.

# 4. Discussion

Recent advances in molecular biology techniques enabling scientists to generate transgenic and knockout mice have allowed for unprecedented investigation of general mammalian biology and pathology, as well as targeted genetic studies. The Cre/loxP system for creating conditional knockout mice and the use of Green Fluorescent Proteins as tags and fusion proteins have become powerful means of achieving a high degree of genomic tailoring. Although these methods are technically difficult to develop, our laboratories have sought to exploit them to further our understanding of the role of PTPA in the response to oxidative stress.

Overall, our goals of generating both conditional knockout and transgenic mice for the PTPA gene have not yet been achieved. Several constructs were created in preparation for a targeting vector to allow the creation of the conditional knockout mice. Only one final cloning step, conceived to increase the length of homology on the 3' arm of the PTPA gene, is required before the plasmid can be electroporated in embryonic stem cells. Furthermore, it appears that the mice designed to express EYFP-fused Ptpa did not express the transgene. This section addresses a number of issues and details that were considered throughout the various stages of theses projects. In addition, a number of recommendations are made that may maximize the chances of obtaining fluorescent-Ptpa transgenic mice in the future.

## 4.1. The Creation of Conditional PTPA Knockout Mice Targeting Vector

The Cre/loxP system is an extremely useful tool in mouse studies because it allows the experimenter to control the location and time of the knockout event at any stage of mouse development. However, this method requires that a number of modifications be made to the mouse genome: two loxP sites must be engineered flanking the exons that are to be deleted by the Cre recombinase, and two selection markers (one within the targeted sequence and one on either the 3' or 5' end of the vector) are to be inserted. This makes the design of the targeting vector complex and challenging. In addition, several precautions must be taken to maximize homologous recombination

efficiency and to minimize the effects that the modified DNA may have on the targeted gene and its protein product. An important limiting factor is the availability of restriction sites for cloning after every cloning step; as each construct is being "assembled," fewer unique sites are present, making subsequent cloning steps more difficult to perform.

### 4.1.1. Targeting Vector Must be Isogenic with Mouse ES Strain

Various ES cell lines are available for the generation of knockout mice. The genomic sequence of PTPA was obtained from the mouse strain 129. This background is significant because it has been reported that differences in genetic background between the ES cell line and the DNA of the targeting vector could decrease the frequency of homologous recombination (te Riele *et al.*, 1992). Therefore, ES cells derived from the 129 mouse strain will eventually be used for gene targeting. Indeed, several studies have shown that this is an efficient strain for the creation of targeted deletions in mice (Dobrovolsky *et al.*, 1996; Ware *et al.*, 2003).

### 4.1.2. Utilizing Selection Markers

Integration of a positive selection marker within the targeting vector is needed to select for ES cells that have incorporated the vector within their genome. However, while this process enriches for cells that have incorporated the targeting vector within their genome, it does not distinguish between random and homologous recombination integration. To eliminate cells having incorporated the construct at non-homologous sites, Mansour *et al.* (1988) developed the "positive/negative selection" strategy. This approach calls for the construction of a targeting vector containing two antibiotic resistance genes: one for positive selection, to be engineered within the genomic DNA sequence of the vector, and another for negative selection, to be added to either extremity of the construct.

The rationale for this design is that randomly integrated exogenous DNA is incorporated in its entirety, whereas the process of homologous recombination eliminates non-homologous ends. Therefore, ES cells that have undergone HR will have integrated only the positive selection marker. Thus, two rounds of selections, one positive and one

negative, are needed to enrich for the correct clones; candidate cells exhibit resistance to the former and retain sensitivity to the latter.

In this study, the neomycin gene conferring resistance to G418 was integrated within the PTPA sequence for positive selection, whereas a puromycin resistance gene was cloned on the 3' extremity of the targeting vector. The expression of both resistance genes is assured by the PGK promoter, which is routinely used in ES cells for targeted deletion applications (Hannan *et al.*, 1993).

### 4.1.3. Use of the Frt/Flp System

The purpose of generating conditional knockout mice is to produce wild-type animals who have a spatially and/or temporally-limited sequence deletion. However, the very presence of a positive selection marker integrated within the targeted genomic DNA may disrupt the normal expression of this gene (Fiering *et al.*, 1995), regardless of the location and timing of Cre expression. To prevent this, we have sought to use the strategy developed by Fiering *et al.* (1995) and Zhao *et al.* (2001), which allows the removal of the positive selection marker using the frt/Flp system. Briefly, the targeting vector is designed such that this gene is flanked by frt sites. ES cell lines established as having integrated the targeting vector via HR are transfected with an eFlp (enhanced Flp) recombinase-expressing vector. This mediates recombination between the frt sites, effectively deleting the selection marker sequence from the genomic DNA. Having lost the resistance gene, the resultant ES cells would be genetically identical to wild-type ES cells with the exception of the two short loxP sites of 34 base pairs each, bringing the genomic modifications to a minimum. Many eFlp-expressing vectors are available commercially. For example, pCAGGS-FLPe, supplied by Gene Bridges (Dresden, Germany, http://www.genebridges.com), has been shown to remove sequences flanked by frt sites in ES cells effectively (Schaft *et al.*, 2001).

In the case of the PTPA targeting construct, we have used an frt-flanked neomycin gene from the pK-11 vector (Meyers *et al.*, 1998). The loxP sites are located 5' and 3' of the frt-neomycin sequence. Therefore, the loxP sites would be left intact upon Flp-mediated recombination. Those ES cells that have lost the marker can be selected by southern blot. Alternatively, cells having lost resistance to G418 would also

indicate the loss of the neomycin gene mediated by Flp. Following this step, the usual protocol for transferring ES cells to a pseudo-pregnant female can be followed.

Although the removal of the PGKNeo cassette is not absolutely required, this additional step provides two advantages. First, it minimizes the degree of modification incurred by the genomic DNA, preventing the potentially disruptive effect of maintaining the selection marker within the mouse genome. In addition, upon removal of the Neo gene, ES cells can be targeted again by the same construct, producing cells that contain the loxP sites on both PTPA alleles. These conditional knockout lines could be useful for investigating the function of PTPA in embryonic stem cells.

### 4.1.4. Length of the Targeting Construct

Homologous recombination between exogenous and genomic DNA is a process that occurs spontaneously in cells at low frequency. More often, rather than undergoing HR and replacing the endogenous sequence with targeting vector, cells will incorporate the vector randomly into their genome. Although the positive/negative selection process enriches for cells that have undergone homologous recombination, it does not increase the frequency of HR *per se*.

One factor that may increase the homologous recombination frequency in ES cells is the length of the homologous sequence. Several reports have indicated that the lower limit of homology is rather low (Hasty *et al.*, 1991; Deng and Capecchi, 1992; Thomas *et al.*, 1992). Hasty *et al.* (1991) reported that as little as 472 bp homology was sufficient for recombination to occur. Subsequently, it was found that longer lengths of homology could increase the frequency of HR significantly (Deng and Capecchi, 1992). A more recent study (Lu *et al.*, 2003), indicated that the relationship between the length of targeting arms and recombination efficiency is more complex. In this study, 8, 16, 24 and 110 kb homology length between the targeting vector and genomic DNA were shown to undergo HR at similar frequencies. The authors hypothesized that recombination frequency depend on several other factors, "such as the targeted locus itself, vector design, and the status of cellular HR machinery."

The completed PTPA-loxP targeting vector will have 5' and 3' arms of homology of 4.1 and 1.8 kb, respectively. According to the HR frequency rates established by Deng

and Capecchi (1992), this should allow for efficient homologous recombination. However, there is no way of anticipating or circumventing the other variables that may affect this efficiency. It may be necessary to "troubleshoot" modifications to the construct if HR frequencies are too low.

### 4.1.5. Incorporation of loxP Sites

The loxP sites must be engineered so that they flank a sequence that is deemed essential for gene function. This sequence will be removed from the mouse genome upon Cre-mediated recombination, translating into a non-functional protein. We have opted to incorporate the loxP sites flanking exons 6 and 7 of the PTPA gene. These two exons correspond to 77 amino acids (approximately 25% of the full length protein). More importantly, they include sequences that are highly conserved in all organisms. Exon 6 is the DNA sequence coding for a portion of the first conserved region, whereas exon 7 corresponds to the entire sequence of the second conserved region (Figure 2, in bold). In addition, a point mutation within this second region in which an aspartic acid residue is substituted with a glycine residue (D213G), completely abolishes yeast Rrd1 function, causing cells to be exhibit a sensitivity to 4-NQO similar to Rrd1-deficient cells (unpublished data). Together, these features indicated that this sequence was a good candidate for targeted deletion of PTPA.

### 4.1.6. Future Directions: Generating Conditional Knockout PTPA Mice

When the targeting construct is finalized, it will be linearized with XhoI (Figure 14). The targeting vector will then be electroporated into ES cells. Cells having integrated the construct within their genome will be selected using G418. The puromycin negative selection will eliminate cells that did not go through homologous recombination. Candidate G418-resistant, puromycin-sensitive cell lines will be screened by southern blot. It is important to note that only one PTPA allele is expected to undergo homologous recombination.

Once candidate ES cells lines are confirmed, they can be transfected with eFlp-expressing plasmid, removing the neomycin resistance gene from the genomic DNA. Cells will then be transferred to the inner cell mass of a blastocyst, to be subsequently

implanted in a pseudo-pregnant female. Since the inner cell mass will consist of ES cells of which only a fraction are carrying the genetic modification, the resultant pups will be chimeras, the loxP sites present merely in a subset of their tissues. Other tissue types will be completely wild-type.

These chimeras will be crossed with wild-type animals and their offspring will be screened by southern blot. This will allow the identification of the founder mice that carry the loxP sites in their germline. Positive offspring will then be mated with the transgenic mice capable of expressing the Cre recombinase so that a fraction of the resulting mice will carry the loxP sites on one PTPA allele as well as the recombinase gene. Finally, two such siblings (carrying both the loxP sites on one PTPA allele and the recombinase gene) will be crossed to obtain mice with the loxP sites on *both* alleles, as well as the ability to express Cre (Figure 17).

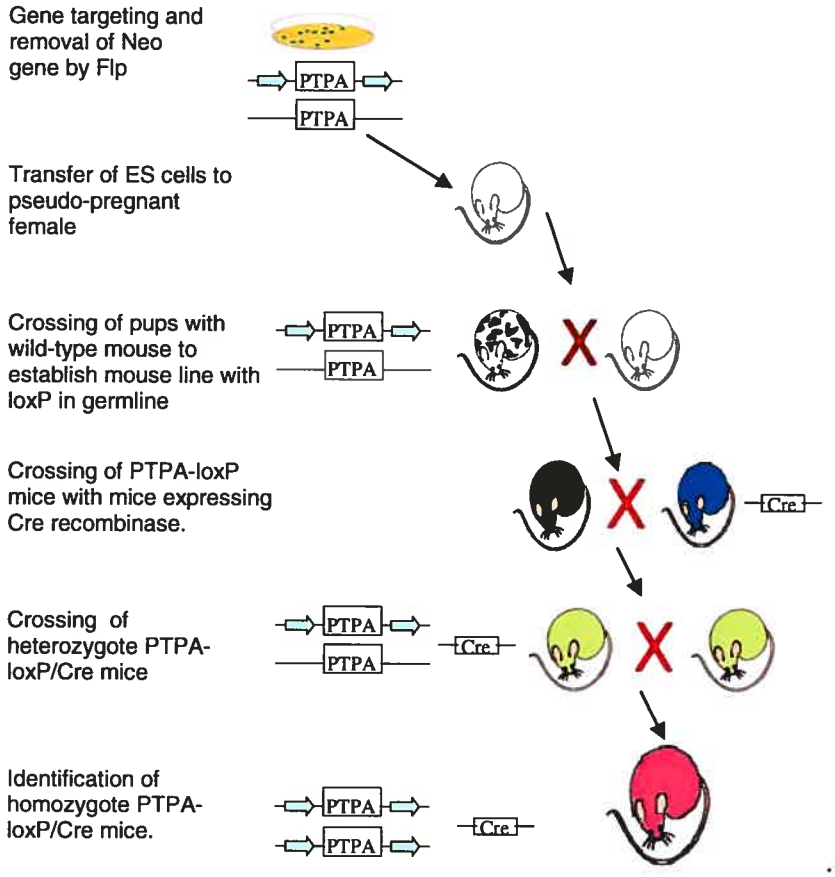


**Figure 17: Generating PTPA-loxP mice.** Arrows indicate loxP sites. Both alleles of the PTPA gene are shown.

A variety of mice expressing Cre under the control of inducible or tissue-specific promoters has been developed. These present interesting options for targeting PTPA deletion once PTPA-loxP mice have been generated. For example, the Tyr::Cre mouse line expresses the recombinase under the control of the tyrosinase gene promoter (Delmas *et al.*, 2003). This tightly regulated promoter drives gene expression in melanoblasts from embryonic day 11.5. Thus, if crossed to PTPA-loxP mice, only cells deriving from this precursor cell type will become PTPA-deficient. The cell lineage includes melanocytes, which is of particular interest given the relationship between UVA-induced oxidative damage and melanoma.

Alternatively, the CreR (T2) is a mouse line that ubiquitously expresses the Cre recombinase upon induction by tamoxifen and certain tamoxifen analogs. This mouse line expresses the recombinase fused to a modified oestrogen binding domain; only upon administration of these drugs does the protein become active. In addition, in the absence of tamoxifen/tamoxifen-analog activation, this mouse line exhibits a very low level of basal Cre activity. Finally, low doses of the drugs can efficiently activate the recombinase. This is a considerable advantage over other inducible Cre mice, in which the recombinase can only be activated when animals are treated with higher doses of drugs, often causing side effects (Feil *et al.*, 1997).

Many other mouse lines expressing the Cre recombinase under the control of inducible or tissue specific promoters are commercially available. The Jackson Laboratory's "Cre deleter" mouse strains and Artemis Pharmaceuticals' Cre Recombinase Zoo provide a wide range of tissue- and time-specific Cre-expressing mice. The PTPA-loxP mice could be crossed with one or several of these Cre animals, making the conditional knockouts very versatile, allowing the study of PTPA function in different tissues and/or at different stages of development.

## 4.2. The Creation of Mice Overexpressing PTPA and Fused to EYFP

In addition to generating PTPA knockout mice, our laboratories were interested in observing the effect of Ptpa protein overexpression on the response to oxidative stress in mice. Generally, transgenic mice are produced more rapidly than knockout mice and are

less prone to embryonic lethality. Therefore, we attempted to generate mice that would express the transgene, tagged to a GFP, ubiquitously, rather than limiting its expression to specific tissues. GFPs are powerful tools for microscopic (intracellular localization of the fusion protein, FACS analysis, etc.) and macroscopic (animal typing and screening) applications. Further, our laboratories did not initially have a reliable anti-Ptpa antibody. Producing Ptpa fused to a GFP was considered advantageous because the tag could be detected by a commercially available anti-GFP antibody.

### 4.2.1. Choice of Green Fluorescent Protein Variant

Since Green Fluorescent Proteins were first discovered and characterized in 1978, applications have evolved tremendously. Mutagenesis experiments have generated a variety of GFPs, characterized by different spectral features and quantum yields. The enhanced GFPs (eGFPs), such as EGFP, EYFP and ECFP, have distinct and only partially overlapping emission and excitation spectra, and different quantum yields. These have been used successfully in cell lines as well as in whole animals (Zhu *et al.* 1999; Frank *et al.*, 2003).

We have opted to generate mice expressing the EYFP-fused Ptpa protein. Used as a tag, EYFP, like other GFPs, can be readily visualized macroscopically in mouse tissues. Thus, once transgene expression is confirmed by western blotting, subsequent screening of transgenic mice could be performed through the empirical observation of fluorescence. In the event that transgene expression is not ubiquitous, adult mouse dissections could be performed to screen macroscopically for expression within specific tissue. In addition to utilizing the rapid, simple and non-invasive method of screening animals described above, EYFP could be detected in primary cell lines derived from transgenic mice Therefore, microscopic observations would allow us to localize and quantify the tagged Ptpa in cells.

The most appealing property of the EYFP variant is its high quantum yield. Like other GFPs, EYFP requires excitation by specific wavelengths to emit its fluorescence. This variant's quantum yield is 0.61, emitting a greater number of photons per excitation photon than other GFPs (Ormo *et al.*, 1996). Consequently, we judged that the use of this variant would best guarantee a strong and clearly visible signal.

### 4.2.2. Detection of Transgene Expression

Upon establishing candidate mouse lines, DNA of individual mice from different families was extracted from tail clippings and screened by southern blotting. Having found several individuals appearing to carry the transgene, we sought to identify animals in which Ptpa-EYFP was expressed. Initially, we dissected several individuals of different mouse lines, isolated a number of tissues from which protein was extracted and performed western blots. Initially, we used an anti-GFP antibody that can detect GFP variants including EYFP. No detectable signal for Ptpa-EYFP was obtained. Western blots were repeated when our laboratories subsequently obtained an anti-Ptpa antibody. Although, this antibody detected the endogenous mouse Ptpa very effectively, it did not reveal the expression of the transgene. Upon dissecting many animals from three families and repeating the procedure several times, it was concluded that no transgene expression could be detected by western blot.

Following our use of molecular techniques to detect Ptpa-EYFP expression, we obtained equipment that would permit the macroscopic detection of fluorescence. A number of costly apparatuses are available commercially for such applications (Budapest, Hungary, www.bls-ltd.com). Our laboratory used a more cost-effective system, the Clare Chemical Spot Lamp Kit and observation goggles (Dolores, USA, www.clarechemical.com). This kit allows macroscopic visualization of even low levels of fluorescence. Its major limitation is that it is not possible to combine it with photographic equipment that would allow pictures of the fluorescence to be taken.

The light source of the Spot Lamp consists of a bright light with an excitation filter limiting the light emission to wavelengths between 400 nm and 520 nm. The goggles act as an emission filter, enabling the viewer to see wavelengths above 540 nm. Although these do not correspond to the emission and excitation maxima of EYFP, the ranges of wavelengths closely match the spectrum of this GFP variant (Ormo M *et al.*, 1996).

Initially, only hairless pups were screened for expression of EYFP because the emitted fluorescence is only readily visible in hairless tissue. These macroscopic observations did not reveal fluorescence. It was hypothesized that only a subset of tissues expresses the Ptpa-EYFP fusion. Therefore, several mice from different mouse lines

were sacrificed, dissected, and their inner organs observed with the Spot Lamp and observation goggles. Again, no EYFP expression was detected, with the exception of one animal whose seminal vesicle appeared to emit fluorescence.

In sum, despite the confirmation that proper integration of the construct into the mouse genome in different mouse lines, none of these was found to overexpress Ptpa or to express EYFP, as ascertained by western blotting using antibodies for mouse Ptpa and GFP. In addition, except for one animal, macroscopic observations did not reveal fluorescence in any tissue.

### 4.2.3. Possible Reasons for the Absence of Transgene Expression

A number of reasons may account for the absence of transgene expression. It was initially hypothesized that transgene expression may have a negative effect on the health of embryos or pups, preventing us from detecting transgenic adults by southern blot. Indeed, this hypothesis was later substantiated in our laboratories (see Section 4.3.). If this were the case, female mice would have given birth to fewer pups per pregnancy, a fraction of the embryos having died because of the transgene expression. Our observation that mice had normal pregnancy and birthing patterns excluded this possibility.

This lack of Ptpa-EYPF expression is more likely due to the choice of the promoter driving the transgene expression. The PTPA-EYFP construct was designed by incorporating a copy of mouse PTPA cDNA into the pEYFP-N1 plasmid (Clontech), which contains a CMV promoter. We relied on the CMV promoter to drive the constitutive expression of the transgene. However, this promoter has been associated with suboptimal patterns of protein expression in animals. One study demonstrated that a transgene is driven in different tissues to variable extents in transgenic animals (Baskar *et al.*, 1996). This finding was confirmed in a more recent study involving CMV promoter-driven GFP expression in mice. Villuendas *et al.* (2001) reported that generally, this promoter does not drive the expression of significant levels of green fluorescent protein in mice tissues, the only exception being male reproductive organs. This is partially consistent with our observation of EYFP in the seminal vesicle in one animal.

Indeed, upon surveying the literature, it appears that the majority of researchers who successfully generated GFP-expressing mice did so utilizing the chicken beta-actin promoter (Okabe *et al.*, 1997; Sato *et al.*, 2001; Frank *et al.*, 2003).

### 4.2.4. Proposed Modifications for Future Transgenic PTPA-GFP Studies

In the future, a number of modifications should be made to increase the chance of obtaining mice with a strong transgene expression and to maximize fluorescence emission. Primarily, the chicken beta-actin promoter should be used, as in other studies reporting strong fluorescence expression in mice. Additionally, the EYFP variant should be replaced with EGFP. EGFP has a broader emission and excitation spectra than EYFP. The former can consequently be visualized macroscopically with a standard hand held UV lamp or the Clare Chemical Spot Lamp, without requiring the use of stringent filters that allow only a narrow range of wavelengths to pass through. In addition, since EGFP has a broad emission/excitation spectrum, the fluorescence in cells isolated from mice can be visualized microscopically using conventional GFP filters and analyzed by FACS using standard parameters. In contrast, EYFP's narrower excitation/emission spectra render microscopic fluorescence visualization and FACS analysis inaccurate unless specific filter sets are acquired and standard FACS parameters modified.

## 4.3. Future Directions for PTPA Conditional Knockout and Transgenic Mice

Using animals to study the role of PTPA in the cellular response to oxidative stress is a promising endeavour. In the short to medium term, much effort will be required to generate mice that will carry and express the appropriate genomic modifications. This is, in and of itself, very labour intensive. In addition, altering Ptpa expression may have a deletrious or lethal effect on the experimental animals, making it difficult to generate the desired lineages.

Indeed, it has been demonstrated that both the suppression and overexpression of Ptpa cause cell dealth. Fellner *et al.* (2003) reported that PTPA-RNAi-transfected HeLa cells underwent apoptosis. Recent unpublished data obtained in our laboratories provides evidence that excess amounts of the protein is equally damaging to the cell; a sharp

decline in survival rates was observed in HCT 116 cells transfected with a plasmid driving the expression of Ptpa-EYFP, 24 and 48 hours post-transfection (see Appendix).

The ultimate goal for developing transgenic and knockout PTPA mice is to gain insight into PTPA function. Preliminary experiments should consist of treating the genetically modified mice with different doses of ROS-inducing agents by feeding them with drugs that are known to produce oxidative stress or by exposing them to UVA. Given the potentially diverse roles of PTPA, it should be expected that a number of phenotypes be observed. As such, it is difficult to outline a detailed experimental plan. Rather, experiments using these mice will have to be continuously refined and adjusted with emerging phenotypes.

# 5. Conclusion

The study of oxidative stress is of great relevance to several contemporary health issues. A better appreciation of the genetic factors underlying the cellular response to ROS will help refine our understanding of the biology of reactive oxygen species and their role in disease, eventually enabling the development of effective preventative and/or curative measures.

The yeast homologue of the mammalian PTPA gene has been shown to play a role in the response to oxidative stress, particularly in maintaining DNA integrity upon ROS insult. Although the no clear gene function emerges from the literature, several lines of evidence suggest that it may also be involved in a variety of other important pathways. Evidence supports a role for this gene in mechanisms related to carcinogenesis. Therefore, our laboratories undertook the task of exploring the role of PTPA in the response to oxidative stress in greater detail, focusing on possible implications for the study carcinogenesis.

The manipulation of the mouse genome to alter gene expression is an extremely powerful, almost indispensable, tool for the study of gene function and pathology, at the level of the entire organism. Indeed, traditional knockout and transgenic mice have become commonplace. These methods are continuously being refined to help achieve a greater "tailoring" of the mouse genome. The Cre/loxP system and the Green Fluorescent Protein allow the generation of powerful, practical and versatile genetically modified mice.

We have sought to exploit these technologies to determine the function of the PTPA gene in mammals. A targeting vector containing the various elements required for the generation of conditional knockout mouse was prepared. One more cloning step is required before the construct could be electroporated to ES cells. In addition, transgenic mice, anticipated to express Ptpa protein fused to a Green Fluorescent Protein-derivative, were produced. Unfortunately, expression of the transgene was not detected. A number of modifications can be made to the construct that was utilized to generate these mice, which will almost certainly yield results that are more fruitful in the future. Once the

mice are finalized, experiments will be performed that will, hopefully, help elucidate the PTPA's function in the response to oxidative stress and related pathologies.

# 6. Appendix

Our laboratories have generated a cell-line in which Ptpa-EYFP is expressed. HCT 116 cells, derived from a primary colon carcinoma of an adult man (Brattain *et al.* 1982), were transfected with the CMV-PTPA-EYFP construct, identical to the one microinjected into fertilized oocytes for producing transgenic mice. Ptpa-EYFP expression was determined by western blot analysis using an anti-GFP antibody (Figure 18a).

A

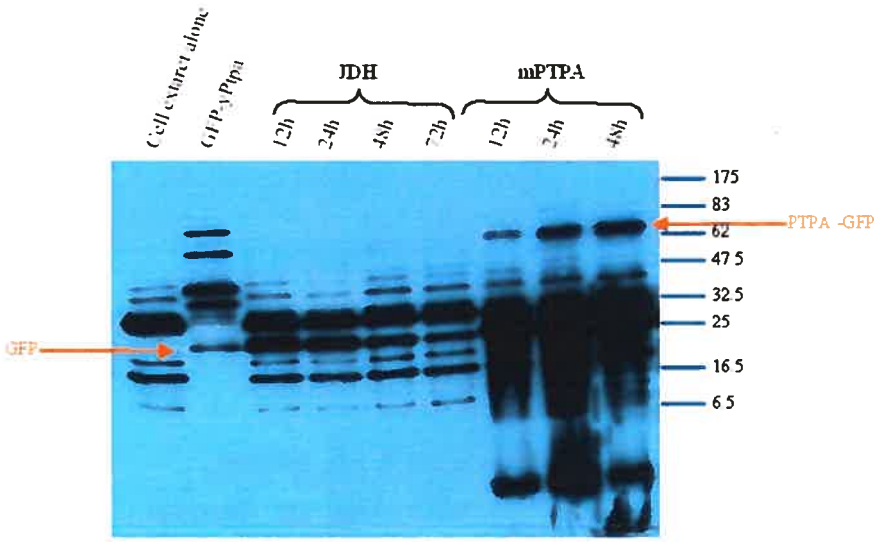


B

| | CMV-PTPA-EYFP-transfected HCT 116 | | CMV-EYFP transfected cells | untransfected cells |
|---|---|---|---|---|
| | 24h | 48h | 48h | 48h |
| total cells count | 4.08 X10$^6$ | 4.33 X10$^6$ | 9.34 X10$^6$ | 9.25 X10$^6$ |
| dead cells | 0.98 X10$^6$ | 1.63 X10$^6$ | 0.66 X10$^6$ | 0.15 X10$^6$ |
| living cells | 3.1 X10$^6$ | 2.7 X10$^6$ | 8.68 X10$^6$ | 9.1 X10$^6$ |
| % survival | 75.98 | 62.35 | 92.86 | 98.37 |

**Figure 18:** Ptpa-EYFP expression decreases survival rates of HCT 116 cells. *A*, Western blotting for detection of Ptpa-EYFP expression using an anti-GFP antibody. *B*, Survival rate of CMV-PTPA-EYFP-transfected cells.

A clear signal immediately above the 62kDa marker band in lanes representing protein extracted from cell 12, 24 and 48 hours post-transfection, indicates that the Ptpa-EYFP construct is expressed.

Concomittant with Ptpa-EYFP expression, a marked decrease in cell survival is observed. In contrast, a culture of CMV-EYFP-transfected HCT 116 cells has a survival rate similar to that of untransfected cells, suggesting that the overexpression of Ptpa is the major cause of the decline in survival rates.

The figure and data were compiled by Sonish Azam and Xiaoming Yang.

# 7. References

Aguilar F, Hussain SP, Cerutti P. Aflatoxin B1 induces the transversion of G-->T in codon 249 of the p53 tumor suppressor gene in human hepatocytes. Proc. Natl. Acad. Sci USA. 90: 8586-8590, 1993.

Ames BN, Shigenaga MK, Hagen TM. Oxidants, antioxidants, and the degenerative diseases of aging. Proc Natl Acad Sci U S A . 90:7915–22, 1993.

Armstrong BK, Kricker A. Cutaneous melanoma. Cancer Surv. 19-20:219-40, 1994.

Austin S, Ziese M, Sternberg N. A novel role for site-specific recombination in maintenance of bacterial replicons. Cell. 25(3):729-36, 1981.

Athar M, Lloyd JR, Bickers DR, Mukhtar H. Malignant conversion of UV radiation and chemically induced mouse skin benign tumors by free-radical-generating compounds. Carcinogenesis. 10(10):1841-5, 1989.

Barzilay G, Hickson ID. Structure and function of apurinic/apyrimidinic endonucleases. Bioessays. 17(8):713-9, 1995.

Brattain MG, Fine WD, Khaled FM, Thompson J, Brattain DE. Heterogeneity of malignant cells from a human colonic carcinoma. Cancer Res. 41(5):1751-6, 1981.

Holger Bastians, Heike Krebber, David Vetrie, Joerg Hoheisel, Peter Lichter, Herwig Ponstingl, Stefan Joos. Localization of the Novel Serine/Threonine Protein Phosphatase 6 Gene (PPP6C) to Human Chromosome Xq22.3. Genomics. 41(2):296-7, 1997.

Bastians H, Ponstingl H. The novel human protein serine/threonine phosphatase 6 is a functional homologue of budding yeast Sit4p and fission yeast ppe1, which are involved in cell cycle regulation. J Cell Sci. 109 (Pt 12):2865-74, 1996.

Baskar JF, Smith PP, Nilaver G, Jupp RA, Hoffmann S, Peffer NJ, Tenney DJ, Colberg-Poley AM, Ghazal P, Nelson JA. The enhancer domain of the human cytomegalovirus major immediate-early promoter determines cell type-specific expression in transgenic mice. J Virol. 70(5):3207-14, 1996.

Beck T, Schmidt A, Hall MN. Starvation induces vacuolar targeting and degradation of the tryptophan permease in yeast. J Cell Biol. 146(6):1227-38, 1999.

Behrend L, Henderson G, Zwacka RM. Reactive oxygen species in oncogenic transformation. Biochem Soc Trans. Pt 6: 1441-4, 2003.

Bird AP. CpG-rich islands and the function of DNA methylation. Nature. 321(6067):209-13, 1986.

Birnboim HC, Doly J. A rapid alkaline extraction procedure for screening recombinant plasmid DNA. Nucleic Acids Res. 7(6):1513-23, 1979.

Brewster JL, de Valoir T, Dwyer ND, Winter E, Gustin MC. An osmosensing signal transduction pathway in yeast. Science. 259(5102):1760-3, 1993.

Broach JR, Hicks JB. Replication and recombination functions associated with the yeast plasmid, 2 mucircle. Cell. 21(2):501-8, 1980.

Cabelof DC, Raffoul JJ, Yanamadala S, Guo Z, Heydari AR. Induction of DNA polymerase beta-dependent base excision repair in response to oxidative stress in vivo. Carcinogenesis. 23(9):1419-25, 2000.

Cadenas E, Davies KJ. Mitochondrial free radical generation, oxidative stress, and aging. Free Radic Biol Med. 29(3-4):222-30, 2000.

Cadet J, Sage E, Douki T. Ultraviolet radiation-mediated damage to cellular DNA. Mutat Res. 571(1-2):3-17, 2005.

Calin, G. A., di Iasio, M. G., Caprini, E., Vorechovsky, I., Natali, P. G., Sozzi, G., Croce, C. M., Barbanti-Brodano, G., Russo, G., and Negrini, M. Oncogene.. 19:1191–1195, 2000.

Cayla X, Goris J, Hermann J, Hendrix P, Ozon R, Merlevede W. Isolation and characterization of a tyrosyl phosphatase activator from rabbit skeletal muscle and Xenopus laevis oocytes. Biochemistry. 29(3):658-67, 1990.

Cayla X, Van Hoof C, Bosch M, Waelkens E, Vandekerckhove J, Peeters B,Merlevede W, Goris J. Molecular cloning, expression, and characterization of PTPA, a protein that activates the tyrosyl phosphatase activity of protein phosphatase 2A. Biol Chem. 269(22):15668-75, 1994.

Chalfie M, Tu Y, Euskirchen G, Ward WW, Prasher DC. Green fluorescent protein as a marker for gene expression.
Science. 263(5148):802-5, 1994.

Chance PF, Rabin BA, Ryan SG, Ding Y, Scavina M, Crain B, Griffin JW, Cornblath DR. Linkage of the gene for an autosomal dominant form of juvenile amyotrophic lateral sclerosis to chromosome 9q34. Am J Hum Genet. 62(3):633-40, 1998.

Chatterjee PK, Shakes LA, Srivastava DK, Garland DM, Harewood KR, Moore KJ, Coren JS. Mutually exclusive recombination of wild-type and mutant loxP sites in vivo facilitates transposon-mediated deletions from both ends of genomic DNA in PACs. Nucleic Acids Res. 32(18):5668-76, 2004.

Cheah SS, Behringer RR. Contemporary gene targeting strategies for the novice. Mol Biotechnol. 19(3): 297-304, 2001.

Cheng KC, Cahill DS, Kasai H, Nishimura S, Loeb LA. 8-Hydroxyguanine, an abundant form of oxidative DNA damage, causes G----T and A----C substitutions. Biol Chem. 267(1):166-72, 1992.

Chernoff J, Li HC, Cheng YS, Chen LB. Characterization of a phosphotyrosyl protein phosphatase activity associated with a phosphoseryl protein phosphatase of Mr = 95,000 from bovine heart. J Biol Chem. 258(12):7852-7, 1983.

Chong YC, Heppner GH, Paul LA, Fulton AM. Macrophage-mediated induction of DNA strand breaks in target tumor cells. Cancer Res. 49(23):6652-7, 1989.

Churg A. Interactions of exogenous or evoked agents and particles: the role of reactive oxygen species. Free Radic Biol Med. 34(10):1230-5, 2003.

Cicchillitti L., Fasanaro P, Biglioli P, Capogrossi MC, Martelli F, Oxidative Stress Induces Protein Phosphatase 2A-dependent Dephosphorylation of the Pocket Proteins pRb, p107, and p130* . PP2A de J. Biol. Chem., 278(21): 19509-19517, 2003.

de Haan JB, Cristiano F, Iannello RC, Kola I. Cu/Zn-superoxide dismutase and glutathione peroxidase during aging. Biochem Mol Biol Int. 35(6):1281-97, 1995.

Delmas V, Martinozzi S, Bourgeois Y, Holzenberger M, Larue L. Cre-mediated recombination in the skin melanocyte lineage. Genesis. 36(2):73-80, 2003.

Deng C, Capecchi MR. Reexamination of gene targeting frequency as a function of the extent of homology between the targeting vector and the target locus. Mol Cell Biol. 12(8):3365-71, 1992.

Di Como CJ, Arndt KT. Nutrients, via the Tor proteins, stimulate the association of Tap42 with type 2A phosphatases. Genes Dev. 10(15):1904-16, 1996.

Dobrovolsky VN, Casciano DA, Heflich RH. Development of a novel mouse tk+/- embryonic stem cell line for use in mutagenicity studies. Environ Mol Mutagen. 28(4):483-9, 1996.

Doetsch PW, Morey NJ, Swanson RL, Jinks-Robertson S. Yeast base excision repair: interconnections and networks. Prog Nucleic Acid Res Mol Biol. 68:29-39, 2001.

Dong XP, Stubenrauch F, Beyer-Finkler E, Pfister. Prevalence of deletions of YY1-binding sites in episomal HPV 16 DNA from cervical cancers. Int J Cancer. 58(6):803-8, 1994.

Douville J, David J, Fortier PK, Ramotar D The yeast phosphotyrosyl phosphatase activator protein, yPtpa1/Rrd1, interacts with Sit4 phosphatase to mediate resistance to 4-nitroquinoline-1-oxide and UVA. Curr Genet, available online as of May 2004.

Droge W. Oxidative stress and aging. Adv Exp Med Biol. 543:191-200, 2003.

Dizdaroglu M, von Sonntag C, Schulte-Frohlinde D. Letter: Strand breaks and sugar release by gamma-irradiation of DNA in aqueous solution.J Am Chem Soc. 97(8):2277-8, 1975.

Engelward BP, Weeda G, Wyatt MD, Broekhof JLM, de Wit J, Donker I, James AM, Gold B, Hoeijmakers JHJ, Samson LD. Base excision repair deficient mice lacking the Aag alkyladenine DNA glycosylase. Proc Natl Acad Sci U S A. 94 (24): 13087–13092, 1997.

Ercal N, Gurer-Orhan H, Aykin-Burns N. Toxic metals and oxidative stress part I: mechanisms involved in metal-induced oxidative damage. Curr Top Med Chem. 1(6):529-39. 2001.

Feil R, Wagner J, Metzger D, Chambon P. Regulation of Cre recombinase activity by mutated estrogen receptor ligand-binding domains. Biochem Biophys Res Commun. 237(3):752-7, 1997.

Fellner T, Lackner DH, Hombauer H, Piribauer P, Mudrak I, Zaragoza K, Juno C, Ogris E. A novel and essential mechanism determining specificity and activity of protein phosphatase 2A (PP2A) in vivo. Genes Dev. 17(17):2138-50, 2003.

Fiering S, Epner E, Robinson K, Zhuang Y, Telling A, Hu M, Martin DI, Enver T, Ley TJ, Groudine M. Targeted deletion of 5'HS2 of the murine beta-globin LCR reveals that it is not essential for proper regulation of the beta-globin locus. Genes Dev. 9(18):2203-13, 1995.

Frank AC, Meyers KA, Welsh IC, O'Brien TP. Development of an enhanced GFP-based dual-color reporter to facilitate genetic screens for the recovery of mutations in mice. Proc Natl Acad Sci U S A. 100(24):14103-8, 2003.

Fortini P, Pascucci B, Parlanti E, D'Errico M, Simonelli V, Dogliotti E. 8-Oxoguanine DNA damage: at the crossroad of alternative repair pathways. Mutat Res. 531(1-2):127-39, 2003.

Foulkes JG, Erikson E, Erikson RL.Separation of multiple phosphotyrosyl-and phosphoseryl-protein phosphatases from chicken brain.J Biol Chem. 258(1):431-8, 1983.

Garcia, A., Cayla, X., & Sontag, E. Protein phosphatase 2A: a definite player in viral and parasitic regulation. Microbes Infect. 2,:401–407, 2000.

Gasdaska, P. Y.; Gasdaska, J. R.; Cochran, S.; Powis, G. Cloning and sequencing of a human thioredoxin reductase. FEBS Lett. 373: 5-9, 1995.

Gentry MS, Hallberg RL. Localization of Saccharomyces cerevisiae Protein Phosphatase 2A Subunits throughout Mitotic Cell Cycle. Mol Biol Cell. 13 (10): 3477–3492, 2002.

J. Götz, A. Probst, E. Ehler, B. Hemmings and W. Kues. Delayed embryonic lethality in mice lacking protein phosphatase 2A catalytic subunit Calpha. Proc. Natl. Acad. Sci. USA 95:12370–12375, 1998.

Grammatico P, Maresca V, Roccella F, Roccella M, Biondo L, Catricala C, Picardo M. Increased sensitivity to peroxidizing agents is correlated with an imbalance of antioxidants in normal melanocytes from melanoma patients. Exp Dermatol. 7(4):205-12, 1998.

Grollman AP, Moriya M. Mutagenesis by 8-oxoguanine: an enemy within. Trends Genet. 9(7):246-9, 1993.

Groves MR, Hanlon N, Turowski P, Hemmings BA & Barford, D. The structure of the protein phosphatase 2A PR65/A subunit reveals the conformation of its 15 tandemly repeated HEAT motifs. Cell 96:99–110, 1999.

Gruijl FR. Photocarcinogenesis: UVA vs UVB. Methods Enzymol. 319:359-66, 2000.

Hannan GN, Lehnert SA, MacAvoy ES, Jennings PA, Molloy PL. An engineered PGK promoter and lac operator-repressor system for the regulation of gene expression in mammalian cells. Gene. 130(2):233-9, 1993.

Grune T, Reinheckel T, Davies KJ. Degradation of oxidized proteins in mammalian cells. Faseb J. 11(7):526-34, 1997.

Hadjantonakis AK, Macmaster S, Nagy A. Embryonic stem cells and mice expressing different GFP variants for multiple non-invasive reporter usage within a single animal. BMC Biotechnol. 2(1):11. 2002.

Hadjantonakis AK, Nagy A. The color of mice: in the light of GFP-variant reporters. Histochem Cell Biol. 115:49–58, 2001.

Hall HI, Miller DR, Rogers JD, Bewerse B. Update on the incidence and mortality from melanoma in the United States. Journal of the American Academy Of Dermatology. 40(1) 35:-42, 1999.

Harman D. Aging: a theory based on free radical and radiation chemistry. J Gerontol. 11: 298-300, 1956.

Harman D. The aging process. Proc Natl Acad Sci USA. 78: 7124-7128, 1981.

Hasty P, Rivera-Perez J, Bradley A. The length of homology required for gene targeting in embryonic stem cells. Mol Cell Biol. 11(11):5586-91, 1991.

Healy, A.M., Zolnierowicz, S., Stapleton, A.E., Goebl, M., DePaoli-Roach, A.A. & Pringle, J.R. CDC55, a Saccharomyces cerevisiae gene involved in cellular morphogenesis: Identification, characterization and homology to the B subunit of mammalian type 2A protein phosphatase. Mol. Cell. Biol. 11: 5767–5780, 1991.

Heller FA, Xue C, Fisher A, Everett AD. Expression and mapping of protein phosphatase 2A alpha in the developing rat heart. Pediatr Res. 43(1):68-76, 1998.

Huang S, Houghton PJ. Targeting mTOR signaling for cancer therapy. Curr Opin Pharmacol. 3(4):371-7, 2003.

Huntly BJ, Bench A, Green AR. Double jeopardy from a single translocation: deletions of the derivative chromosome 9 in chronic myeloid leukemia. Blood. 102(4):1160-8, 2003.

Ichiba M, Maeta Y, Mukoyama T, Saeki T, Yasui S, Kanbe T, Okano J, Tanabe Y,Hirooka Y, Yamada S, Kurimasa A, Murawaki Y, Shiota G. Expression of 8-hydroxy-2'-deoxyguanosine in chronic liver disease and hepatocellular carcinoma. Liver Int. 23(5):338-45, 2003.

Amsterdam A, Lin S, Hopkins, N. The *Aequorea victoria* green fluorescent protein can be used as a reporter in live zebrafish embryos. *Devel Biol.* 171:123-129, (1995).

Ikawa M, Kominami K, Yoshimura Y, Tanaka K, Nishimune Y, Okabe M. A rapid and non-invasive selection of transgenic embryos before implantation using green fluorescent protein (GFP). FEBS Lett. 375(1-2):125-8, 199

Ito A, Koma YI, Watabe K.A mutation in protein phosphatase type 2A as a cause of melanoma progression. Histol Histopathol. 18(4):1313-9, 2003.

Jackson AL, Loeb LA. The contribution of endogenous sources of DNA damage to the multiple mutations in cancer. Mut Res. 477(1-2): 7-21.

Jacob RA, Burri BJ. Oxidative damage and defense. Am J Clin Nutr. 63(6):985S-990S, 1996

Janssens, V. & Goris, J. Protein phosphatase 2A: a highly regulated family of serine/threonine phosphatases implicated in cell growth and signaling. Biochem. J. 353, 417–439, 2001.

Janssens V, Van Hoof C, De Baere I, Merlevede W, Goris J. Functional analysis of the promoter region of the human phosphotyrosine phosphatase activator gene: Yin Yang 1 is essential for core promoter activity. Biochem J. 344(3):755-63, 1999.

Janssens V, Van Hoof C, De Baere I, Merlevede W, Goris J. The phosphotyrosyl phosphatase activator gene is a novel p53 target gene. J Biol Chem. 275(27):20488-95, 2000.

Janssens V, van Hoof C, Martens E, de Baere I, Merlevede W, Goris J. Identification and characterization of alternative splice products encoded by the human phosphotyrosyl phosphatase activator gene. Eur J Biochem. 267(14):4406-13, 2000.

Jones CA, Huberman E, Cunningham ML, Peak MJ. Mutagenesis and cytotoxicity in human epithelial cells by farand near-ultraviolet radiations: action spectra. Radiat Res. 110:244-54, 1987;

Jones S, Lambert S, Williams GT, Best JM, Sampson JR, Cheadle JP. Increased frequency of the k-ras G12C mutation in MYH polyposis colorectal adenomas. Br J Cancer. 90(8):1591-3, 2004.

Kaneko Y, Frizzera G, Maseki N, Sakurai M, Komada Y, Sakurai M, Hiyoshi Y,Nakadate H, Takeda T. A novel translocation, t(9;17)(q34;q23), in aggressive childhood lymphoblastic lymphoma. Leukemia. 2(11):745-8, 1998.

Karaiskou A, Jessus C, Brassac T, Ozon R. Phosphatase 2A and polo kinase, two antagonistic regulators of cdc25 activation and MPF auto-amplification. J Cell Sci. 112:3747-56, 1998.

Kappus H. Oxidative stress in chemical toxicity. Arch Toxicol. 60(1-3):144-9, 1987.

Kim KJ, Chakrabarty I, Li GZ, Grosch S, Kaina B, Runger TM. Modulation of base excision repair alters cellular sensitivity to UVA1 but not to UVB1. Photochem Photobiol. 75(5):507-12, 2002.

Kim YB, Oh SH, Sok DE, Kim MR. Neuroprotective effect of maltol against oxidative stress in brain of mice challenged with kainic acid. Nutr Neurosci.7(1):33-9, 2004.

Kimura F, Florl AR, Seifert HH, Louhelainen J, Maas S, Knowles MA, Schulz WA. Destabilization of chromosome 9 in transitional cell carcinoma of the urinary bladder. Br J Cancer. 85(12):1887-93, 2001.

Kley N, Chung RY, Fay S, Loeffler JP, Seizinger BR. Repression of the basal c-fos promoter by wild-type p53. Nucleic Acids Res. 20(15):4083-7, 1992.

Klungland A, Rosewell I, Hollenbach S, Larsen E, Daly G, Epe B, Seeberg E, Lindahl T, Barnes DE. Accumulation of premutagenic DNA lesions in mice defective in removal of oxidative base damage. Proc Natl Acad Sci U S A. 96(23):13300-5, 1999.

Kreutzer,D.A. and Essigmann,J.M. Oxidized, deaminated cytosines are a source of C→T transitions in vivo. Proc. Natl Acad. Sci. USA. 95: 3578–3582, 1998.

Kruman II, Pedersen WA, Springer JE, Mattson MP. ALS-linked Cu/Zn-SOD mutation increases vulnerability of motor neurons toexcitotoxicity by a mechanism involving increased oxidative stress and perturbed calcium homeostasis. Exp Neurol. 160(1):28-39, 1999.

Latarjet R. Influence de l'ozone atmospherique sur l'activite biologique du rayonnement solaire. Rev. Opt. Theor. Instrum. **14**: 398–411, 1935,

Lebovitz R. L., Zhang H., Vogel H., Cartwright J., Jr., Dionne L., Lu N., Huang S., Matzuk M. M. Neurodegeneration, myocardial injury, and perinatal death in mitochondrial superoxide dismutase-deficient mice. Proc. Natl. Acad. Sci. USA, 93: 9782-9787, 1996.

Le Page F, Kwoh EE, Avrutskaya A, Gentil A, Leadon SA, Sarasin A, Cooper PK. Transcription-coupled repair of 8-oxoguanine: requirement for XPG, TFIIH, and CSB and implications for Cockayne syndrome. Cell. 101(2):159-71, 2000.

Ley RD. Ultraviolet radiation A-induced precursors of cutaneous melanoma in Monodelphis domestica. Cancer Res. 57:3682-4, 1997.

Lin XH, Walter J, Scheidtmann K, Ohst K, Newport J, Walter G. Protein phosphatase 2A is required for the initiation of chromosomal DNA replication. Proc Natl Acad Sci U S A. 95(25):14693-8, 1998.

Loeb LA, Preston BD. Mutagenesis by apurinic/apyrimidinic sites. Annu Rev Genet. 20:201-30, 1986.

Longin S, Jordens J, Martens E, Stevens I, Janssens V, Rondelez E, De Baere I, Derua R, Waelkens E, Goris J, Van Hoof C. An inactive protein phosphatase 2A population is associated with methylesterase and can be reactivated by the phosphotyrosyl phosphatase activator. Biochem J. 380(Pt 1):111-9, 2004

Lopez-Torres M, Thiele JJ, Shindo Y, Han D, Packer L. Topical application of alpha-tocopherol modulates the antioxidant network and diminishes ultraviolet-induced oxidative damage in murine skin. Br J Dermatol. 138(2):207-15, 1998.

Lu ZH, Books JT, Kaufman RM, Ley TJ. Long targeting arms do not increase the efficiency of homologous recombination in the beta-globin locus of murine embryonic stem cells. Blood. 102(4):1531-3.

Lundgren K, Wulf HC. Cytotoxicity and genotoxicity of UVA irradiation in Chinese hamster ovary cells measured by specific locus mutations, sister chromatid exchanges and chromosome aberrations. Photochem Photobiol. 47:559-63, 1998.

Mansour SL, Thomas KR, Capecchi MR. Disruption of the proto-oncogene int-2 in mouse embryo-derived stem cells: a general strategy for targeting mutations to non-selectable genes. Nature. 336(6197):348-52, 1998.

Marnett LJ. Oxyradicals and DNA damage. Carcinogenesis. 21(3):361-370, 2000.

Mayer, R.E., Khew-Goodall, Y., Stone, S.R. & Hemmings, Structure and expression of protein phosphatase PP2A. Adv. Prot. Phosphatases 6: 125–143, 1991.

Meyers EN, Lewandoski M, Martin GR. An Fgf8 mutant allelic series generated by Cre- and Flp-mediated recombination. Nat Genet. 18(2):136-41, 1998.
McCullough AK, Dodson ML, Lloyd RS. Initiation of base excision repair: glycosylase mechanisms and structures. Annu Rev Biochem. 68:255-85, 1999.

Mermoud JE, Cohen P, Lamond AI. Ser/Thr-specific protein phosphatases are required for both catalytic steps of pre-mRNA splicing. Nucleic Acids Res. 20(20):5263-9, 1992.

Minowa O, Arai T, Hirano M, Monden Y, Nakai S, Fukuda M, Itoh M, Takano H, Hippou Y, Aburatani H, Masumura K, Nohmi T, Nishimura S, Noda T. Mmh/Ogg1 gene inactivation results in accumulation of 8-hydroxyguanine in mice. Proc Natl Acad Sci U S A. 97(8):4156-61, 2000.

Mitchell DA, Sprague GF Jr. The phosphotyrosyl phosphatase activator, Ncs1p (Rrd1p), functions with Cla4p to regulate the G(2)/M transition in Saccharomyces cerevisiae. Mol Cell Biol. 21(2):488-500, 2001.

Mitra S, Izumi T, Boldogh I, Bhakat KK, Hill JW, Hazra TK. Choreography of oxidative damage repair in mammalian genomes.Free Radic Biol Med. 33(1):15-28, 2002.

Moan J, Dahlback A, Setlow RB. Epidemiological support for an hypothesis for melanoma induction indicating a role for UVA radiation. Photochem Photobiol . 70: 243-247, 1999.

Muller H, Helin K. The E2F transcription factors: key regulators of cell proliferation. Biochim Biophys Acta. 1470(1):M1-12, 2000.

Nayak BK, Das BR. Differential binding of NF1 transcription factor to P53 gene promoter and its depletion in human breast tumours. Mol Biol Rep. 26(4):223-30, 1999.

Nath N., Chari S. N., Rathi A. B. Superoxide dismutase in diabetic polymorphonuclear leukocytes. Diabetes. 33: 586-589, 1984

Noor R, Mittal S, Iqbal J. Superoxide dismutase--applications and relevance to human diseases. Med Sci Monit. 8(9):RA210-5, 2002.

Norata GD, Pirillo A, Catapano AL. Statins and oxidative stress during atherogenesis. J Cardiovasc Risk. 10(3):181-9, 2003.

Ocampo MT, Chaung W, Marenstein DR, Chan MK, Altamirano A, Basu AK, Boorstein RJ, Cunningham RP, Teebor GW. Targeted deletion of mNth1 reveals a novel DNA repair enzyme activity. Mol Cell Biol. 22(17):6111-21, 2002.

Okabe M, Ikawa M, Kominami K, Nakanishi T, Nishimune Y. 'Green mice' as a source of ubiquitous green cells. FEBS Lett. 407 :313-9, 1997

Orban PC, Chui D, Marth JD. Tissue- and site-specific DNA recombination in transgenic mice. Proc Natl Acad Sci U S A. 89(15):6861-5, 1992.

Ormo M, Cubitt AB, Kallio K, Gross LA, Tsien RY, Remington SJ. Crystal structure of the Aequorea victoria green fluorescent protein. Science. 273(5280):1392-5, 1996.

Osterod M, Larsen E, Le Page F, Hengstler JG, Van Der Horst GT, Boiteux S, Klungland A, Epe B. A global DNA repair mechanism involving the Cockayne syndrome B (CSB) gene product can prevent the in vivo accumulation of endogenous oxidative DNA base damage. Oncogene. 21(54):8232-9, 28 2000.

Ou K, Seow TK, Liang RC, Ong SE, Chung MC. Proteome analysis of a human heptocellular carcinoma cell line, HCC-M: an update. Electrophoresis. 22(13):2804-11, 2001.

Parija T, Das BR. Involvement of YY1 and its correlation with c-myc in NDEA induced hepatocarcinogenesis, its prevention by d-limonene. Mol Biol Rep. 30(1):41-6, 2003.

Paz-Elizur T, Krupsky M, Blumenstein S, Elinger D, Schechtman E, Livneh Z. DNA repair activity for oxidative damage and risk of lung cancer. J Natl Cancer Inst. 95(17):1312-9, 2003.

Picardo M, Grammatico P, Roccella F, Roccella M, Grandinetti M, Del Porto G, Passi S. Imbalance in the antioxidant pool in melanoma cells and normal melanocytes from patients with melanoma. J Invest Dermatol. 107(3):322-6, 1996.

Prendergast. Chemical and physical properties of aequorin and the green fluorescent protein isolated from Aequorea forskalea. Biochemistry. 17(17):3448-53, 1978.

Powers T, Walter P. Regulation of ribosome biogenesis by the rapamycin-sensitive TOR-signaling pathway in Saccharomyces cerevisiae. Mol Biol Cell. 10(4):987-1000, 1999.

Pryor,W.A. Oxy-radicals and related species: their formation, lifetimes and reactions. Annu. Rev. Physiol. 48: 657–667, 1986.

Ramotar D, Belanger E, Brodeur I, Masson JY, Drobetsky EA. A yeast homologue of the human phosphotyrosyl phosphatase activator PTPA is implicated in protection against oxidative DNA damage induced by the model carcinogen 4-nitroquinoline 1-oxide. J Biol Chem. 273(34):21489-96, 1998.

Richa J. Production of transgenic mice. Molec Biotechnology. 17(3):261-8.

Rempola B, Kaniak A, Migdalski A, Rytka J, Slonimski PP, di Rago JP. Functional analysis of RRD1 (YIL153w) and RRD2 (YPL152w), which encode two putative activators of the phosphotyrosyl phosphatase activity of PP2A in Saccharomyces cerevisiae. Mol Gen Genet. 262(6):1081-92, 2000.

Roos D, van Bruggen R, Meischl C. Oxidative killing of microbes by neutrophils. Microbes Infect. 5(14):1307-15, 2000.

Rodriguez CI, Buchholz F, Galloway J, Sequerra R, Kasper J, Ayala R, Stewart AF, Dymecki SM. High-efficiency deleter mice show that FLPe is an alternative to Cre-loxP. Nat Genet. 25(2):139-40, 2000.

Ruediger R, Pham HT, Walter G. Alterations in protein phosphatase 2A subunit interaction in human carcinomas of the lung and colon with mutations in the A beta subunit gene. Oncogene. 20: 1892–1899, 2001.

Rybanska I, Pirsel M. Involvement of the nucleotide excision repair proteins in the removal of oxidative DNA base damage in mammalian cells. Neoplasma. 50(6):389-95, 2003.

Sambrook J. Fritsch E.F. and T. Maniatis. Molecular Cloning A Laboratory Manual. Cold Spring Harbor Laboratory Press, 2nd edition. 1.74, 1989.

Sandri MI, Isaacs RJ, Ongkeko WM, Harris AL, Hickson ID, Broggini M, Vikhanskaya F. p53 regulates the minimal promoter of the human topoisomerase IIalpha gene. Nucleic Acids Res. 24(22):4464-70, 1996.

Sato M, Watanabe T, Oshida A, Nagashima A, Miyazaki JI, Kimura M. Usefulness of double gene construct for rapid identification of transgenic mice exhibiting tissue-specific gene expression. Mol Reprod Dev. 60(4):446-56, 2001.

Schaft J, Ashery-Padan R, van der Hoeven F, Gruss P, Stewart AF. Efficient FLP recombination in mouse ES cells and oocytes. Genesis. 31, 6-10, 2001.

Schmelzle T, Hall MN. TOR, a central controller of cell growth.Cell. 103(2):253-62, 2000.

Scott AD, Neishabury M, Jones DH, Reed SH, Boiteux S, Waters R. Spontaneous mutation, oxidative DNA damage, and the roles of base and nucleotide excision repair in the yeast Saccharomyces cerevisiae. Yeast. 15(3):205-18, 1999.

Setlow RB, Grist E, Thompson K,Woodhead AD. Wavelengths effective in induction of malignant melanoma. Proc Natl Acad Sci U S A. 90:6666-70, 1993.

Seow TK, Ong SE, Liang RC, Ren EC, Chan L, Ou K, Chung MC. Two-dimensional electrophoresis map of the human hepatocellular carcinoma cell line, HCC-M, and identification of the separated proteins by mass spectrometry. Electrophoresis. 21(9):1787-813, 2000.

Shibutani S, Takeshita M, Grollman AP. Insertion of specific bases during DNA synthesis past the oxidation-damaged base. Nature. 349(6308):431-4. 1991.

Sterenborg HJ, Van der Leun JC. Tumorigenesis by a long wavelength UV-A source. Photochem Photobiol. 51(3):325-30, 1990.

Suganuma M, Fujiki H, Suguri H, Yoshizawa S, Hirota M, Nakayasu M, Ojika M, Wakamatsu K, Yamada K, Sugimura T. Okadaic acid: an additional non-phorbol-12-tetradecanoate-13-acetate-type tumor promoter. Proc Natl Acad Sci U S A. 85(6):1768-71, 1998

Sunesen M, Stevnsner T, Brosh Jr RM, Dianov GL, Bohr VA. Global genome repair of 8-oxoG in hamster cells requires a functional CSB gene product. Oncogene. 21(22):3571-8, 2002.

Takagi Y, Futamura M, Yamaguchi K, Aoki S, Takahashi T, Saji S. Alterations of the PPP2R1B gene located at 11q23 in human colorectal cancers. Gut. 47(2):268-71, 2000.

Teoule R, Cadet J. Radiation-induced degradation of the base component in DNA and related substances--final products. Mol Biol Biochem Biophys. 27:171-203, 1978

te Riele H, Maandag ER, Berns A. Highly efficient gene targeting in embryonic stem cells through homologous recombination with isogenic DNA constructs.Proc Natl Acad Sci U S A. 89(11):5128-32, 1992.

Thomas KR, Deng C, Capecchi MR. High-fidelity gene targeting in embryonic stem cells by using sequence replacement vectors. Mol Cell Biol. 12, 2919–23, 1992.

Turrens JF. Mitochondrial formation of reactive oxygen species. Physiol. 552(Pt 2):335-44, 2003.

Van der Vliet A, Bast A. Effect of oxidative stress on receptors and signal transmission. Chem Biol Interact. 85(2-3):95-116, 1992.

Van Hoof C, Aly MS, Garcia A, Cayla X, Cassiman JJ, Merlevede W, Goris J. Structure and chromosomal localization of the human gene of the phosphotyrosyl phosphatase activator (PTPA) of protein phosphatase 2A. Genomics. 28(2):261-72, 1995.

Van Hoof C, Cayla X, Bosch M, Merlevede W, Goris J. The phosphotyrosyl phosphatase activator of protein phosphatase 2A. A novel purification method, immunological and enzymic characterization. Eur J Biochem. 226(3):899-907, 1994.

Van Hoof C, Janssens V, De Baere I, de Winde JH, Winderickx J, Dumortier F, Thevelein JM, Merlevede W, Goris J. The Saccharomyces cerevisiae homologue YPA1 of the mammalian phosphotyrosyl phosphatase activator of protein phosphatase 2A controls progression through the G1 phase of the yeast cell cycle. J Mol Biol. 302(1):103-20, 2000.

Van Hoof C, Janssens V, De Baere I, Stark MJ, de Winde JH, Winderickx J, Thevelein JM, Merlevede W, Goris J. The Saccharomyces cerevisiae phosphotyrosyl phosphatase activator proteins are required for a subset of the functions disrupted by protein phosphatase 2A mutations. Exp Cell Res. 264(2):372-87, 2001.

Van Hoof C, Janssens V, Dinishiotu A, Merlevede W, Goris J. Functional analysis of conserved domains in the phosphotyrosyl phosphatase activator. Molecular cloning of the homologues from Drosophila melanogaster and Saccharomyces cerevisiae. Biochemistry. 37(37):12899-908, 1998.

Van Remmen H, Ikeno Y, Hamilton M, Pahlavani M, Wolf N, Thorpe SR, Alderson NL, Baynes JW, Epstein CJ, Huang TT, Nelson J, Strong R, Richardson A. Life-long reduction in MnSOD activity results in increased DNA damage and higher incidence of cancer but does not accelerate aging. Physiol Genomics. 16(1):29-37, 2003.

van Zyl, W., Huang, W. D., Sneddon, A. A., Stark, M., Camier, S., Werner, M., Marck, C., Sentenac, A. and Broach, J. R. Inactivation of the protein phosphatase 2A regulatory

subunit A results in morphological and transcriptional defects in Saccharomyces cerevisiae. Mol. Cell. Biol. 12: 4946–4959, 1992.

Villuendas G, Gutierrez-Adan A, Jimenez A, Rojo C, Roldan ER, Pintado B. CMV-driven expression of green fluorescent protein (GFP) in male germ cells of transgenic mice and its effect on fertility. Int J Androl. 24(5):300-5, 2001.

von Lindern M, Poustka A, Lerach H, Grosveld G. The (6;9) chromosome translocation, associated with a specific subtype of acute nonlymphocytic leukemia, leads to aberrant transcription of a target gene on 9q34. Mol Cell Biol. 10(8):4016-26, 1990.

Waelkens E, Goris J, Merlevede W. Purification and properties of polycation-stimulated phosphorylase phosphatases from rabbit skeletal muscle. J Biol Chem. 262(3):1049-59. 1987.

Walker LJ, Craig RB, Harris AL, Hickson ID. A role for the human DNA repair enzyme HAP1 in cellular protection against DNA damaging agents and hypoxic stress. Nucleic Acids Res. 22(23):4884-9, 1994.

Wang SS, Esplin ED, Li JL, Huang L, Gazdar A, Minna J, Evans GA. Alterations of the PPP2R1B gene in human lung and colon cancer. Science. 282(5387):284-7, 1998.

Wang S, Hazelrigg T. Implications for bcd mRNA localization from spatial distribution of exu protein in Drosophila oogenesis. Nature. 369:400-403, 1994.

Ward, JF. DNA damage produced by ionizing radiation in mammalian cells: identities, mechanisms of formation and reparability. Prog Nucleic Acid Res Mol Biol. **35**, 95–125

Ware CB, Siverts LA, Nelson AM, Morton JF, Ladiges WC. Utility of a C57BL/6 ES line versus 129 ES lines for targeted mutations in mice. Transgenic Res. 12(6):743-6. 2003.

Yokota J, Kohno T. Molecular footprints of human lung cancer progression. Cancer Sci. 95(3):197-204, 2004.

Zhao R, Fahs SA, Weiler H, Duncan SA. An efficient method to successively introduce transgenes into a given genomic locus in the mouse. BMC Dev Biol. 1(1):10, 2001.

Zhao Y, Boguslawski G, Zitomer RS, DePaoli-Roach AA, Saccharomyces cerevisiae homologs of mammalian B and B' subunits of protein phosphatase 2A direct the enzyme to distinct cellular functions. J. Biol. Chem. 272 : 8256–8262, 1997.

Zhu J, Musco ML, Grace MJ. Three-color flow cytometry analysis of tricistronic expression of eBFP, eGFP, and eYFP using EMCV-IRES linkages. Cytometry. 37(1):51-9, 1999.

Zolnierowicz, S., Van Hoof, C., Andjelkovic, N., Cron, P., Stevens, J., Merlevede, W., Goris, J. & Hemmings. The variable subunit associated with protein phosphatases 2A0 defines a novel multimember family of regulatory subunits. Biochem. J. 317: 187–194, 2002.